ANALYSIS AND SIMULATION OF THE BACKSCATTERING ENHANCEMENT PHENOMENON FROM RANDOMLY DISTRIBUTED POINT SCATTERERS

A THESIS SUBMITTED TO
THE GRADUATE SCHOOL OF NATURAL AND APPLIED SCIENCES
OF
MIDDLE EAST TECHNICAL UNIVERSITY

BY

KARTAL ŞAHİN AĞAR

IN PARTIAL FULFILLMENT OF THE REQUIREMENTS
FOR
THE DEGREE OF MASTER OF SCIENCE
IN
ELECTRICAL AND ELECTRONICS ENGINEERING

AUGUST 2007

Approval of the thesis:

ANALYSIS AND SIMULATION OF THE BACKSCATTERING ENHANCEMENT PHENOMENON FROM RANDOMLY DISTRIBUTED POINT SCATTERERS

submitted by **KARTAL ŞAHİN AĞAR** in partial fulfillment of the requirements for the degree of **Master of Science in Electrical and Electronics Engineering, Middle East Technical University** by,

Prof. Dr. Canan Özgen
Dean, Graduate School of **Natural and Applied Sciences** _____

Prof. Dr. İsmet Erkmen
Head of Department, **Electrical and Electronics Eng.** _____

Assoc. Prof. Dr. Seyit Sencer Koç
Supervisor, **Electrical and Electronics Eng. Dept., METU** _____

Examining Committee Members:

Prof. Dr. Canan Toker
Electrical and Electronics Engineering Dept., METU _____

Assoc. Prof. Dr. Seyit Sencer Koç
Electrical and Electronics Engineering Dept., METU _____

Prof. Dr. Gülbin Dural
Electrical and Electronics Engineering Dept., METU _____

Assist. Prof. Dr. Lale Alatan
Electrical and Electronics Engineering Dept., METU _____

Prof. Dr. Adnan Köksal
Electrical and Electronics Engineering Dept., HÜ _____

Date: 31.08.2007

I hereby declare that all information in this document has been obtained and presented in accordance with academic rules and ethical conduct. I also declare that, as required by these rules and conduct, I have fully cited and referenced all material and results that are not original to this work.

Name, Last name: Kartal Şahin, AĞAR

Signature :

ABSTRACT

ANALYSIS AND SIMULATION OF THE BACKSCATTERING ENHANCEMENT PHENOMENON FROM RANDOMLY DISTRIBUTED POINT SCATTERERS

AĞAR, Kartal Şahin

Department of Electrical and Electronics Engineering

Supervisor: Assoc. Prof. Dr. Seyit Sencer KOÇ

August 2007, 122 pages

This thesis investigates analysis and simulation of the backscattering enhancement phenomenon from randomly distributed point scatterers. These point scatterers are randomly distributed within a cube or a sphere and then the backscattering enhancement phenomenon from both cubical and spherical distributions are examined throughout the thesis. The general characteristic differences between cubical and spherical distribution about the scattering phenomenon are observed. T-matrix method is used for analytic investigations of the backscattering enhancement and also a certain number of approximate formulas are obtained. As for Monte Carlo simulation method, it is used for simulated investigations of the backscattering enhancement. Some Monte Carlo simulations are prepared by using MATLAB programming language and verified by showing their confidence intervals. Both analytic and simulated investigations of the backscattering enhancement due to single and double scattering are analyzed; however, only simulated investigation of the backscattering enhancement due to multiple scattering are analyzed because of its computational complexity. The thesis traces differences between single scattering and multiple scattering from randomly distributed point scatterers. Effects of both incident field frequency and point

scatterer density on the backscattering enhancement are indicated. The thesis seeks answers to questions such as which conditions cause the backscattering enhancement phenomenon from randomly distributed point scatterers, why we need to consider multiple scattering to examine the backscattering phenomenon and how we can discriminate the backscattering enhancement from the specular enhancement.

Keywords: Backscattering Enhancement Phenomenon, Point Scatterers, Monte Carlo Simulation, Single Scattering, Multiple Scattering.

ÖZ

RASGELE DAĞITILMIŞ NOKTASAL SAÇICILARINDAN GERİ SAÇILIM ARTIRILMASI OLGUSUNUN İRDELENMESİ VE SİMÜLASYONU

AĞAR, Kartal Şahin
Yüksek Lisans, Elektrik ve Elektronik Mühendisliği
Tez Yöneticisi: Doç. Dr. Seyit Sencer KOÇ

Ağustos 2007, 122 sayfa

Bu çalışma, rasgele dağıtılmış noktasal saçıcılar üzerinden geri saçılım artırılması olgusunun irdelenmesini ve simülasyonunu araştırmıştır. Bu noktasal saçıcılar bir küpün veya bir kürenin içerisine rasgele dağıtıldıktan sonra hem kübik hem de küresel dağılımlar üzerinden geri saçılım artırılması olgusu çalışmanın başından sonuna kadar incelenmiştir. Kübik ve küresel dağılımların saçılım olgusu hususundaki genel karakteristik farkları gözlemlenmiştir. T-matris metodu geri saçılım artırılması olgusunun analitik araştırması için kullanılmış ve ayrıca birtakım yaklaşık formüller elde edilmiştir. Monte Carlo simülasyon metodu ise geri saçılım artırılması olgusunun simülasyon araştırması için kullanılmıştır. Bazı Monte Carlo simülasyonları MATLAB programlama dili kullanılarak hazırlanmış ve güven aralıkları gösterilerek doğruluğu kanıtlanmıştır. Tekli ve çiftli saçılımda oluşan geri saçılım artırılması olgusunun hem irdelenmesi hem de simülasyonunu araştırılmıştır; ancak, hesaplama karmaşıklığı nedeniyle çoklu saçılımda oluşan geri saçılım artırılması olgusu sadece simülasyonlarla incelenmiştir. Bu çalışma, rasgele dağıtılmış noktasal saçıcılar üzerinden oluşan tekli saçılım ile çoklu saçılım arasındaki farkları araştırmıştır. Hem gelen sinyalin frekansının hem de noktasal saçıcı yoğunluğunun geri saçılım artırımı üzerindeki etkilerine işaret edilmiştir. Bu çalışmada, hangi koşullar altında rasgele dağılmış noktasal saçıcılar üzerinden geri

saçılım artırımı olgusunun oluştuğu, neden geri saçılım artırımı olgusunu incelemek için çoklu saçılımı hesaba katma ihtiyacı duyulduğu ve geri saçılım artırımının aynasal saçılım artırımından nasıl ayırt edilebileceği gibi sorular yanıtlanmaya çalışılmıştır.

Anahtar Kelimeler: Geri Saçılım Artırılması Olayı, Noktasal Saçıcılar, Monte Carlo Simülasyonu, Tekli Saçılım, Çoklu Saçılım.

ACKNOWLEDGMENTS

I would certainly like to express my deepest gratitude to my supervisor Assoc. Prof. Dr. Seyit Sencer KOÇ for his guidance, advice, criticism, encouragements and insight throughout the research.

I would also like to give heartfelt thanks to my parents for their moral support and encouragement.

TABLE OF CONTENTS

LIST OF TABLES

TABLES

LIST OF FIGURES

FIGURES

LIST OF SYMBOLS

T : T-matrix

ψ_{inc} : Incident Field

ψ_{sca} : Scatted Field

$\psi(\vec{r}_a)$: Total Field at observation point $\left[\psi(\vec{r}_a) = \psi_{inc}(\vec{r}_a) + \psi_{sca}(\vec{r}_a)\right]$

j_n : Spherical Bessel Function of First Kind

$h_n^{(1)}$: Spherical Hankel Function of First Kind

$h_n^{(2)}$: Spherical Hankel Function of Second Kind

k : Wave Number

$\vec{k}_i$: Incident Wave Vector

$\vec{k}_s$: Scattered Wave Vector

$Y(\theta, \vartheta)$: Surface Harmonics

$\vec{r}_n$: A position vector of n th scatterer

$\vec{r}_a$: A position vector of the observation point

$\vec{r}_s$: A vector from a scatterer to the observation point

G^0 : Free-Space Green's Function

f : A Constant which is $\left[i4\pi T\right]/k$

$\phi(\vec{r}_n)$: Effective Field

G_n^a : A symbol which denotes scattering from n to a

$G_n^a G_m^n$: A symbol which denotes scattering from m to n and then from n to a

$G_n^a G_m^n G_v^m$: A symbol which denotes scattering from *v* to *m* and then from *m* to *n* and then from *n* to *a*

$\psi^{(1)}(\vec{r}_a)$: Single Scattered Field

$\psi^{(2)}(\vec{r}_a)$: Double Scattered Field

$\psi^{(2)^*}(\vec{r}_a)$: Conjugate of the Double Scattered Field

$I_{sca}(\vec{r})$: Scattered Field Intensity

I_{11} : Field Intensity due to single scattering

I_{22} : Field Intensity due to double scattering

I_{12} : Field Intensity due to interaction of single and double scattering

$< I_{sca} >$: Total scattered mean field intensity

$p(\vec{r}_n, \vec{r}_{n'})$: Probability Density Function

θ_s : Scattering Angle which is between incident field and scattered field

MC : Run number of Monte Carlo simulation

E : Expected Variable

$Var(.)$: Variance

$Std(.)$: Standard Deviation

CI : Confidence Interval

z : *z*-score (standardized score) for the particular confidence interval

$\left|J(\vec{r}_1, \vec{r}_2)\right|$: Absolute value of the Jacobian

$\vec{\sigma}$: Sum of the incident and scattered wave vectors $\left[\vec{\sigma} = \vec{k}_i + \vec{k}_s = 2k\sin(\theta_s/2)\hat{\sigma}\right]$

$\vec{\delta}$: Subtraction of the incident and scattered wave vectors $\left[\vec{\delta} = \vec{k}_i - \vec{k}_s = 2k\cos(\theta_s/2)\hat{\delta}\right]$

δ_{nm} : Kronecker Delta

α_{11} : Ensemble average of $e^{i\left[(\vec{k}_i-\vec{k}_s).(\vec{r}_n-\vec{r}_{n'})\right]}$ which is single scattering expression

$\alpha_{22}^{(c)}$: Ensemble average of $\sum_{n=1}^{N}\sum_{\substack{m=1\\m\neq n}}^{N}\sum_{n'=1}^{N}\sum_{\substack{m'=1\\m'\neq n'}}^{N} e^{i\vec{k}_s.(\vec{r}_{n'}-\vec{r}_n)} e^{i\vec{k}_i.(\vec{r}_m-\vec{r}_{m'})} \frac{e^{ik|\vec{r}_n-\vec{r}_m|}}{|\vec{r}_n-\vec{r}_m|}\frac{e^{-ik|\vec{r}_{n'}-\vec{r}_{m'}|}}{|\vec{r}_{n'}-\vec{r}_{m'}|}$ which is double scattering expression for all cases

$\alpha_{22}^{(1)}$: Ensemble average of $\frac{1}{|\vec{r}_n-\vec{r}_m|^2}$ which is double scattering expression for case 1

$\alpha_{22}^{(2)}$: Ensemble average of $\frac{e^{i(\vec{k}_i+\vec{k}_s).(\vec{r}_m-\vec{r}_n)}}{|\vec{r}_m-\vec{r}_n|^2}$ which is double scattering expression for case 2

$\alpha_{22}^{(3)}$: Ensemble average of $\frac{e^{i\vec{k}_i.(\vec{r}_m-\vec{r}_{m'})}e^{ik|\vec{r}_m-\vec{r}_n|}e^{-ik|\vec{r}_{m'}-\vec{r}_n|}}{|\vec{r}_m-\vec{r}_n||\vec{r}_{m'}-\vec{r}_n|}$ which is double scattering expression for case 3

$\alpha_{22}^{(4)}$: Ensemble average of $e^{i\vec{k}_s.(\vec{r}_m-\vec{r}_n)}e^{i\vec{k}_i.(\vec{r}_m-\vec{r}_{m'})}\frac{e^{ik|\vec{r}_m-\vec{r}_n|}}{|\vec{r}_m-\vec{r}_n|}\frac{e^{-ik|\vec{r}_{m'}-\vec{r}_m|}}{|\vec{r}_{m'}-\vec{r}_m|}$ which is double scattering expression for case 4

$\alpha_{22}^{(5)}$: Ensemble average of $e^{i\vec{k}_s.(\vec{r}_{n'}-\vec{r}_n)}\frac{e^{ik|\vec{r}_m-\vec{r}_n|}}{|\vec{r}_m-\vec{r}_n|}\frac{e^{-ik|\vec{r}_m-\vec{r}_{n'}|}}{|\vec{r}_m-\vec{r}_{n'}|}$ which is double scattering expression for case 5

$\alpha_{22}^{(6)}$: Ensemble average of $e^{i\vec{k}_s.(\vec{r}_{n'}-\vec{r}_n)}e^{i\vec{k}_i.(\vec{r}_m-\vec{r}_n)}\frac{e^{ik|\vec{r}_m-\vec{r}_n|}}{|\vec{r}_m-\vec{r}_n|}\frac{e^{-ik|\vec{r}_n-\vec{r}_{n'}|}}{|\vec{r}_n-\vec{r}_{n'}|}$ which is double scattering expression for case 6

$\alpha_{22}^{(7)}$: Ensemble average of $e^{i\vec{k}_s.(\vec{r}_{n'}-\vec{r}_n)}e^{i\vec{k}_i.(\vec{r}_m-\vec{r}_{m'})}\frac{e^{ik|\vec{r}_m-\vec{r}_n|}}{|\vec{r}_m-\vec{r}_n|}\frac{e^{-ik|\vec{r}_{m'}-\vec{r}_{n'}|}}{|\vec{r}_{m'}-\vec{r}_{n'}|}$ which is double scattering expression for case 7

$\alpha_{12}^{(c)}$: Ensemble average of $\sum_{n=1}^{N}\sum_{n'=1}^{N}\sum_{\substack{m'=1\\m'\neq n'}}^{N}\frac{e^{-ik|\vec{r}_{n'}-\vec{r}_{m'}|}}{|\vec{r}_{n'}-\vec{r}_{m'}|}e^{-i\vec{k}_s.(\vec{r}_n-\vec{r}_{n'})}e^{i\vec{k}_i.(\vec{r}_n-\vec{r}_{m'})}$ which is interaction of single and double scattering expression for all cases

$\alpha_{12}^{(1)}$: Ensemble average of $\frac{e^{-ik|\vec{r}_n-\vec{r}_{n'}|}}{|\vec{r}_n-\vec{r}_{n'}|}e^{-i\vec{k}_s.(\vec{r}_n-\vec{r}_{n'})}$ which is interaction of single and double scattering expression for case 1

$\alpha_{12}^{(2)}$: Ensemble average of $\frac{e^{-ik|\vec{r}_{m'}-\vec{r}_n|}}{|\vec{r}_{m'}-\vec{r}_n|}e^{i\vec{k}_i.(\vec{r}_n-\vec{r}_{m'})}$ which is interaction of single and double scattering expression for case 2

$\alpha_{12}^{(3)}$: Ensemble average of $\frac{e^{-ik|\vec{r}_{m'}-\vec{r}_{n'}|}}{|\vec{r}_{m'}-\vec{r}_{n'}|}e^{-i\vec{k}_s.(\vec{r}_n-\vec{r}_{n'})}e^{i\vec{k}_i.(\vec{r}_n-\vec{r}_{m'})}$ which is interaction of single and double scattering expression for case 3

CHAPTER 1

INTRODUCTION

The scattered field is clearly determined as the field radiated in space from obstacles which are illuminated by an incident electromagnetic field. In this thesis, these obstacles are considered as randomly distributed point scatterers and the incident field is assumed as a plane wave for simplicity. Backscattered field basically represents the field scattered back towards the direction of the incident field. If these scattered fields are constructively interfered in the backscattering direction, this special phenomenon is called as the backscattering enhancement. This phenomenon has been one of the important subjects for radar engineering, remote sensing, astronomy and bioengineering. The backscattering enhancement has been investigated mostly from an academic point of view, [13].

The only source of information about the properties of randomly distributed point scatterers is the intensity and polarization of their scattered field which is measured remotely and this scattered field is also a function of incident field frequency and the overall shape of distribution. In order to obtain the approximate size, composition, shape and structure of this distribution from critical data about the scattered field, one has to gradually resolve the inverse problem using simple structures as model scatterers which are considered as both cubical and spherical distributions of the point scatterers throughout this thesis, [9]. This inverse problem is the event of defining the characteristics of randomly distributed point scatterers from measurement of radiation. Therefore, we reasonably investigate the backscattering enhancement phenomenon from randomly distributed point scatterers in this study.

The single scattering is defined as an external radiation that is scattered only one times from randomly distributed point scatterers. As for the multiple scattering, it is

defined as an external radiation that arises due to the scattering of an incident field after interaction with more than one randomly distributed point scatterers. When an electromagnetic incident field interacts with randomly distributed point scatterers in a cubical or spherical volume medium, some of the scattered fields interfere constructively to a higher level. To aid remotely-sensed data analysis, a model may be used to simulate the interactions between randomly distributed point scatterers and the radiant energy. Usually, such models include only single scattering. In reality, multiple scattering has important contribution in intensity of the backscattering enhancement, [11]. This contribution of the multiple scattering is shown in this thesis and also analytic studies of both single and multiple scattering phenomena are presented in more detail in Chapter 2.

Theoretical and experimental studies of multiple scattering from randomly distributed point scatterers have a large scientific interest in academic research as well as in the industry. Although the multiple scattering theory has been investigated since the end of 1960s, the complexity of the calculation has limited the range of applications, [12].

We describe a rather simple approach for separating not only single scattering but also double scattering from the total intensity of multiple scattering. We consider the situation in which the scattering orders can be separated, which gives additional information about the scattering medium, [10]. The double scattering is the first multiple scattering mechanism in the distribution volume and we illustrate that it has the dominant effect on the backscattering enhancement. The double order scattering from spherical distribution is presented and an approximate formula of the mean field intensity due to double scattering is obtained in Chapter 3. The Monte Carlo simulation technique for studying scattering from randomly distributed point scatterers is employed. The reliability of the data obtained due to single scattering has been checked by comparing the results of the computer simulation with analytical calculations in Chapter 4. It has been shown that the significant contribution of multiple scattering can vary by an order of magnitude, [10].

Statistics is necessary in order to gather relevant information from results of experiments and the probability theory is used to estimate results of experiments. Therefore, a certain number of errors are involved whenever an experiment is run. Confidence intervals definitely give us an estimated amount of error involved in result data of our experiments. They tell us about the accuracy of the statistical estimates, [6]. In this study, we have computed the 95% confidence interval for the MC simulation due to both single scattering and multiple scattering in Chapter 4 so that the accuracy of our simulation results can be verified.

Multiple scattering of a field is commonly encountered when the density of randomly distribution point scatterers is large enough, so that an incident field interacts with more than one point scatterer in the medium before leaving it, [8]. This phenomenon is important for a number of applications: For example, Military Area (remote sensing, underwater vision and acoustic), Industrial Area (design of efficient headlamps for foggy driving), Biomedical Optics Area (imaging of small tumors in opaque tissues), Astronomy Area (discovering of quasars) and Simulation Systems for Training Area, [29]. Effects of the point scatterer density on the backscattering enhancement are discussed in Chapter 4. A classical method for simulating multiple scattering is the Monte Carlo technique. This type of program is able to simulate a complex process as a rapid succession of elementary events for which probabilities are known. Therefore, each event is governed by a random number, [8]. Calculation of the multiple scattering is too complex; hence, its consistent calculation costs too much CPU time and memory allocation. Solution of the multiple scattering processes becomes too complicated after the density of randomly distributed point scatterers becomes higher. However, research of multiple scattering is growing because of the modern computer age. This thesis calculates the mean field intensity due to multiple scattering by using Monte Carlo simulation technique in Chapter 4.

Since the enhancement effect occurs in the backscattering direction, the angular width of the backscattering enhancement effect becomes a critical issue. Because, when the angular width is too small relative to the beam width of the receiving antenna, the backscattering enhancement effect is not to be observed, [7]. The

determination of backscattering enhancement angle width is of great significance. For example, in measuring scattering coefficients with a receiving antenna that has a certain beam width, it is necessary to know the enhancement angle width. The backscattering enhancement angle width is affected by the incident field frequency. If the frequency gets higher, the backscattering enhancement angle width gets narrower, [15]. Effect of the incident field frequency on the backscattering enhancement from randomly distributed point scatterers are illustrated in Chapter 4.

This thesis proves that the backscattering enhancement is observed due to multiple scattering; however, there is an enhancement from cubical distribution due to single scattering. This enhancement is defined as the specular enhancement not the backscattering enhancement. Because of the cubical structure, the surface of the cubical distributed point scatterers is flat. If a surface is flat, the wave is scattered in the specular direction, which situation corresponds to Snell's law, [14]. This type of enhancement is illustrated in Chapter 4.

Briefly, this study includes analytic studies of the backscattering enhancement from randomly distributed point scatterers illustrated in Chapter 3 and it also includes simulated studies of the backscattering enhancement from randomly distributed point scatterers presented in Chapter 4. The backscattering enhancement has been analyzed for two different geometries, namely spherical distribution and cubical distribution throughout this study.

CHAPTER 2

THE POINT SCATTERERS

2.1 Single Scattering from Point Scatterers

In this thesis, the transition matrix method (or T-matrix method) is used to calculate the scattered field. The transition matrix (or T-matrix) depends only on the particle, its structural composition, size, shape, and orientation and also T-matrix is independent of the incident field. This means that for any particular particle, the T-matrix only needs to be calculated once, and then it can be used for repeated calculations. This is a significant advantage over many other methods which are widely utilized for calculating scattering where the entire calculation needs to be repeated, [2]. Throughout the thesis, we use point scatterers as scatterers whose radii are nearly zero. Therefore, we need to use the T-matrix for a point scatterer. T-matrix of a point scatterer consists of only one element which is nm=00 and all other elements are zero. This means that the value of T-matrix for a point scatterer is $T_{00} = T$ and later we are to assume that T is equal to 1 for a point scatterer. Let us write the incident and the scattered fields in terms of a spherical harmonic expansion as follows:

$$\left.\begin{aligned} \psi_{inc} &= \sum_{nm} a_{nm} j_n(kr_s) Y_{nm}(\theta,\vartheta) \\ \psi_{sca} &= \sum_{nm} b_{nm} h_n^{(1)}(kr_s) Y_{nm}(\theta,\vartheta) \end{aligned}\right\} \tag{2.1}$$

where $Y_{nm}(\theta,\vartheta)$ are the surface harmonics, a_{nm} are the coefficients for the incident field and b_{nm} are the coefficients for the scattered field. $\vec{r}_s$ is a vector from the scatterer to the observation point. The position vector of a point scatterer $\vec{r}_n$ and the position vector of the observation point $\vec{r}_a$ are shown in Figure 2.1.

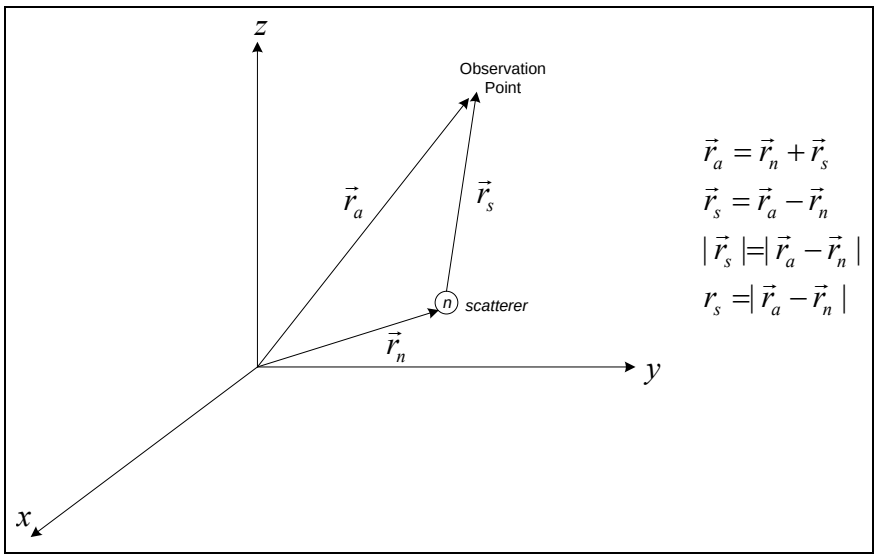

Figure 2.1: Scattering from a single point scatterer and the position vectors.

In Eq. (2.1), $j_n(kr_s)$ is the spherical Bessel function of the first kind of order *n* and $h_n^{(1)}(kr_s)$ is the spherical Hankel function of the first kind of order *n*. Note that the spherical Hankel functions are linear combinations of the spherical Bessel function of the first kind and the spherical Bessel function of the second kind as follows:

$$\left.\begin{aligned} h_n^{(1)}(x) &= j_n(x) + iy_n(x) \\ h_n^{(2)}(x) &= j_n(x) - iy_n(x) \end{aligned}\right\} \tag{2.2}$$

The scattered field coefficients b_{nm} and the incident field coefficients a_{nm} are related by means of a T-matrix as follows:

$$b_{nm} = T_{nm} a_{nm} \tag{2.3}$$

Since a point scatterer has a T-matrix which is defined as $T_{nm} = 0$ for $n \neq 0$, we can consider only *nm*=00 value. The scattered field at the observation point (see Figure 2.1) from only one point scatterer consists of a single term of the scattered field summation which is given in Eq. (2.1). This single term can be written as

$$\psi_{sca}(\vec{r}_a) = b_{00} h_0^{(1)}(kr_s) Y_{00} \tag{2.4}$$

We can insert $b_{00} = T_{00} a_{00}$ into Eq. (2.4) to get

$$\psi_{sca}(\vec{r}_a) = T_{00} a_{00} h_0^{(1)}(kr_s) Y_{00} \tag{2.5}$$

The scattered field from a point scatterer (in the far-field) can be found by using the expression of the spherical Hankel function of first kind of order 0 which is

$$\boxed{\begin{aligned} h_0^{(1)}(x) &= -i\frac{e^{ix}}{x} \\ h_0^{(1)}(kr_s) &= -i\frac{e^{ikr_s}}{kr_s} \end{aligned}} \tag{2.6}$$

and we get

$$\psi_{sca}(\vec{r}_a) = -i\frac{e^{ikr_s}}{kr_s} T_{00} a_{00} Y_{00} \tag{2.7}$$

The scattered field is related to the incident field at the location of the point scatterer. Therefore, we need to calculate $\psi_{inc}(\vec{r}_s = 0)$ or $\psi_{inc}(\vec{r}_n)$ by using the incident field written in Eq. (2.1). Thus, the incident field for a single point scatterer is written as

$$\begin{aligned} \psi_{inc}(\vec{r}_s) &= a_{00} j_0(kr_s) Y_{00} \\ \psi_{inc}(\vec{r}_n) = \psi_{inc}(\vec{r}_s = 0) &= a_{00} j_0(0) Y_{00} \qquad ; j_0(0) = 1 \\ \psi_{inc}(\vec{r}_n) &= a_{00} Y_{00} \end{aligned} \tag{2.8}$$

Substituting $a_{00} = \psi_{inc}(\vec{r}_n)/Y_{00}$ and $T_{00} = T$ into Eq. (2.7), we get

$$\psi_{sca}(\vec{r}_a) = -i\frac{e^{ikr_s}}{kr_s} T \psi_{inc}(\vec{r}_n) \tag{2.9}$$

where $\vec{r}_s$ is a vector from the scatterer to the observation point (see Figure 2.1) and its amplitude is written as $|\vec{r}_s| = |\vec{r}_a - \vec{r}_n|$ or $r_s = |\vec{r}_a - \vec{r}_n|$. The scattered field at the observation point (see Figure 2.1) can be expressed as

$$\begin{aligned} \psi_{sca}(\vec{r}_a) &= \frac{-ie^{ik|\vec{r}_a - \vec{r}_n|}}{k|\vec{r}_a - \vec{r}_n|} T \psi_{inc}(\vec{r}_n) \\ \psi_{sca}(\vec{r}_a) &= \frac{i4\pi T}{k} \frac{-e^{ik|\vec{r}_a - \vec{r}_n|}}{4\pi|\vec{r}_a - \vec{r}_n|} \psi_{inc}(\vec{r}_n) \end{aligned} \tag{2.10}$$

Using the free-space Green's function as $G^0(\vec{r}_a,\vec{r}_n) = -e^{ik|\vec{r}_a-\vec{r}_n|}/\left(4\pi\,|\,\vec{r}_a-\vec{r}_n\,|\right)$ and defining the constant f as $i4\pi T/k$, the scattered field can be written as

$$\psi_{sca}(\vec{r}_a) = fG^0(\vec{r}_a,\vec{r}_n)\psi_{inc}(\vec{r}_n) \tag{2.11}$$

where $\vec{r}_n$ and $\vec{r}_a$ denote the position vector of the point scatterer and the position vector of the observation point, respectively. For simplicity, we can use a symbol $G_n^a = fG^0(\vec{r}_a,\vec{r}_n)$ which denotes scattering from the scatterer at $\vec{r}_n$ to the observation point at $\vec{r}_a$. Finally, the scattered field at the observation point becomes

$$\boxed{\psi_{sca}(\vec{r}_a) = G_n^a\psi_{inc}(\vec{r}_n)} \tag{2.12}$$

Note that the single scattering phenomenon can be defined as the radiation which is scattered only one times from randomly distributed point scatterers so above defined scattered field can also be called as the single scattered field.

2.2 Multiple Scattering from Point Scatterers

Consider a distribution of N point scatterers located at $\vec{r}_1,\vec{r}_2,...\vec{r}_n...,\vec{r}_N$, which is depicted in Figure 2.2. Define the wave $\phi(\vec{r}_n)$ incident upon the scatterer at $\vec{r}_n$ as the "effective field". The effective field $\phi(\vec{r}_n)$ consists of the incident wave $\psi_{inc}(\vec{r}_n)$ and the wave scattered from all the particles except the one at $\vec{r}_n$. The effective field is stated as

$$\phi(\vec{r}_n) = \psi_{inc}(\vec{r}_n) + \psi_{sca}(\vec{r}_1) + ... + \psi_{sca}(\vec{r}_{n-1}) + \psi_{sca}(\vec{r}_{n+1}) + ... + \psi_{sca}(\vec{r}_N) \tag{2.13}$$

which may be written as

$$\phi(\vec{r}_n) = \psi_{inc}(\vec{r}_n) + \sum_{\substack{t=1 \\ t\neq n}}^{N}\psi_{sca}(\vec{r}_t) \tag{2.14}$$

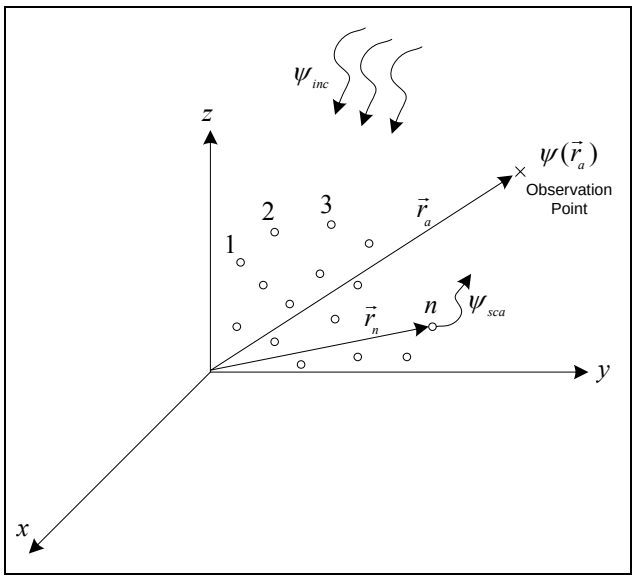

Figure 2.2: A distribution of N point scatterers.

Substituting the scattered field $\psi_{sca}(\vec{r}_t)$ defined by $fG^0(\vec{r}_n,\vec{r}_t)\phi(\vec{r}_t)$ into Eq. (2.14), we have

$$\phi(\vec{r}_n) = \psi_{inc}(\vec{r}_n) + \sum_{\substack{t=1 \\ t\neq n}}^{N} fG^0(\vec{r}_n,\vec{r}_t)\phi(\vec{r}_t) \tag{2.15}$$

If the effective field $\phi(\vec{r}_n)$ is known at all locations of the scatterers, the total field $\psi(\vec{r}_a) = \psi_{inc}(\vec{r}_a) + \psi_{sca}(\vec{r}_a)$ at any observation point $\vec{r}_a$ can be written as

$$\boxed{\psi(\vec{r}_a) = \psi_{inc}(\vec{r}_a) + \sum_{n=1}^{N} fG^0(\vec{r}_a,\vec{r}_n)\phi(\vec{r}_n)} \tag{2.16}$$

We note that the effective field $\phi(\vec{r}_n)$ can be eliminated from Eqs. (2.15) and (2.16) and then a simple solution to the field at any observation point $\psi(\vec{r}_a)$ can be acquired.

In Eq. (2.15), we have N unknowns which are the effective field at positions of the scatterers, i.e. $\phi(\vec{r}_n)$ $;n = 1,2,...,N$. The effective field $\phi(\vec{r}_n)$ can be written for any n=1,2,…,N ; thus, Eq. (2.15) defines N equations in the N unknowns, which are the

effective fields at the exact location of the *N* scatterers. This equation can be written in matrix form as follows:

$$\begin{aligned} \bar{\phi} &= \bar{\psi}_{inc} + \bar{\bar{G}}\bar{\phi} \\ \bar{\phi} - \bar{\bar{G}}\bar{\phi} &= \bar{\psi}_{inc} \\ (1 - \bar{\bar{G}})\bar{\phi} &= \bar{\psi}_{inc} \\ (\bar{I} - \bar{\bar{G}})\bar{\phi} &= \bar{\psi}_{inc} \end{aligned} \tag{2.17}$$

Note that the symbol $\bar{\bar{G}}$ is the Green's function matrix which consists of elements depending on both $\vec{r}_n$ and $\vec{r}_t$, $\bar{\phi}$ is the effective field vector which consists of elements depending on $\vec{r}_n$, and $\bar{\psi}_{inc}$ is the incident field vector which consists of elements depending on $\vec{r}_n$. If we write Eq. (2.17) as follows:

$$\bar{\phi} = \left[\bar{I} - \bar{\bar{G}}\right]^{-1} \bar{\psi}_{inc} \tag{2.18}$$

The effective field vector $\bar{\phi}$ can be calculated from matrix multiplication of the inverse matrix $\left[\bar{I} - \bar{\bar{G}}\right]^{-1}$ with the incident field vector $\bar{\psi}_{inc}$.

The elements of the Green's matrix are given by

$$\left[\bar{\bar{G}}\right]_{mn} = fG^0(\vec{r}_n, \vec{r}_m)[1 - \delta_{nm}] \tag{2.19}$$

where δ_{nm} is the Kronecker delta. We first write the below serial expansion:

$$\frac{1}{1-x} = [1-x]^{-1} = 1 + x + x^2 + x^3 + \ldots \qquad ;\text{for } -1 < x < 1 \tag{2.20}$$

If we write $\left[\bar{I} - \bar{\bar{G}}\right]^{-1}$ in the same manner:

$$\left[\bar{I} - \bar{\bar{G}}\right]^{-1} = 1 + \bar{\bar{G}} + \bar{\bar{G}}^2 + \bar{\bar{G}}^3 \ldots = \sum_{t=0}^{\infty} \bar{\bar{G}}^t \tag{2.21}$$

Thus, the solution to Eq. (2.18) is:

$$\bar{\phi} = \left[\bar{I} - \bar{\bar{G}}\right]^{-1} \bar{\psi}_{inc} = \sum_{t=0}^{\infty} \bar{\bar{G}}^t \bar{\psi}_{inc} \tag{2.22}$$

$$\overline{\phi} = \sum_{t=0}^{\infty} \overline{\overline{G}}^{t} \overline{\psi}_{inc} = \overline{\psi}_{inc} + \overline{\overline{G}}\,\overline{\psi}_{inc} + \overline{\overline{G}}^{2}\overline{\psi}_{inc} + \ldots \tag{2.23}$$

The total field at the observation point $\vec{r}_a$ is $\psi(\vec{r}_a) = \psi_{inc}(\vec{r}_a) + \psi_{sca}(\vec{r}_a)$:

$$\psi(\vec{r}_a) = \psi_{inc}(\vec{r}_a) + \sum_{n=1}^{N} fG^0(\vec{r}_a - \vec{r}_n)\phi(\vec{r}_n) \tag{2.24}$$

We insert Eq. (2.22) into Eq. (2.24) and get

$$\psi(\vec{r}_a) = \psi_{inc}(\vec{r}_a) + \sum_{n=1}^{N} fG^0(\vec{r}_a - \vec{r}_n)\left\{\sum_{t=0}^{\infty} \overline{\overline{G}}^{t} \overline{\psi}_{inc}\right\}_n \tag{2.25}$$

We can use shorthand symbols ψ^a to denote the total field at the observation point $\vec{r}_a$ and ψ^a_{inc} to denote the incident field at the observation point $\vec{r}_a$ (see Figure 2.2). A solution to the total field at the observation point ψ^a can be done by iterating, this process is defined in the following manner:

$$\psi^a = \psi^a_{inc} + \sum_{n=1}^{N} G^a_n \left\{ \psi^n_{inc} + \sum_{\substack{m=1 \\ m\neq n}}^{N} G^n_m \psi^m_{inc} + \sum_{\substack{m=1 \\ m\neq n}}^{N} G^n_m \left(\sum_{\substack{v=1 \\ v\neq m}}^{N} G^m_v \psi^v_{inc} \right) + \ldots \right\} \tag{2.26}$$

We obtain the total field at the observation point ψ^a:

$$\psi^a = \underbrace{\psi^a_{inc}}_{\substack{incident \\ field}} + \underbrace{\sum_{n=1}^{N} G^a_n \psi^n_{inc}}_{\substack{\text{sin}gle \\ scattering}} + \underbrace{\sum_{n=1}^{N}\sum_{\substack{m=1 \\ m\neq n}}^{N} G^a_n G^n_m \psi^m_{inc}}_{\substack{double \\ scattering}} + \underbrace{\sum_{n=1}^{N}\sum_{\substack{m=1 \\ m\neq n}}^{N}\sum_{\substack{v=1 \\ v\neq m}}^{N} G^a_n G^n_m G^m_v \psi^v_{inc} + \ldots.}_{\substack{triple \\ scattering}} \tag{2.27}$$

In this study, the symbols $G^a_n = fG^0(\vec{r}_a, \vec{r}_n)$, $G^a_n G^n_m = fG^0(\vec{r}_a, \vec{r}_n) fG^0(\vec{r}_n, \vec{r}_m)$ and $G^a_n G^n_m G^m_v = fG^0(\vec{r}_a, \vec{r}_n) fG^0(\vec{r}_n, \vec{r}_m) fG^0(\vec{r}_m, \vec{r}_v)$ are used for shorthand.

Note that the multiple scattering phenomenon can be clearly defined as the radiation which is scattered many times from randomly distributed point scatterers so above defined the total field except the incident field ψ^a_{inc} is called as the total scattered field or the multiple scattered field and it is given by

$$\psi_{sca}^{a} = \underbrace{\sum_{n=1}^{N} G_n^a \psi_{inc}^n}_{\substack{\text{sin}\,gle \\ scattering}} + \underbrace{\sum_{n=1}^{N}\sum_{\substack{m=1 \\ m\neq n}}^{N} G_n^a G_m^n \psi_{inc}^m}_{\substack{double \\ scattering}} + \underbrace{\sum_{n=1}^{N}\sum_{\substack{m=1 \\ m\neq n}}^{N}\sum_{\substack{v=1 \\ v\neq m}}^{N} G_n^a G_m^n G_v^m \psi_{inc}^v + ...}_{\substack{triple \\ scattering}} \tag{2.28}$$

which is the multiple scattered field at the observation point ψ_{sca}^{a} :

Note also that the term $G_n^a G_m^n$ describes scattering of the incident field from the point scatterer *m* to the point scatterer *n* and then from the point scatterer *n* to the observation point $\vec{r}_a$, hence a double scattering term. Similarly, $G_n^a G_m^n G_v^m$ describes scattering of the incident field first by the point scatterer *v* to the point scatterer *m* and then from the point scatterer *m* to the point scatterer *n* and finally from the point scatterer *n* to the observation point $\vec{r}_a$, hence a triple scattering term. These scattering processes are shown in Figure 2.3.

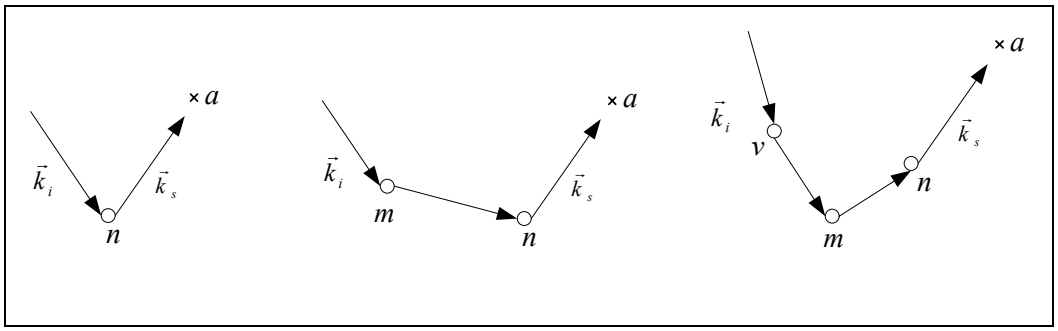

Figure 2.3: (a) The single scattering phenomenon. (b) The double scattering phenomenon. (c) The triple scattering phenomenon.

CHAPTER 3

ANALYTIC INVESTIGATION OF THE BACKSCATTERING ENHANCEMENT FROM RANDOMLY DISTRIBUTED POINT SCATTERERS

This Chapter thoroughly includes analytic studies of the backscattering enhancement from randomly distributed point scatterers. We begin this analysis by considering some terms of the total field at the observation point. These terms are given by Eq. (2.27). The first term of this summation is the incident field. The second term represents all the singly scattered fields denoted by $\psi_{sca}^{(1)}$. The third summation accounts for all the doubly scattered fields denoted by $\psi_{sca}^{(2)}$. The fourth summation accounts for all the triple scattering denoted by $\psi_{sca}^{(3)}$ and so on, [1]. If we consider only the scattered fields at the observation point, except the incident field, the total scattered field at the observation point can be written as

$$\begin{aligned} \psi_{sca}(\vec{r}) &= \psi_{sca}^{(1)}(\vec{r}) + \psi_{sca}^{(2)}(\vec{r}) + \psi_{sca}^{(3)}(\vec{r}) + \ldots \\ \psi_{sca}(\vec{r}) &= \sum_{n=1}^{\infty} \psi_{sca}^{(n)}(\vec{r}) \end{aligned} \tag{3.1}$$

The total field intensity is obtained by multiplying the total scattered field $\psi_{sca}(\vec{r})$ and its conjugate $\psi_{sca}^{*}(\vec{r})$ and is given by

$$\boxed{I_{sca}(\vec{r}) = \psi_{sca}(\vec{r})\psi_{sca}^{*}(\vec{r})} \tag{3.2}$$

Using Eq. (3.1) to express $\psi_{sca}(\vec{r})\psi_{sca}^{*}(\vec{r})$, we get

$$I_{sca}(\vec{r}) = \sum_{n=1}^{\infty}\sum_{n'=1}^{\infty} \psi_{sca}^{(n)}(\vec{r})\psi_{sca}^{(n')^{*}}(\vec{r}) \tag{3.3}$$

Expanding the serial summations in Eq. (3.3), the total scattered field intensity (or the field intensity due to multiple scattering) is expressed as

$$I_{sca}(\vec{r}) = \underbrace{\psi^{(1)}\psi^{(1)^*}}_{I_{11}} + \underbrace{\left[\psi^{(1)}\psi^{(2)^*} + \psi^{(2)}\psi^{(1)^*}\right]}_{I_{12}} + \underbrace{\psi^{(2)}\psi^{(2)^*}}_{I_{22}} + \ldots \tag{3.4}$$

Using Eq. (3.4) the total scattered mean field intensity (or the mean field intensity due to multiple scattering) over all possible distributions of N particles can be obtained and is given by

$$\underbrace{< I_{sca} >}_{\substack{average\\ scattering\\ field}} = \underbrace{< I_{11} >}_{\substack{average\\ sin\,gle\\ scattering\\ field}} + \underbrace{< I_{12} >}_{\substack{average\\ int\,eraction\\ of\\ sin\,gle\&double\\ scattering\\ field}} + \underbrace{< I_{22} >}_{\substack{average\\ double\\ scattering\\ field}} \ldots . \tag{3.5}$$

where <..> denotes the ensemble average (or mean) over all possible distributions of N particles.

3.1 Mean Field Intensity due to Single Scattering Phenomenon

The single scattering phenomenon is shown in Figure 2.3 (a). The second term of Eq. (2.27) represents all the single scattering denoted by $\psi_{sca}^{(1)}$ and given by

$$\psi^{(1)}(\vec{r}_a) = \sum_{n=1}^{N} G_n^a \psi_{inc}(\vec{r}_n) \tag{3.6}$$

In the calculation, we assume that the incident wave is a plane wave:

$$\psi_{inc}(\vec{r}) = e^{i\vec{k}_i \cdot \vec{r}} \tag{3.7}$$

Substituting the Green's function $G_n^a = -f\left[e^{ik|\vec{r}_a - \vec{r}_n|} / \left(4\pi\,|\,\vec{r}_a - \vec{r}_n\,|\right)\right]$ and the incident field expression $\psi_{inc}(\vec{r}) = e^{i\vec{k}_i \cdot \vec{r}}$ into Eq. (3.6), we get

$$\psi^{(1)}(\vec{r}_a) = \sum_{n=1}^{N} -f\,\frac{e^{ik|\vec{r}_a - \vec{r}_n|}}{4\pi\,|\,\vec{r}_a - \vec{r}_n\,|} e^{i\vec{k}_i \cdot \vec{r}_n} \tag{3.8}$$

The mean field intensity due to single scattering can be written as

$$< I_{11} >=< \psi^{(1)}(\vec{r}_a)\psi^{(1)^*}(\vec{r}_a) > \tag{3.9}$$

Combining Eq. (3.8) and Eq. (3.9), we have

$$< I_{11} >=< \left[\sum_{n=1}^{N} - f \frac{e^{ik|\vec{r}_a - \vec{r}_n|}}{4\pi |\vec{r}_a - \vec{r}_n|} e^{i\vec{k}_i . \vec{r}_n} \right] \left[\sum_{n'=1}^{N} - f^* \frac{e^{-ik|\vec{r}_a - \vec{r}_{n'}|}}{4\pi |\vec{r}_a - \vec{r}_{n'}|} e^{-i\vec{k}_i . \vec{r}_{n'}} \right] > \tag{3.10}$$

where the variable n is used for $\psi^{(1)}(\vec{r}_a)$ and the variable n' is used for $\psi^{(1)^*}(\vec{r}_a)$. Also we note that $|\vec{r}_a - \vec{r}_n|$ approaches $|\vec{r}_a|$ in the far-field approximation.

$$< I_{11} >= \sum_{n=1}^{N} \sum_{n'=1}^{N} \frac{|f|^2}{(4\pi r_a)^2} < e^{i\left[(\vec{k}_i - \vec{k}_s).(\vec{r}_n - \vec{r}_{n'})\right]} > \tag{3.11}$$

$$< I_{11} >= \frac{|f|^2}{(4\pi r_a)^2} \sum_{n=1}^{N} \sum_{n'=1}^{N} < e^{i\left[(\vec{k}_i - \vec{k}_s).(\vec{r}_n - \vec{r}_{n'})\right]} > \tag{3.12}$$

where $\vec{k}_i = k\hat{r}_i$ is the incident wave vector and $\hat{r}_i$ is a unit vector in the direction from the source to the point scatterer and $\vec{k}_s = k\hat{r}_s$ is the scattered wave vector and $\hat{r}_s$ is a unit vector in the direction from the point scatterer to the observation point (see Figure 2.3 (a)). Lastly, the wave number is denoted by $k = 2\pi/\lambda$. Note that when the equality $\vec{r}_n = \vec{r}_{n'}$ occurs, the exponent term becomes zero and the expression of the mean field intensity due to single scattering $e^{i\left[(\vec{k}_i - \vec{k}_s).(\vec{r}_n - \vec{r}_{n'})\right]}$ becomes equal to one. This mentioned condition occurs *N* times in Eq. (3.12). We can insert *N* into that summation so that this condition ($\vec{r}_n = \vec{r}_{n'}$) can be detached from the summation and it is given by

$$< I_{11} >= \frac{|f|^2}{(4\pi r_a)^2} \left[N + \sum_{n=1}^{N} \sum_{\substack{n'=1 \\ n' \neq n}}^{N} \underbrace{< e^{i\left[(\vec{k}_i - \vec{k}_s).(\vec{r}_n - \vec{r}_{n'})\right]} >}_{\alpha_{11}} \right] \tag{3.13}$$

We can use shorthand symbol α_{11} to denote an ensemble average of $e^{i\left[(\vec{k}_i - \vec{k}_s).(\vec{r}_n - \vec{r}_{n'})\right]}$ which is single scattering expression and it is taken from Eq. (3.13) and given by

$$\alpha_{11} =< e^{i\left[(\vec{k}_i - \vec{k}_s).(\vec{r}_n - \vec{r}_{n'})\right]} > \tag{3.14}$$

From this point, we give some relevant information about the ensemble average (or mean) and the probability density function. We first write the ensemble average of a function *f* and explain how the ensemble average of this function can be calculated.

Let us state the ensemble average of *f* as

$$< f >= \iint..\int fp(\vec{r}_1,\vec{r}_2,...,\vec{r}_n,...,\vec{r}_N)d\vec{r}_1 d\vec{r}_2...d\vec{r}_n...d\vec{r}_N \tag{3.15}$$

where the ensemble average (or mean) is given in terms of a probability density function $p(\vec{r}_1,\vec{r}_2,...,\vec{r}_n,...,\vec{r}_N)$. Now we consider a case where the point scatterer density is low and the scatterer size is much smaller than the distances between scatterers. In this case, we can neglect the finite size of scatterers and we can assume that the location and characteristics of each scatterer are independent of the locations and characteristics of other scatterers. This means that all scatterers are considered as **point scatterers**, **[**1]. Under this assumption, we get

$$p(\vec{r}_1,\vec{r}_2,...,\vec{r}_n,...,\vec{r}_N) = p(\vec{r}_1)p(\vec{r}_2)p(\vec{r}_3)...p(\vec{r}_n)...p(\vec{r}_N) \tag{3.16}$$

This expression represents that probability density function of each point scatterers can be written in a separate way. Probability of finding the scatterer *n* within a volume $d\vec{r}_n$ is given by $p(\vec{r}_n)d\vec{r}_n$:

$$\begin{aligned} p(\vec{r}_n)d\vec{r}_n &= \frac{\text{number of scatterers within } d\vec{r}_n = dx_n dy_n dz_n}{\text{total number of scatterers in } V} \\ &= \frac{w(\vec{r}_n)d\vec{r}_n}{N} \end{aligned} \tag{3.17}$$

where $w(\vec{r}_n)$ is <u>the number density</u> or <u>the number of scatterers per unit volume</u>. Thus, we get

$$p(\vec{r}_n) = \frac{w(\vec{r}_n)}{N} \tag{3.18}$$

Note that if the number density $w(\vec{r}_n)$ is uniform throughout the volume *V*, then

$$w(\vec{r}_n) = \frac{N}{V} \;,\quad p(\vec{r}_n) = \frac{w(\vec{r}_n)}{N} \quad ==>\; p(\vec{r}_n) = \frac{1}{V} \tag{3.19}$$

The average is now given by

$$< f >= \iint .. \int f \frac{w(\vec{r}_1)w(\vec{r}_2)...w(\vec{r}_N)}{N^N} d\vec{r}_1 d\vec{r}_2 ... d\vec{r}_N \tag{3.20}$$

If f depends on the location of a single scatterer n, then writing $f(\vec{r}_n)$, we obtain

$$< f(\vec{r}_n) >= \int f(\vec{r}_n) \frac{w(\vec{r}_n)}{N} d\vec{r}_n \tag{3.21}$$

If f depends on the locations of two different scatterers m and n, then writing $f(\vec{r}_n, \vec{r}_m)$, we obtain

$$< f(\vec{r}_n, \vec{r}_m) >= \iint f(\vec{r}_n, \vec{r}_m) \frac{w(\vec{r}_n)w(\vec{r}_m)}{N^2} d\vec{r}_n d\vec{r}_m \tag{3.22}$$

After all of the above expressions about finding the ensemble average (or mean) of a function f, we can now calculate α_{11} by using these definitions. Therefore, the expression $e^{i\left[(\vec{k}_i - \vec{k}_s).(\vec{r}_n - \vec{r}_{n'})\right]}$ is to be multiplied with the probability density function $p(\vec{r}_n, \vec{r}_{n'})$ and then the following integral must be evaluated.

$$\alpha_{11} = \iint p(\vec{r}_n, \vec{r}_{n'}) e^{i\left[(\vec{k}_i - \vec{k}_s).(\vec{r}_n - \vec{r}_{n'})\right]} d\vec{r}_n d\vec{r}_{n'} \tag{3.23}$$

Since the scatterers are the point scatterers, it is assumed that their positions are independent, i.e., under this assumption, we have

$$p(\vec{r}_n, \vec{r}_{n'}) = p(\vec{r}_n) p(\vec{r}_{n'}) \tag{3.24}$$

and also that if the density $p(\vec{r}_n)$ is uniform throughout the total volume V, then

$$p(\vec{r}_n) = p(\vec{r}_{n'}) = \frac{1}{V} \tag{3.25}$$

$$p(\vec{r}_n, \vec{r}_{n'}) = p(\vec{r}_n) p(\vec{r}_{n'}) = \frac{1}{V^2} \tag{3.26}$$

Finally, substituting Eq. (3.26) into Eq. (3.23), we get the integral form of α_{11}:

$$\boxed{\alpha_{11} = \iint \frac{1}{V^2} e^{i\left[(\vec{k}_i - \vec{k}_s).(\vec{r}_n - \vec{r}_{n'})\right]} d\vec{r}_n d\vec{r}_{n'}} \tag{3.27}$$

3.1.1 The Particles are Distributed within a Cube

We next consider a scenario in which the particles are distributed uniformly within a cube whose dimension is $D=2d$, this scenario is depicted in Figure 3.1:

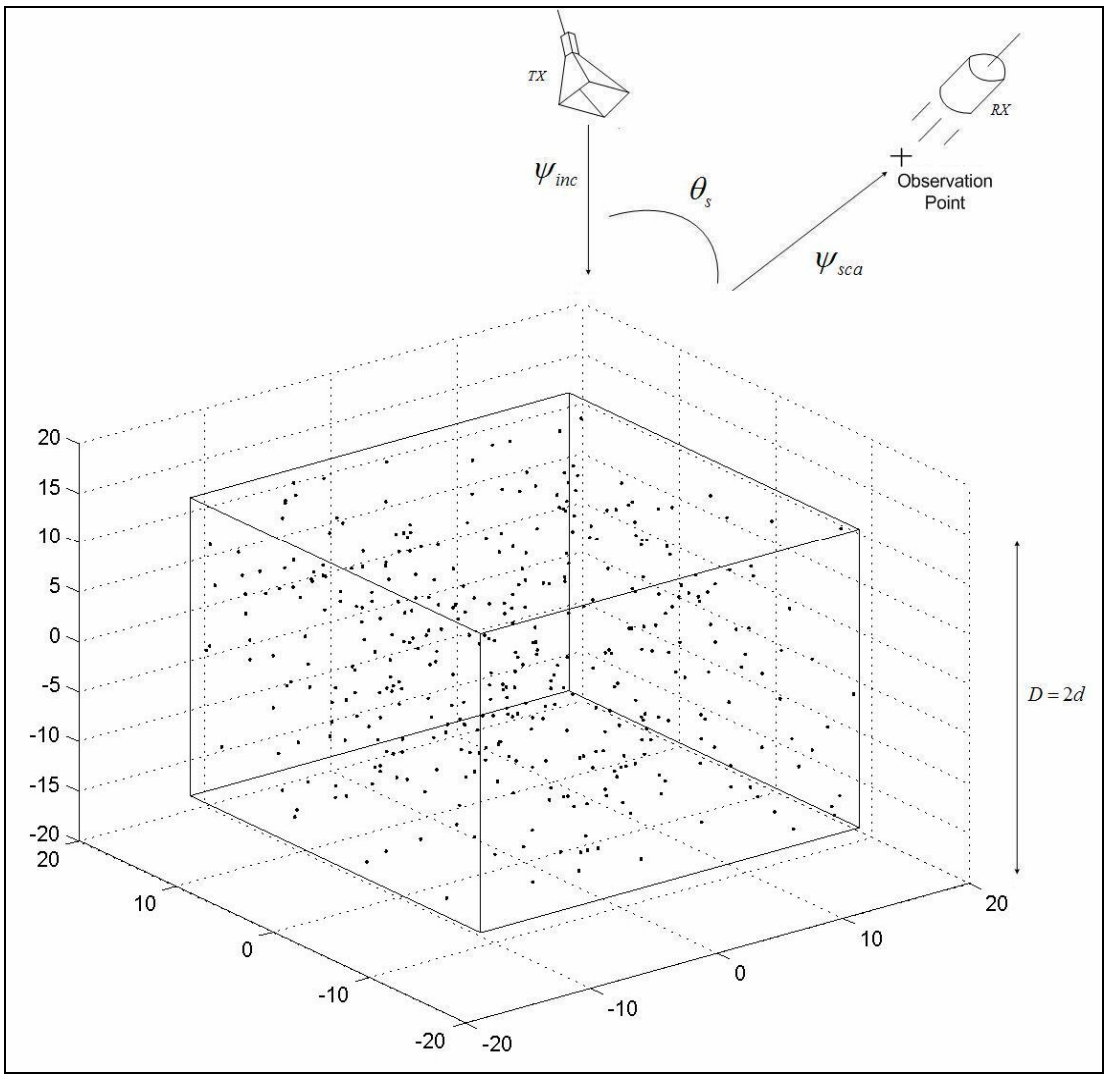

Figure 3.1: The particles are distributed within a cube whose dimension $D=2d$.

In order to understand the fundamentals of a scattering phenomenon let us consider just only one of these scatterers. The incident wave vector and the scattered wave vector of a single point scatterer are examined and depicted in Figure 3.2.

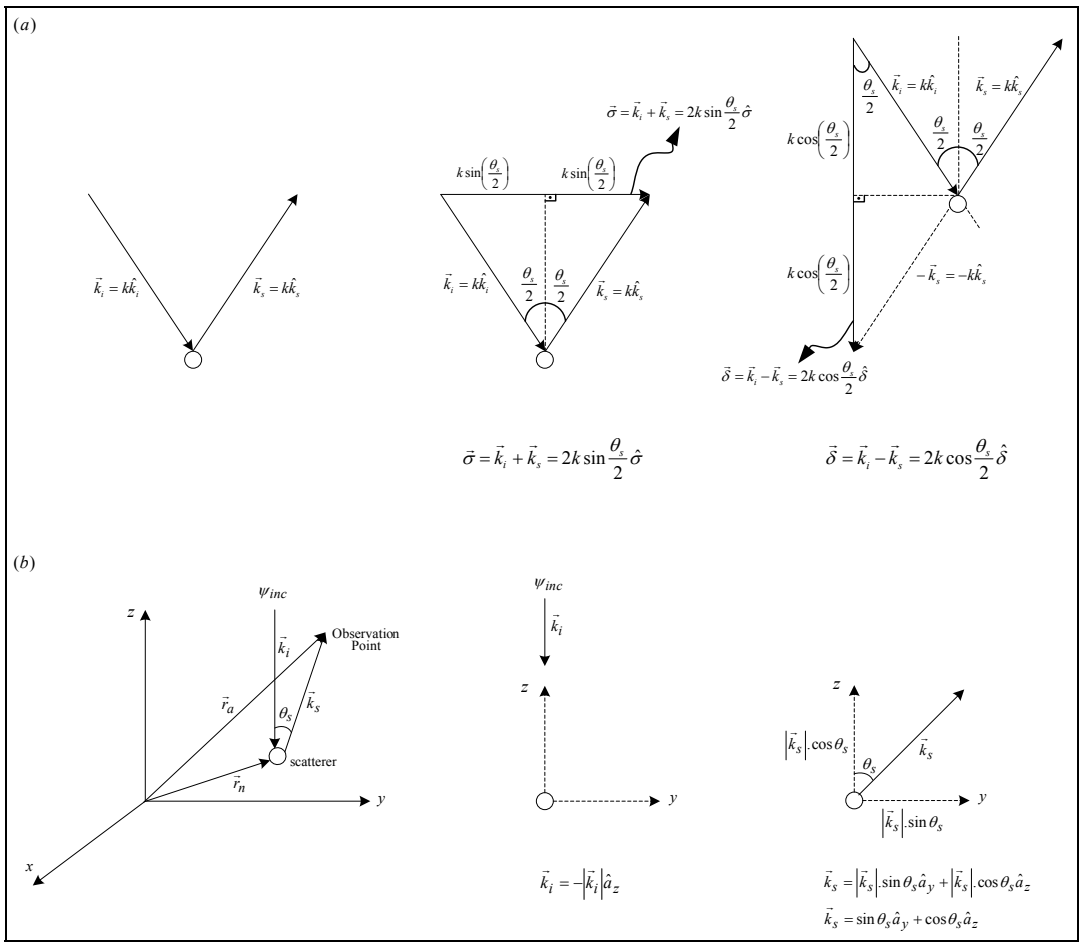

Figure 3.2: (a) Representation of relation between the incident wave vector and the scattered wave vector. (b) The incident wave vector and the scattered wave vector in the Cartesian coordinate system.

In the far-field approximation, the scattering angle is assumed as θ_s depicted in the Figure 3.2. If we consider the incident field in the *–z* direction (see Figure 3.2 (b)), the incident wave vector for this field is written as $\vec{k}_i = -\hat{a}_z$ and the scattered wave vector can be written as $\vec{k}_s = \sin\theta_s\hat{a}_y + \cos\theta_s\hat{a}_z$. If we insert these two wave vectors into Eq. (3.27), this integral can be evaluated to give:

$$\alpha_{11}(\theta_s) = \frac{\sin^2\left[kD\cos^2(\theta_s/2)\right]\sin^2\left[kd\sin\theta_s\right]}{(kD)^4\cos^6(\theta_s/2)\sin^2(\theta_s/2)} \tag{3.28}$$

where particles are confined to $-d \le x \le d$, $-d \le y \le d$ and $-d \le z \le d$. In other words, this cube's dimension is *D=2d* (see Figure 3.1).

The scattering angle θ_s is the angle between the incident wave vector direction and the scattered wave vector direction. Also, α_{11} from cubical distribution depends on the scattering angle θ_s. Note that if the scattering angle θ_s approaches forward scattering direction, π, α_{11} from cubical distribution is

$$\lim_{\theta_s \to \pi} \alpha_{11}(\theta_s) = 1 \tag{3.29}$$

Note also that if the scattering angle θ_s approaches backscattering direction, 0, α_{11} from cubical distribution is

$$\lim_{\theta_s \to 0} \alpha_{11}(\theta_s) = \frac{\sin^2(kD)}{(kD)^2} \le \frac{1}{(kD)^2} \tag{3.30}$$

In the limit as the volume of the cube goes to infinity, i.e., $D \to \infty$, in Eq. (3.30) α_{11} from cubical distribution becomes equal to 0:

$$\lim_{\theta_s \to 0} \alpha_{11}(\theta_s) \le \frac{1}{(kD)^2} \xrightarrow[D \to \infty]{} 0 \tag{3.31}$$

We substitute Eq. (3.28) into Eq. (3.13) in order to get the mean field intensity due to single scattering $< I_{11} >$ from cubical distribution:

$$< I_{11} >= \frac{|f|^2}{(4\pi r_a)^2}\left[N + \sum_{n=1}^{N} \sum_{\substack{n'=1 \\ n' \neq n}}^{N} \frac{\sin^2\left[kD\cos^2(\theta_s/2)\right]\sin^2\left[kd\sin\theta_s\right]}{(kD)^4 \cos^6(\theta_s/2)\sin^2(\theta_s/2)} \right] \tag{3.32}$$

In the above equation, the terms in the double summation are independent of the summation variables. Thus, a factor *(N−1)* comes from the first summation and a factor *N* comes from the second summation, and then we have

$$< I_{11} >= \frac{|f|^2}{(4\pi r_a)^2}\left[N + N(N-1) \frac{\sin^2\left[kD\cos^2(\theta_s/2)\right]\sin^2\left[kd\sin\theta_s\right]}{(kD)^4 \cos^6(\theta_s/2)\sin^2(\theta_s/2)} \right] \tag{3.33}$$

To depict this case, we arrange Eq. (3.33) by multiplying both sides of this Eq. with constant $(4\pi r_a)^2 / |f|^2$, and then we get

$$< I_{11} > . \frac{(4\pi r_a)^2}{|f|^2} = \left[N + N(N-1) \frac{\sin^2\left[kD\cos^2(\theta_s/2)\right]\sin^2\left[kd\sin\theta_s\right]}{(kD)^4 \cos^6(\theta_s/2)\sin^2(\theta_s/2)} \right] \tag{3.34}$$

This is the mean field intensity due to single scattering from cubical distribution of the point scatterers $< I_{11} >$ and is plotted in Figure 3.3 as a function of the scattering angle.

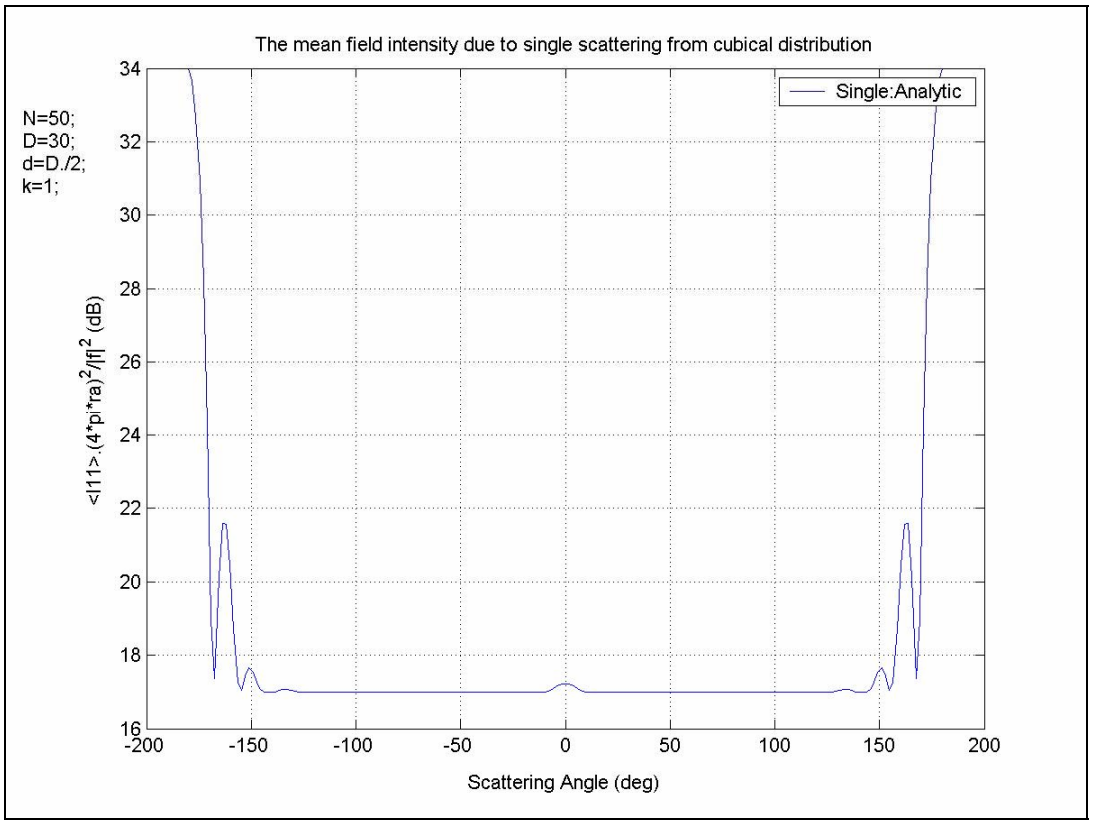

Figure 3.3: The mean field intensity due to single scattering from cubical distribution: *N*=50, *D*=30 and *k*=1.

As can be seen from Figure 3.3, a peak occurs in the backscattering direction from cubical distribution which is due to specular-like reflection since the incident field is normal to the surface of this cube, and this case is investigated in more detail in Section 4.3. In this study, we also prove that the backscattering enhancement is only constituted due to multiple scattering. We note that the mean field intensities are calculated in the decibel (dB) units throughout this thesis. The decibel (dB) is the logarithmic quantity and determined in a common way when referring to measurements of power or intensity. The basic decibel quantity is given by $f(x)_{dB} = 10\log_{10}\left(f(x)\right)$.

3.1.2 The Particles are Distributed within a Sphere

We next consider a scenario in which the particles are distributed within a sphere whose diameter is $D=2a$, this scenario is depicted in Figure 3.4:

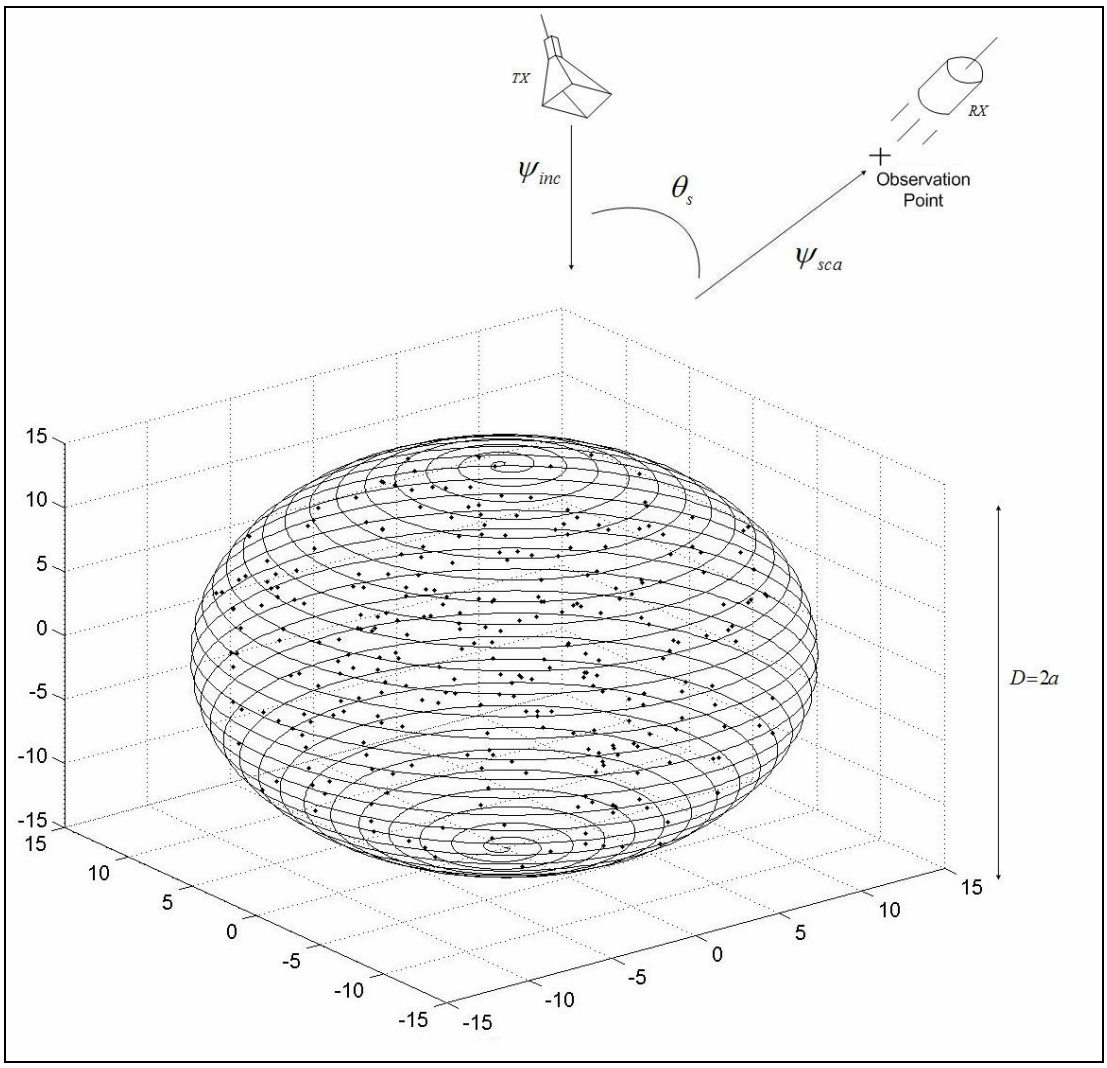

Figure 3.4: The particles are distributed within a sphere whose diameter is D=2a.

If we insert $\vec{k}_i = -\hat{a}_z$ and $\vec{k}_s = \sin\theta_s \hat{a}_y + \cos\theta_s \hat{a}_z$ into Eq. (3.27), this integral, for spherical distribution, can be evaluated and then α_{11} is obtained as

$$\alpha_{11}(\theta_s) = \frac{9\left[kD\cos\left(kD\cos(\theta_s/2)\right)\cos(\theta_s/2) - \sin\left(kD\cos(\theta_s/2)\right)\right]^2}{(kD)^6\cos^6(\theta_s/2)} \quad (3.35)$$

Note that if the scattering angle θ_s approaches forward scattering direction, π, α_{11} from spherical distribution is

$$\lim_{\theta_s\to\pi}\alpha_{11}(\theta_s) = 1 \quad (3.36)$$

Note also that if the scattering angle θ_s approaches backscattering direction, 0, α_{11} from spherical distribution is

$$\lim_{\theta_s\to 0}\alpha_{11}(\theta_s) = \frac{9\left[kD\cos(kD) - \sin(kD)\right]^2}{(kD)^6} \cong \frac{9}{(kD)^4} \quad (3.37)$$

In the limit as the volume of the sphere goes to infinity, i.e., $D\to\infty$, in Eq. (3.37) α_{11} from spherical distribution becomes equal to 0:

$$\lim_{\theta_s\to 0}\alpha_{11}(\theta_s) \cong \frac{9}{(kD)^4} \xrightarrow[D\to\infty]{} 0 \quad (3.38)$$

We substitute Eq. (3.35) into Eq. (3.13) in order to get the mean field intensity due to single scattering $< I_{11} >$ from spherical distribution:

$$< I_{11} >= \frac{|f|^2}{(4\pi r_a)^2}\left[N + \sum_{n=1}^{N}\sum_{\substack{n'=1\\ n'\neq n}}^{N}\frac{9\left[kD\cos\left(kD\cos(\theta_s/2)\right)\cos(\theta_s/2) - \sin\left(kD\cos(\theta_s/2)\right)\right]^2}{(kD)^6\cos^6(\theta_s/2)}\right] \quad (3.39)$$

In the above equation, the terms in the double summation are independent of the summation variables. Thus, a factor *(N−1)* comes from the first summation and a factor *N* comes from the second summation, and we have

$$< I_{11} >= \frac{|f|^2}{(4\pi r_a)^2}\left[N + N(N-1)\frac{9\left[kD\cos\left(kD\cos(\theta_s/2)\right)\cos(\theta_s/2) - \sin\left(kD\cos(\theta_s/2)\right)\right]^2}{(kD)^6\cos^6(\theta_s/2)}\right] \quad (3.40)$$

To depict this case, we arrange Eq. (3.40) by multiplying both sides of this Eq. with constant $(4\pi r_a)^2/|f|^2$, and then we get

$$< I_{11} > \cdot\frac{(4\pi r_a)^2}{|f|^2} = \left[N + N(N-1)\frac{9\left[kD\cos\left(kD\cos(\theta_s/2)\right)\cos(\theta_s/2) - \sin\left(kD\cos(\theta_s/2)\right)\right]^2}{(kD)^6\cos^6(\theta_s/2)}\right] \quad (3.41)$$

This is the mean field intensity due to single scattering from spherical distribution of the point scatterers $< I_{11} >$ and is plotted in Figure 3.5 as a function of the scattering angle.

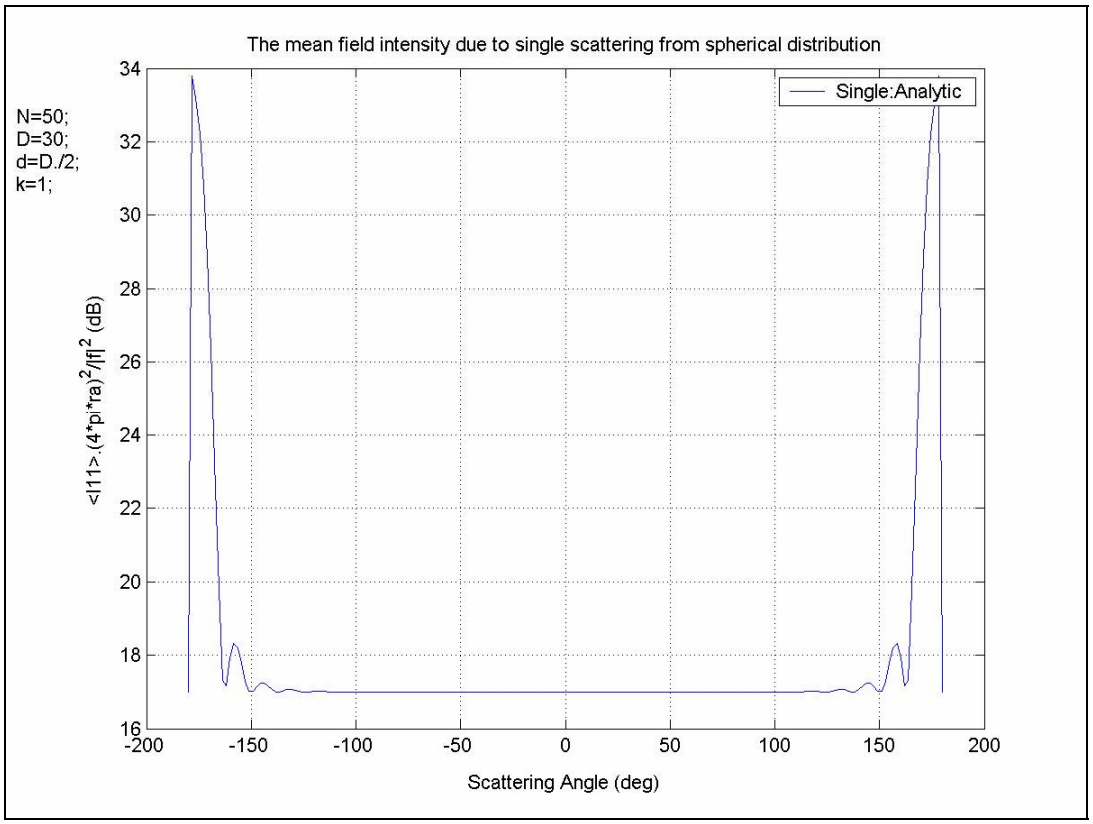

Figure 3.5: The mean field intensity due to single scattering from spherical distribution: *N*=50, *D*=30 and *k*=1.

As can be seen from Figure 3.3, any kind of the enhancement in the backscattering direction from spherical distribution does not occur while the incident field is normal to the surface of this sphere. Meanwhile, forward scattering intensity in the direction of ± 180 degrees can be seen clearly from the above figure while the incident field is in the direction of 0 degrees.

Comparison of cubical and spherical distributions, for *N*=50, *D*=30, is shown in Figure 3.6.

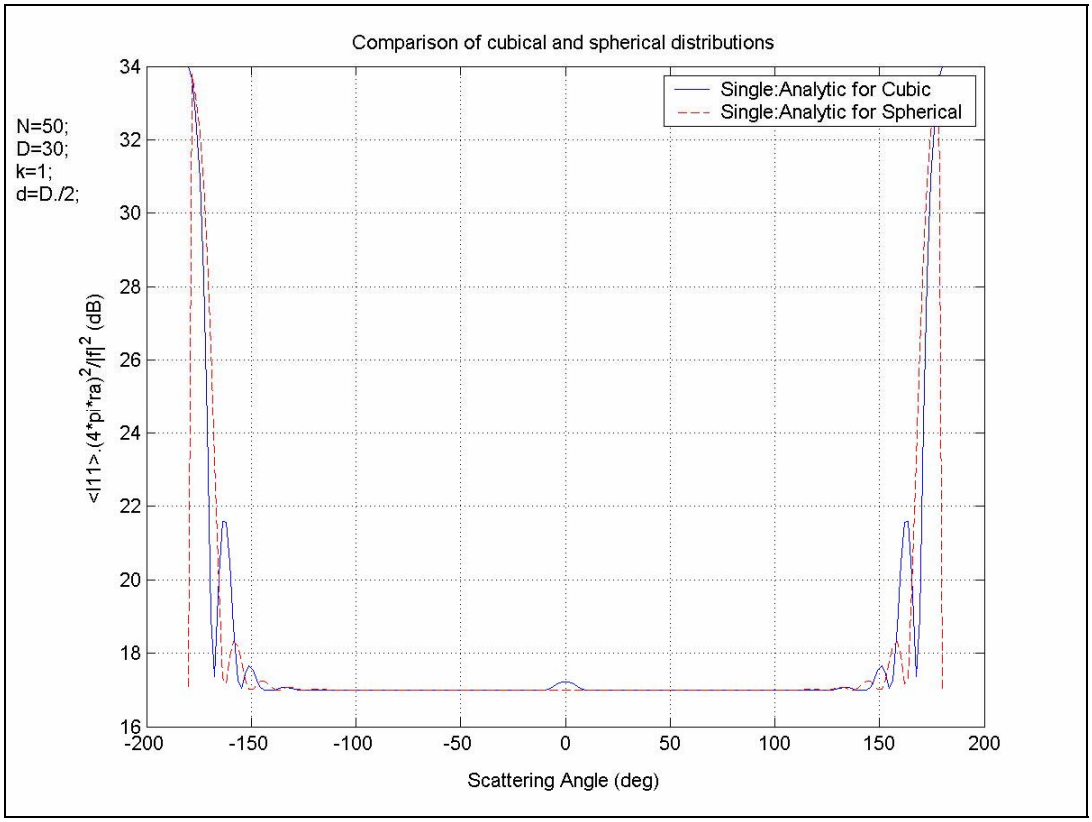

Figure 3.6: Comparison of cubical and spherical distributions: *N*=50 and *D*=30.

It can be seen from the above results that a specular enhancement is observed for the cubical distribution; however, no enhancement is observed for the spherical distribution in the any direction. From this result, we can conclude that the overall distribution of the point scatterers influences the result.

3.2 Mean Field Intensity due to Double Scattering Phenomenon

3.2.1 The Particles are Distributed within a Sphere

The double scattering phenomenon is shown in Figure 2.3 (b). The double scattering is the first multiple scattering mechanism in the distribution volume and it is one of the low-order multiple scattering terms. The third term of Eq. (2.27) represents all the double scattering denoted by $\psi_{sca}^{(2)}$ and given by

$$\psi_{sca}^{(2)} = \sum_{n=1}^{N} \sum_{\substack{m=1 \\ m \neq n}}^{N} G_n^a G_m^n \psi_{inc}^m \tag{3.42}$$

After we substitute the Green's functions, which are written as $G_n^a = -f\left[e^{ik|\vec{r}_a - \vec{r}_n|} / \left(4\pi |\vec{r}_a - \vec{r}_n|\right)\right]$ and $G_m^n = -f\left[e^{ik|\vec{r}_n - \vec{r}_m|} / \left(4\pi |\vec{r}_n - \vec{r}_m|\right)\right]$, and the incident field expression $\psi_{inc}(\vec{r}_m) = e^{i\vec{k}_i \cdot \vec{r}_m}$ into Eq. (3.42), the double scattered field $\psi_{sca}^{(2)}$ is

$$\psi^{(2)}(\vec{r}_a) = \sum_{n=1}^{N} \sum_{\substack{m=1 \\ m \neq n}}^{N} f^2 \frac{e^{ik|\vec{r}_a - \vec{r}_n|}}{4\pi |\vec{r}_a - \vec{r}_n|} \frac{e^{ik|\vec{r}_n - \vec{r}_m|}}{4\pi |\vec{r}_n - \vec{r}_m|} e^{i\vec{k}_i \cdot \vec{r}_m} \tag{3.43}$$

The mean field intensity due to double scattering $< I_{22} >$ can be written as

$$< I_{22} > = < \psi^{(2)}(\vec{r}_a) \psi^{(2)^*}(\vec{r}_a) > \tag{3.44}$$

Combining Eq. (3.43) and Eq. (3.44), we have

$$\begin{aligned} < I_{22} > &= \frac{|f|^4}{(4\pi)^4 r_a^2} \underbrace{\sum_{\substack{m,n \\ n \neq m}} \sum_{\substack{m',n' \\ n' \neq m'}} < e^{i\vec{k}_s \cdot (\vec{r}_{n'} - \vec{r}_n)} e^{i\vec{k}_i \cdot (\vec{r}_m - \vec{r}_{m'})} \frac{e^{ik|\vec{r}_n - \vec{r}_m|}}{|\vec{r}_n - \vec{r}_m|} \frac{e^{-ik|\vec{r}_{n'} - \vec{r}_{m'}|}}{|\vec{r}_{n'} - \vec{r}_{m'}|} >}_{\alpha_{22}^{(c)}} \\ < I_{22} > &= \frac{|f|^4}{(4\pi)^4 r_a^2} \underbrace{\sum_{n=1}^{N} \sum_{\substack{m=1 \\ m \neq n}}^{N} \sum_{n'=1}^{N} \sum_{\substack{m'=1 \\ m' \neq n'}}^{N} < e^{i\vec{k}_s \cdot (\vec{r}_{n'} - \vec{r}_n)} e^{i\vec{k}_i \cdot (\vec{r}_m - \vec{r}_{m'})} \frac{e^{ik|\vec{r}_n - \vec{r}_m|}}{|\vec{r}_n - \vec{r}_m|} \frac{e^{-ik|\vec{r}_{n'} - \vec{r}_{m'}|}}{|\vec{r}_{n'} - \vec{r}_{m'}|} >}_{\alpha_{22}^{(c)}} \end{aligned} \tag{3.45}$$

where the variables m and n are used for $\psi^{(2)}(\vec{r}_a)$ and the variables m' and n' are used for $\psi^{(2)^*}(\vec{r}_a)$. Also, we can use shorthand symbol $\alpha_{22}^{(c)}$ in order to denote an ensemble average of $\sum_{n=1}^{N} \sum_{\substack{m=1 \\ m \neq n}}^{N} \sum_{n'=1}^{N} \sum_{\substack{m'=1 \\ m' \neq n'}}^{N} e^{i\vec{k}_s \cdot (\vec{r}_{n'} - \vec{r}_n)} e^{i\vec{k}_i \cdot (\vec{r}_m - \vec{r}_{m'})} \frac{e^{ik|\vec{r}_n - \vec{r}_m|}}{|\vec{r}_n - \vec{r}_m|} \frac{e^{-ik|\vec{r}_{n'} - \vec{r}_{m'}|}}{|\vec{r}_{n'} - \vec{r}_{m'}|}$ which is double scattering expression for all cases and the superscript c stands for the cases that are defined below. The mean field intensity due to double scattering in Eq. (3.45) can be written in a simple way:

$$< I_{22} > = \frac{|f|^4}{(4\pi)^4 r_a^2} \left[\alpha_{22}^{(c)}\right] \tag{3.46}$$

and $\alpha_{22}^{(c)}$ is stated clearly as

$$\alpha_{22}^{(c)} = \sum_{n=1}^{N}\sum_{\substack{m=1\\m\neq n}}^{N}\sum_{n'=1}^{N}\sum_{\substack{m'=1\\m'\neq n'}}^{N} < e^{i\vec{k}_s\cdot(\vec{r}_{n'}-\vec{r}_n)} e^{i\vec{k}_i\cdot(\vec{r}_m-\vec{r}_{m'})} \frac{e^{ik|\vec{r}_n-\vec{r}_m|}}{|\vec{r}_n-\vec{r}_m|} \frac{e^{-ik|\vec{r}_{n'}-\vec{r}_{m'}|}}{|\vec{r}_{n'}-\vec{r}_{m'}|} > \tag{3.47}$$

The expression $\sum_{n=1}^{N}\sum_{\substack{m=1\\m\neq n}}^{N}\sum_{n'=1}^{N}\sum_{\substack{m'=1\\m'\neq n'}}^{N} e^{i\vec{k}_s\cdot(\vec{r}_{n'}-\vec{r}_n)} e^{i\vec{k}_i\cdot(\vec{r}_m-\vec{r}_{m'})} \frac{e^{ik|\vec{r}_n-\vec{r}_m|}}{|\vec{r}_n-\vec{r}_m|} \frac{e^{-ik|\vec{r}_{n'}-\vec{r}_{m'}|}}{|\vec{r}_{n'}-\vec{r}_{m'}|}$ is to be multiplied with the probability density function $p(\vec{r}_m,\vec{r}_n,\vec{r}_{m'},\vec{r}_{n'})$ and then integrated in order to calculate $\alpha_{22}^{(c)}$. This integral can be considered separately for seven possible cases. $\alpha_{22}^{(c)}$ can be also written as using these seven possible cases (see Figure 3.7) in the following manner:

$$\begin{aligned}\alpha_{22}^{(c)} &= N(N-1)\alpha_{22}^{(1)} + N(N-1)\alpha_{22}^{(2)} + N(N-1)(N-2)\,\alpha_{22}^{(3)} + \\ &N(N-1)(N-2)\,\alpha_{22}^{(4)} + N(N-1)(N-2)\,\alpha_{22}^{(5)} + \\ &N(N-1)(N-2)\,\alpha_{22}^{(6)} + N(N-1)(N-2)(N-3)\,\alpha_{22}^{(7)}\end{aligned} \tag{3.48}$$

The coefficients of the above equation are the total number of possible ways to choose each one of their conditions (see Figure 3.7). The term $N(N-1)$ of these coefficients is a common multiplier. Thus, this equation can be simplified in the following way:

$$\alpha_{22}^{(c)} = N(N-1)\left[\begin{aligned}&\alpha_{22}^{(1)} + \alpha_{22}^{(2)} + (N-2)\,\alpha_{22}^{(3)} + (N-2)\,\alpha_{22}^{(4)} + \\ &(N-2)\,\alpha_{22}^{(5)} + (N-2)\,\alpha_{22}^{(6)} + (N-2)(N-3)\,\alpha_{22}^{(7)}\end{aligned}\right] \tag{3.49}$$

We will next explain what these seven possible cases are and how the total number of possible ways can be computed. Depending on the choice of m' and n', we are evaluating the correlation of the ray with a different ray. There are seven possible cases shown in Figure 3.7. In this figure, the dashed line refers to conjugate of the double scattered field $\psi^{(2)^*}(\vec{r}_a)$ and the continuous line refers to the double scattered field $\psi^{(2)}(\vec{r}_a)$. We use basic principle of counting to determine the number of different ways occurring in Figure 3.7. Let us describe how this principle is applied to our cases.

In case 1, we can choose point scatter m' to be the same scatterer as m th one. From N randomly distributed point scatterers, this can be done in N different ways. After

this, there remain ($N-1$) point scatterers. Thus, $n' = n$ can be chosen in ($N-1$) different ways from the remaining ($N-1$) point scatterers. After the sequence of these two choosing processes, the total number of possible ways to choose $m' = m \,\&\, n' = n$ is $N(N-1)$.

Case 2 is very similar to case 1. Actually, case 2 is conjugate of case 1. Therefore, we can say directly that the total number of possible ways to choose $m' = n \,\&\, n' = m$ is again $N(N-1)$.

In case 3, we can choose the point scatter m' from N randomly distributed point scatterers in N different ways. After this, there remain ($N-1$) point scatterers among which $m' \neq n$ can be chosen in ($N-1$) different ways. Then, there remain ($N-2$) point scatterers. Thus, $n' = n$ can be chosen in ($N-2$) different ways from the remaining ($N-2$) point scatterers. After the sequence of these three choosing processes, the total number of possible ways to choose $m' \neq m, m' \neq n \,\&\, n' = n$ is $N(N-1)(N-2)$.

Case 4, case 5 and case 6 have the same kind of choosing methods as case 3. Therefore, we can say directly the total number of possible ways to choose each one of their conditions is $N(N-1)(N-2)$.

In case 7, we can choose the point scatter m' from N randomly distributed point scatterers in N different ways. After this, there remain ($N-1$) point scatterers among which $m' \neq n$ can be chosen in ($N-1$) different ways. Then, there remain ($N-2$) point scatterers among which $n' \neq m$ can be chosen in ($N-2$) different ways leaving ($N-3$) point scatterers. Finally, $n' \neq n$ can be chosen in ($N-3$) different ways from the remaining ($N-3$) point scatterers. After the sequence of these four choosing processes, the total number of possible ways to choose $m' \neq m, m' \neq n, n' \neq m \,\&\, n' \neq n$ is $N(N-1)(N-2)(N-3)$.

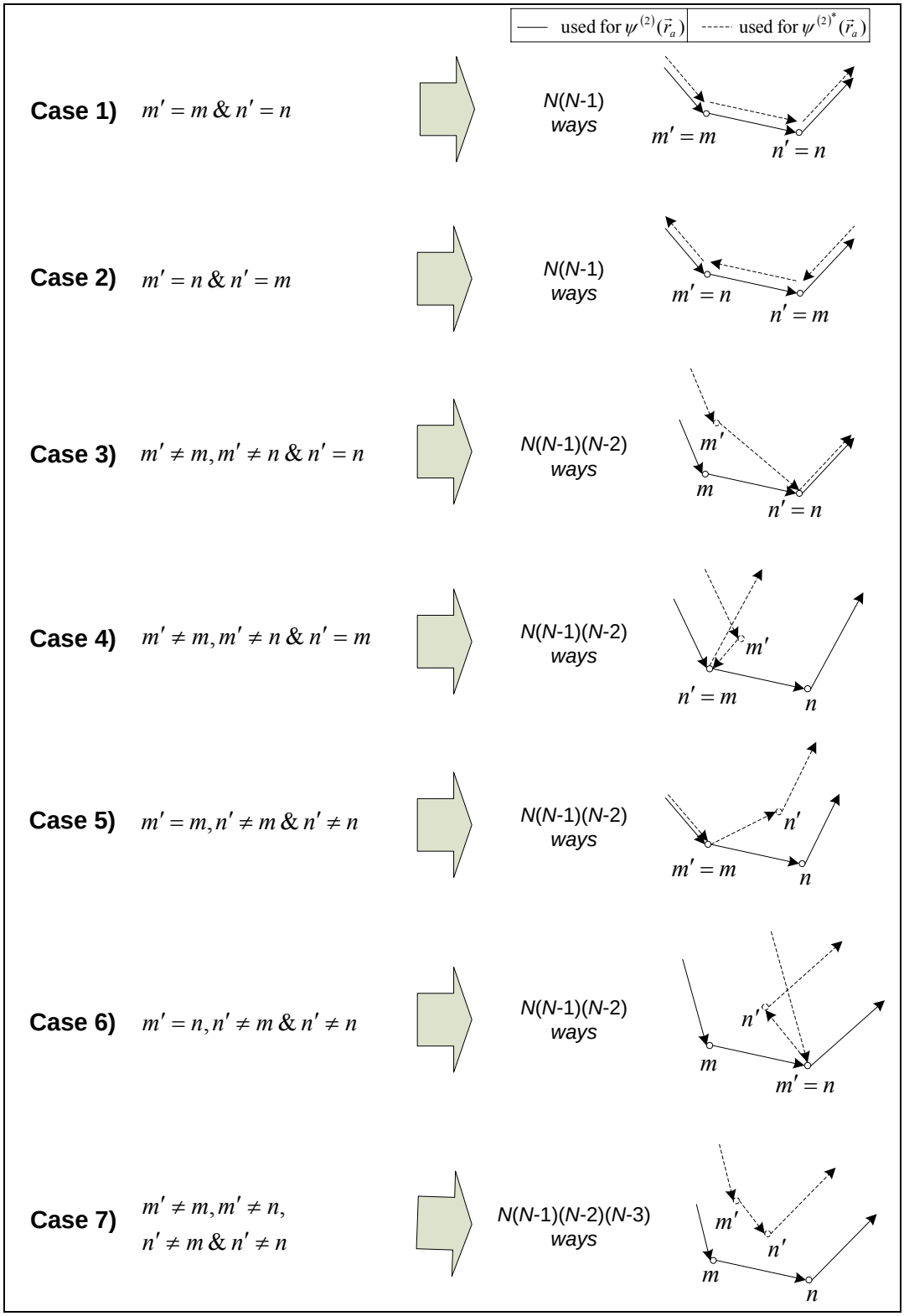

Figure 3.7: Seven possible cases of $\alpha_{22}^{(c)}$.

3.2.1.1 Case 1: $m' = m \,\&\, n' = n$

Case 1 is defined by the condition $m' = m \,\&\, n' = n$. In order to get a result, we insert m instead of m' and n instead of n' into Eq. (3.47) as follows:

$$\begin{aligned}
\alpha_{22}^{(1)} &= < e^{i\vec{k}_s.(\vec{r}_n - \vec{r}_n)} e^{i\vec{k}_i.(\vec{r}_m - \vec{r}_m)} \frac{e^{ik|\vec{r}_n - \vec{r}_m|}}{|\vec{r}_n - \vec{r}_m|} \frac{e^{-ik|\vec{r}_n - \vec{r}_m|}}{|\vec{r}_n - \vec{r}_m|} > \\
\alpha_{22}^{(1)} &= < e^{i\vec{k}_s.(0)} e^{i\vec{k}_i.(0)} \frac{e^{ik|\vec{r}_n - \vec{r}_m| - ik|\vec{r}_n - \vec{r}_n|}}{|\vec{r}_n - \vec{r}_m||\vec{r}_n - \vec{r}_m|} > \\
\alpha_{22}^{(1)} &= < e^0 e^0 \frac{e^0}{|\vec{r}_n - \vec{r}_m||\vec{r}_n - \vec{r}_m|} >
\end{aligned} \tag{3.50}$$

After all, we obtain an ensemble average of $1/|\vec{r}_n - \vec{r}_m|^2$ and it is denoted by $\alpha_{22}^{(1)}$:

$$\alpha_{22}^{(1)} = < \frac{1}{|\vec{r}_n - \vec{r}_m|^2} > \tag{3.51}$$

Expression $1/|\vec{r}_n - \vec{r}_m|^2$ is multiplied with the probability density function $p(\vec{r}_m, \vec{r}_n)$ and then integrated to obtain its ensemble average:

$$\begin{aligned}
\alpha_{22}^{(1)} &= < \frac{1}{|\vec{r}_n - \vec{r}_m|^2} > = \iint p(\vec{r}_m, \vec{r}_n) \frac{1}{|\vec{r}_n - \vec{r}_m|^2} d\vec{r}_m d\vec{r}_n \\
\alpha_{22}^{(1)} &= \iint p(\vec{r}_m, \vec{r}_n) \frac{1}{|\vec{r}_n - \vec{r}_m|^2} d\vec{r}_m d\vec{r}_n
\end{aligned} \tag{3.52}$$

This integral is quite difficult to compute. Therefore, we can use change of variables technique in order to evaluate this integral. Change of variables is one of the basic techniques in replacing one variable with another to obtain a simpler form integral. Now, we can apply this technique to above integral by introducing the variables $\vec{r}_m = \vec{r}_m(\vec{r}_1, \vec{r}_2) = \vec{r}_2 + \vec{r}_1/2$ and $\vec{r}_n = \vec{r}_n(\vec{r}_1, \vec{r}_2) = \vec{r}_2 - \vec{r}_1/2$. We suppose that the region S' in the $\vec{r}_1\vec{r}_2$−plane is transformed into a region S in the $\vec{r}_m\vec{r}_n$−plane, [33]. Under this transformation, we can write the explicit statement of this technique as

$$\iint_S f(\vec{r}_m, \vec{r}_n) d\vec{r}_m d\vec{r}_n = \iint_{S'} f(\vec{r}_1, \vec{r}_2) |J(\vec{r}_1, \vec{r}_2)| d\vec{r}_1 d\vec{r}_2 \tag{3.53}$$

where $\left|J(\vec{r}_1,\vec{r}_2)\right|$ is the absolute value of the Jacobian which is defined as a determinant of a 2x2 matrix. This determinant is given by

$$J(\vec{r}_1,\vec{r}_2)=\begin{vmatrix}\dfrac{\partial\vec{r}_m}{\partial\vec{r}_1} & \dfrac{\partial\vec{r}_m}{\partial\vec{r}_2}\\ \dfrac{\partial\vec{r}_n}{\partial\vec{r}_1} & \dfrac{\partial\vec{r}_n}{\partial\vec{r}_2}\end{vmatrix}=\left(\frac{\partial\vec{r}_m}{\partial\vec{r}_1}\cdot\frac{\partial\vec{r}_n}{\partial\vec{r}_2}\right)-\left(\frac{\partial\vec{r}_m}{\partial\vec{r}_2}\cdot\frac{\partial\vec{r}_n}{\partial\vec{r}_1}\right)=1 \tag{3.54}$$

After evaluating the absolute value of the Jacobian, the relationship between the element of area $d\vec{r}_m d\vec{r}_n$ and the corresponding area element $d\vec{r}_1 d\vec{r}_2$ is given by

$$\begin{aligned} dS &= d\vec{r}_m d\vec{r}_n = \left|J(\vec{r}_1,\vec{r}_2)\right| d\vec{r}_1 d\vec{r}_2 \quad ; \quad \left|J(\vec{r}_1,\vec{r}_2)\right|=1 \\ dS &= d\vec{r}_m d\vec{r}_n = d\vec{r}_1 d\vec{r}_2 \end{aligned} \tag{3.55}$$

Let us rearrange the variables, the area elements and the absolute value of the Jacobian in the following manner:

$$\boxed{\begin{aligned} &\vec{r}_1 = \vec{r}_m - \vec{r}_n \\ &\vec{r}_2 = \frac{\vec{r}_m + \vec{r}_n}{2} \\ &d\vec{r}_1 d\vec{r}_2 = d\vec{r}_m d\vec{r}_n \quad \left|J(\vec{r}_1,\vec{r}_2)\right|=1 \end{aligned}} \tag{3.56}$$

After the change of variables and using joint probability density function of two point scatterers, $p(\vec{r}_m,\vec{r}_n)=p(\vec{r}_m)p(\vec{r}_n)=1/V^2$ we get a simpler form integral as

$$\alpha_{22}^{(1)}=\frac{1}{V^2}\iint\frac{1}{|\vec{r}_1|^2}d\vec{r}_1 d\vec{r}_2 \tag{3.57}$$

$$\alpha_{22}^{(1)}=\frac{1}{V^2}\underbrace{\int_V d\vec{r}_2}_{V}\int_V\frac{1}{r_1^2}d\vec{r}_1 \tag{3.58}$$

$$\alpha_{22}^{(1)}=\frac{1}{V}\int_V\frac{1}{r_1^2}d\vec{r}_1 \tag{3.59}$$

After the change of variables, the volume of above simpler integral is also varied. In a condition of the infinite volume assumption, we can take integral over the sphere and this gives us the approximate result. In order to evaluate the above volume

integral, we'll first have to convert all the terms of $\vec{r}_1$ into spherical polar terms in the following way:

$$\alpha_{22}^{(1)} = \frac{1}{V}\int_{\varphi=0}^{2\pi}\int_{\theta=0}^{\pi}\int_{r=0}^{a}\frac{1}{r^2}r^2\sin\theta dr d\theta d\varphi \tag{3.60}$$

Finally, solution to this integral is

$$\boxed{\alpha_{22}^{(1)} = \frac{4\pi}{V}a \quad \xrightarrow[V=\frac{4}{3}\pi a^3]{} \quad \alpha_{22}^{(1)} = \frac{3}{a^2}} \tag{3.61}$$

3.2.1.2 Case 2: $m' = n \,\&\, n' = m$

Case 2 is defined by the condition $m' = n \,\&\, n' = m$. In order to get a result, we insert n instead of m' and m instead of n' into Eq. (3.47) as follows:

$$\begin{aligned}
\alpha_{22}^{(2)} &= < e^{i\vec{k}_s.(\vec{r}_m-\vec{r}_n)} e^{i\vec{k}_i.(\vec{r}_m-\vec{r}_n)} \frac{e^{ik|\vec{r}_n-\vec{r}_m|}}{|\vec{r}_n-\vec{r}_m|}\frac{e^{-ik|\vec{r}_m-\vec{r}_n|}}{|\vec{r}_m-\vec{r}_n|} > \\
\alpha_{22}^{(2)} &= < e^{i\vec{k}_s.(\vec{r}_m-\vec{r}_n)} e^{i\vec{k}_i.(\vec{r}_m-\vec{r}_n)} \frac{e^{ik|\vec{r}_m-\vec{r}_n|}}{|\vec{r}_m-\vec{r}_n|}\frac{e^{-ik|\vec{r}_m-\vec{r}_n|}}{|\vec{r}_m-\vec{r}_n|} > \\
\alpha_{22}^{(2)} &= < e^{i(\vec{k}_i+\vec{k}_s).(\vec{r}_m-\vec{r}_n)} \frac{e^{ik|\vec{r}_m-\vec{r}_n|-ik|\vec{r}_m-\vec{r}_n|}}{|\vec{r}_m-\vec{r}_n|^2} > \\
\alpha_{22}^{(2)} &= < e^{i(\vec{k}_i+\vec{k}_s).(\vec{r}_m-\vec{r}_n)} \frac{1}{|\vec{r}_m-\vec{r}_n|^2} >
\end{aligned} \tag{3.62}$$

After all, we obtain an ensemble average of $\left[e^{i(\vec{k}_i+\vec{k}_s).(\vec{r}_m-\vec{r}_n)}\right]/|\vec{r}_m-\vec{r}_n|^2$ and it is denoted by $\alpha_{22}^{(2)}$:

$$\alpha_{22}^{(2)} = < \frac{e^{i(\vec{k}_i+\vec{k}_s).(\vec{r}_m-\vec{r}_n)}}{|\vec{r}_m-\vec{r}_n|^2} > \tag{3.63}$$

Expression $\left[e^{i(\vec{k}_i+\vec{k}_s).(\vec{r}_m-\vec{r}_n)}\right]/|\vec{r}_m-\vec{r}_n|^2$ is multiplied with the probability density function $p(\vec{r}_m,\vec{r}_n)$ and then integrated to obtain its ensemble average:

$$\alpha_{22}^{(2)} =< \frac{e^{i(\vec{k}_i+\vec{k}_s).(\vec{r}_m-\vec{r}_n)}}{|\vec{r}_m-\vec{r}_n|^2} >= \iint p(\vec{r}_m,\vec{r}_n)\frac{e^{i(\vec{k}_i+\vec{k}_s).(\vec{r}_m-\vec{r}_n)}}{|\vec{r}_m-\vec{r}_n|^2}d\vec{r}_m d\vec{r}_n$$
$$\alpha_{22}^{(2)} = \iint p(\vec{r}_m,\vec{r}_n)\frac{e^{i(\vec{k}_i+\vec{k}_s).(\vec{r}_m-\vec{r}_n)}}{|\vec{r}_m-\vec{r}_n|^2}d\vec{r}_m d\vec{r}_n \tag{3.64}$$

This integral is quite difficult to compute. Therefore, we make change of variables in the following manner:

$$\boxed{\begin{aligned}&\vec{r}_1 = \vec{r}_m - \vec{r}_n \\ &\vec{r}_2 = \frac{\vec{r}_m+\vec{r}_n}{2} \\ &d\vec{r}_1 d\vec{r}_2 = d\vec{r}_m d\vec{r}_n \quad |J(\vec{r}_1,\vec{r}_2)| = 1\end{aligned}} \tag{3.65}$$

After the change of variables and using joint probability density function of two point scatterers $p(\vec{r}_m,\vec{r}_n) = p(\vec{r}_m)p(\vec{r}_n) = 1/V^2$, we have

$$\alpha_{22}^{(2)} = \frac{1}{V^2}\iint_V \frac{e^{i(\vec{\sigma}).(\vec{r}_1)}}{r_1^2}d\vec{r}_1 d\vec{r}_2 \tag{3.66}$$

where $\vec{\sigma} = \vec{k}_s + \vec{k}_i = 2k\sin(\theta_s/2)\hat{\sigma}$ is the sum of the incident and scattered wave vectors and $\hat{k}_i.\hat{k}_s = \cos(\pi-\theta_s)$ is the scalar product of the incident and scattered wave unit vectors.

$$\alpha_{22}^{(2)} = \frac{1}{V^2}\underbrace{\int_V d\vec{r}_2}_{V}\int_V \frac{e^{i(\vec{\sigma}).(\vec{r}_1)}}{r_1^2}d\vec{r}_1 \tag{3.67}$$

$$\alpha_{22}^{(2)} = \frac{1}{V}\int_V \frac{e^{i(\vec{\sigma}).(\vec{r}_1)}}{r_1^2}d\vec{r}_1 \tag{3.68}$$

In order to evaluate the above volume integral, we'll first have to convert all the terms of $\vec{r}_1$ into spherical polar terms in the following way:

$$\alpha_{22}^{(2)} = \frac{1}{V}\int_{\varphi=0}^{2\pi}\int_{\theta=0}^{\pi}\int_{r=0}^{a}\frac{e^{ir\sigma\cos\theta}}{r^2}r^2\sin\theta dr d\theta d\varphi \tag{3.69}$$

Solution to this integral is $\alpha_{22}^{(2)}$ is

$$\boxed{\alpha_{22}^{(2)} = \frac{4\pi}{V}\frac{Si(a\sigma)}{\sigma} \xrightarrow[V=\frac{4}{3}\pi a^3]{} \alpha_{22}^{(2)} = \frac{3}{a^2}\frac{Si(a\sigma)}{a\sigma}} \tag{3.70}$$

where $Si(a\sigma) = \int_0^{a\sigma} \frac{\sin t}{t} dt$ is the Sine integral and $\sigma = |\vec{\sigma}| = |\vec{k}_s + \vec{k}_i| = 2k\sin(\theta_s/2)$ is the amplitude of the sum of the incident and scattered wave vectors. Some properties of the Sinc function and the Sine integral are given in Appendix G. As can be seen from the above equation, $\alpha_{22}^{(2)}$ has the form Sine integral divided by $a\sigma$ and also σ depends on the scattering angle. Therefore, we expect $\alpha_{22}^{(2)}$ to give rise to the backscattering enhancement. In Section 3.2.1.8, we show that $\alpha_{22}^{(2)}$ is the main cause of the backscattering enhancement. In order to see this contribution, $\alpha_{22}^{(2)}$ is plotted in Figure 3.8 as a function of the scattering angle.

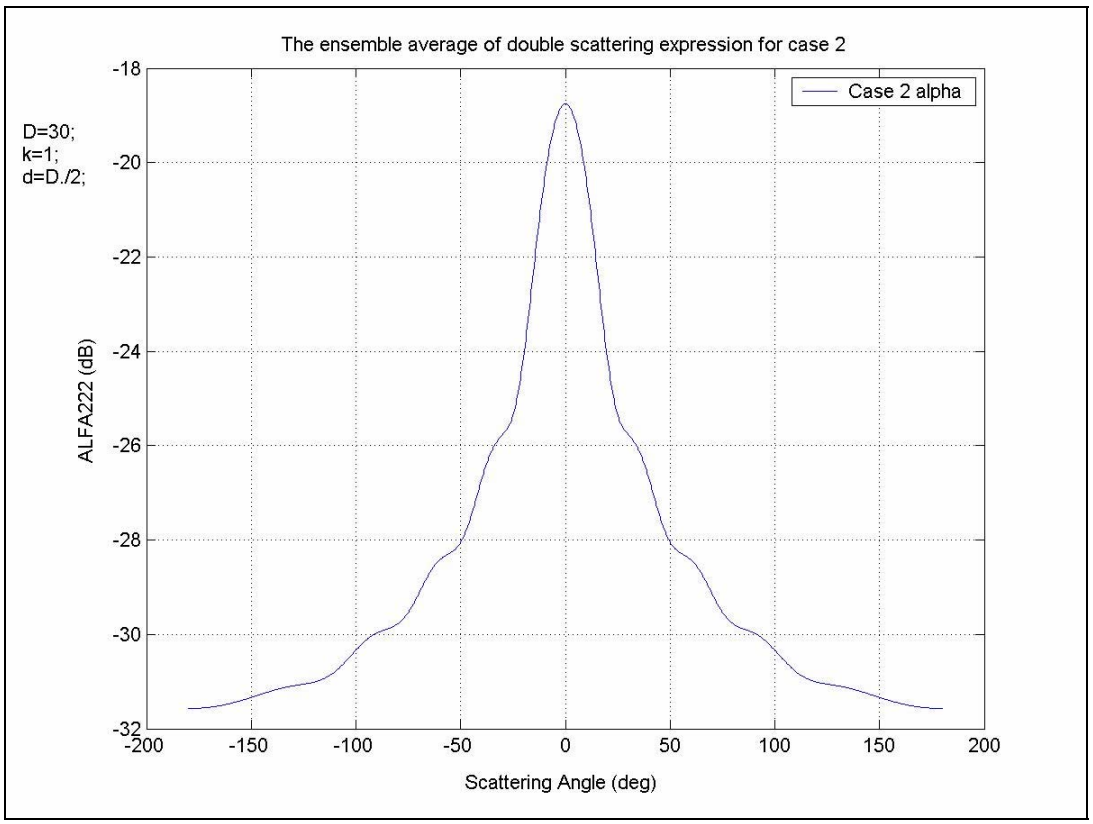

Figure 3.8: $\alpha_{22}^{(2)}$, the ensemble average of $\left[e^{i(\vec{k}_i+\vec{k}_s).(\vec{r}_m-\vec{r}_n)}\right]/|\vec{r}_m - \vec{r}_n|^2$ which is double scattering expression for case 2.

NOTE:

If we insert the approximation $\lim_{\sigma\to 0}\left[Si(\sigma a)\right]/\sigma = a$ into Eq. (3.70), we get

$$\lim_{\sigma\to 0}\alpha_{22}^{(2)} = \lim_{\sigma\to 0}\frac{4\pi}{V}\frac{Si(\sigma a)}{\sigma} = \frac{4\pi}{V}a \tag{3.71}$$

This limit $\lim_{\sigma\to 0}\alpha_{22}^{(2)}$ is equal to $\alpha_{22}^{(1)}$ as expected $\left(\lim_{\sigma\to 0}\alpha_{22}^{(2)} = (4\pi/V)a = \alpha_{22}^{(1)}\right)$.

If we insert the infinite volume approach $\lim_{a\to\infty}\left[Si(\sigma a)\right]/\sigma = (\pi/2)/\sigma$ into Eq. (3.70) in the following manner, we get

$$\lim_{a\to\infty}\alpha_{22}^{(2)} = \lim_{a\to\infty}\frac{4\pi}{V}\frac{Si(\sigma a)}{\sigma} = \frac{4\pi}{V}\frac{\pi/2}{\sigma} = \frac{2\pi^2}{V\sigma} \tag{3.72}$$

Inserting $\vec{\sigma} = \vec{k}_i + \vec{k}_s = 2k\sin(\theta_s/2)\hat{\sigma}$; $(\sigma = 2k\sin(\theta_s/2))$ into Eq. (3.72), we have

$$\lim_{a\to\infty}\alpha_{22}^{(2)} = \frac{2\pi^2}{V\sigma} = \frac{2\pi^2}{V2k\sin\frac{\theta_s}{2}} = \frac{\pi^2}{Vk\sin\frac{\theta_s}{2}} \tag{3.73}$$

When we consider infinite volume assumption for the sphere ($a\to\infty$), $\alpha_{22}^{(2)}$ approaches $\pi^2/\left[Vk\sin(\theta_s/2)\right]$.

Note that we can take integral over the sphere and this gives us the approximate results in a condition of the infinite volume assumption. In the following chapter, these approximate numerical results are tested by MC simulations and we prove that the results nicely agree with each other. This obviously indicates that the infinite volume assumption is not too bad. Since there is no other way to evaluate integrals of $\alpha_{22}^{(2)}$ and also we use this assumption to evaluate the others.

3.2.1.3 Case 3: $m' \neq m, m' \neq n \,\&\, n' = n$

Case 3 is defined by the condition $m' \neq m, m' \neq n \,\&\, n' = n$. In order to get a result, we insert n instead of n' into Eq. (3.47) as follows:

$$\alpha_{22}^{(3)} =< e^{i\vec{k}_s.(\vec{r}_n-\vec{r}_n)} e^{i\vec{k}_i.(\vec{r}_m-\vec{r}_{m'})} \frac{e^{ik|\vec{r}_n-\vec{r}_m|}}{|\vec{r}_n-\vec{r}_m|} \frac{e^{-ik|\vec{r}_n-\vec{r}_{m'}|}}{|\vec{r}_n-\vec{r}_{m'}|} > \tag{3.74}$$

which can be rearranged into the form:

$$\alpha_{22}^{(3)} =< e^{i\vec{k}_s.(\vec{r}_n-\vec{r}_n)} e^{i\vec{k}_i.(\vec{r}_m-\vec{r}_{m'})} \frac{e^{ik|\vec{r}_m-\vec{r}_n|}}{|\vec{r}_m-\vec{r}_n|} \frac{e^{-ik|\vec{r}_{m'}-\vec{r}_n|}}{|\vec{r}_{m'}-\vec{r}_n|} > \tag{3.75}$$

$$\alpha_{22}^{(3)} =< e^{i\vec{k}_s.(0)} e^{i\vec{k}_i.(\vec{r}_m-\vec{r}_{m'})} \frac{e^{ik|\vec{r}_m-\vec{r}_n|}}{|\vec{r}_m-\vec{r}_n|} \frac{e^{-ik|\vec{r}_{m'}-\vec{r}_n|}}{|\vec{r}_{m'}-\vec{r}_n|} > \tag{3.76}$$

After all, we obtain an ensemble average and this is denoted by $\alpha_{22}^{(3)}$:

$$\alpha_{22}^{(3)} =< \frac{e^{i\vec{k}_i.(\vec{r}_m-\vec{r}_{m'})} e^{ik|\vec{r}_m-\vec{r}_n|} e^{-ik|\vec{r}_{m'}-\vec{r}_n|}}{|\vec{r}_m-\vec{r}_n||\vec{r}_{m'}-\vec{r}_n|} > \tag{3.77}$$

Expression $\left[e^{i\vec{k}_i.(\vec{r}_m-\vec{r}_{m'})} e^{ik|\vec{r}_m-\vec{r}_n|} e^{-ik|\vec{r}_{m'}-\vec{r}_n|}\right] / |\vec{r}_m-\vec{r}_n||\vec{r}_{m'}-\vec{r}_n|$ is multiplied with the probability density function $p(\vec{r}_m,\vec{r}_n,\vec{r}_{m'})$ and then integrated to obtain its ensemble average:

$$\begin{aligned}
\alpha_{22}^{(3)} &=< \frac{e^{i\vec{k}_i.(\vec{r}_m-\vec{r}_{m'})} e^{ik|\vec{r}_m-\vec{r}_n|} e^{-ik|\vec{r}_{m'}-\vec{r}_n|}}{|\vec{r}_m-\vec{r}_n||\vec{r}_{m'}-\vec{r}_n|} > \\
\alpha_{22}^{(3)} &= \iiint p(\vec{r}_m,\vec{r}_n,\vec{r}_{m'}) \frac{e^{i\vec{k}_i.(\vec{r}_m-\vec{r}_{m'})} e^{ik|\vec{r}_m-\vec{r}_n|} e^{-ik|\vec{r}_{m'}-\vec{r}_n|}}{|\vec{r}_m-\vec{r}_n||\vec{r}_{m'}-\vec{r}_n|} d\vec{r}_m d\vec{r}_n d\vec{r}_{m'} \\
\alpha_{22}^{(3)} &= \iiint p(\vec{r}_m,\vec{r}_n,\vec{r}_{m'}) \frac{e^{i\vec{k}_i.(\vec{r}_m-\vec{r}_{m'})} e^{ik|\vec{r}_m-\vec{r}_n|} e^{-ik|\vec{r}_{m'}-\vec{r}_n|}}{|\vec{r}_m-\vec{r}_n||\vec{r}_{m'}-\vec{r}_n|} d\vec{r}_m d\vec{r}_n d\vec{r}_{m'}
\end{aligned} \tag{3.78}$$

This integral is quite difficult to compute. Therefore, we make change of variables in the following manner:

$$\boxed{\begin{aligned}
&\vec{r}_1 = \vec{r}_m - \vec{r}_n \\
&\vec{r}_2 = \vec{r}_{m'} - \vec{r}_n \quad ==> \vec{r}_1 - \vec{r}_2 = \vec{r}_m - \vec{r}_{m'} \\
&\vec{r}_3 = \frac{\vec{r}_m + \vec{r}_{m'}}{2} \\
&d\vec{r}_1 d\vec{r}_2 d\vec{r}_3 = d\vec{r}_m d\vec{r}_n d\vec{r}_{m'} \quad \left|J(\vec{r}_1,\vec{r}_2,\vec{r}_3)\right| = 1
\end{aligned}} \tag{3.79}$$

After the change of variables and using joint probability density function of three point scatterers $p(\vec{r}_m,\vec{r}_n,\vec{r}_{m'}) = p(\vec{r}_m)p(\vec{r}_n)p(\vec{r}_{m'}) = 1/V^3$, we have

$$\alpha_{22}^{(3)} = \frac{1}{V^3}\iiint \frac{e^{i\vec{k}_i.(\vec{r}_1-\vec{r}_2)}e^{ik|\vec{r}_1|}e^{-ik|\vec{r}_2|}}{|\vec{r}_1||\vec{r}_2|}d\vec{r}_1 d\vec{r}_2 d\vec{r}_3 \tag{3.80}$$

$$\alpha_{22}^{(3)} = \frac{1}{V^3}\int_V d\vec{r}_3 \iint_V \frac{e^{i\vec{k}_i.(\vec{r}_1-\vec{r}_2)}e^{ik|\vec{r}_1|}e^{-ik|\vec{r}_2|}}{|\vec{r}_1||\vec{r}_2|}d\vec{r}_1 d\vec{r}_2 \tag{3.81}$$

$$\alpha_{22}^{(3)} = \frac{1}{V^3}\int_V d\vec{r}_3 \iint_V \frac{e^{i\vec{k}_i.(\vec{r}_1-\vec{r}_2)}e^{ik(r_1-r_2)}}{r_1 r_2}d\vec{r}_1 d\vec{r}_2 \tag{3.82}$$

Now, the above integral is quite complicated. Thus, we separate it into component parts as follows:

$$\alpha_{22}^{(3)} = \frac{1}{V^3}\underbrace{\int_V d\vec{r}_3}_{V}\underbrace{\int_V \frac{e^{i\vec{k}_i.(\vec{r}_1)}e^{ik(r_1)}}{r_1}d\vec{r}_1}_{I}\underbrace{\int_V \frac{e^{-i\vec{k}_i.(\vec{r}_2)}e^{-ik(r_2)}}{r_2}d\vec{r}_2}_{I^*} \tag{3.83}$$

where the first integral is equal to volume V. Also, the last two integrals are conjugate of each other. Hence, with respect to the equivalence $I.I^* = |I|^2$, $\alpha_{22}^{(3)}$ is written as

$$\alpha_{22}^{(3)} = \frac{1}{V^2}\left|\int_V \frac{e^{i(\vec{k}_i.\vec{r}+kr)}}{r}d\vec{r}\right|^2 \tag{3.84}$$

In order to evaluate the above volume integral, we'll first have to convert all the terms of $\vec{r}$ into spherical polar terms in the following way:

$$\alpha_{22}^{(3)} = \frac{1}{V^2}\left|\int_{\varphi=0}^{2\pi}\int_{\theta=0}^{\pi}\int_{r=0}^{a}\frac{e^{ikr(1+\cos\theta)}}{r}r^2\sin\theta dr d\theta d\varphi\right|^2 \tag{3.85}$$

Solution to this integral is given by

$$\alpha_{22}^{(3)} = \frac{2\pi^2}{k^4V^2}\left[1+2(ka)^2-\cos(2ka)-2ka\sin(2ka)\right] \tag{3.86}$$

When we consider infinite volume assumption for the sphere ($a \to \infty$), the term $\left[1+2(ka)^2-\cos(2ka)-2ka\sin(2ka)\right]$ can approach the term with the largest degree, such as $\left[2(ka)^2\right]$.

$$\alpha_{22}^{(3)} \cong \frac{2\pi^2}{k^4 V^2}\left[2(ka)^2\right] \tag{3.87}$$

After expressing the volume of the sphere in terms of its radius as $V = (4/3)\pi a^3$, $\alpha_{22}^{(3)}$ is determined as

$$\boxed{\alpha_{22}^{(3)} \cong \frac{9}{4k^2a^4}} \tag{3.88}$$

3.2.1.4 Case 4: $m' \neq m, m' \neq n \,\&\, n' = m$

Case 4 is defined by the condition $m' \neq m, m' \neq n \,\&\, n' = m$. In order to get a result, we insert *m* instead of n' into Eq. (3.47) as follows:

$$\alpha_{22}^{(4)} = < e^{i\vec{k}_s.(\vec{r}_m - \vec{r}_n)} e^{i\vec{k}_i.(\vec{r}_m - \vec{r}_{m'})} \frac{e^{ik|\vec{r}_n - \vec{r}_m|}}{|\vec{r}_n - \vec{r}_m|} \frac{e^{-ik|\vec{r}_m - \vec{r}_{m'}|}}{|\vec{r}_m - \vec{r}_{m'}|} > \tag{3.89}$$

which can be rearranged into the form:

$$\alpha_{22}^{(4)} = < e^{i\vec{k}_s.(\vec{r}_m - \vec{r}_n)} e^{i\vec{k}_i.(\vec{r}_m - \vec{r}_{m'})} \frac{e^{ik|\vec{r}_m - \vec{r}_n|}}{|\vec{r}_m - \vec{r}_n|} \frac{e^{-ik|\vec{r}_{m'} - \vec{r}_m|}}{|\vec{r}_{m'} - \vec{r}_m|} > \tag{3.90}$$

Expression $e^{i\vec{k}_s.(\vec{r}_m - \vec{r}_n)} e^{i\vec{k}_i.(\vec{r}_m - \vec{r}_{m'})} \left[e^{ik|\vec{r}_m - \vec{r}_n|} / |\vec{r}_m - \vec{r}_n|\right]\left[e^{-ik|\vec{r}_{m'} - \vec{r}_m|} / |\vec{r}_{m'} - \vec{r}_m|\right]$ is multiplied with the probability density function $p(\vec{r}_m, \vec{r}_n, \vec{r}_{m'})$ and then integrated to obtain its ensemble average:

$$\alpha_{22}^{(4)} = < e^{i\vec{k}_s.(\vec{r}_m - \vec{r}_n)} e^{i\vec{k}_i.(\vec{r}_m - \vec{r}_{m'})} \frac{e^{ik|\vec{r}_m - \vec{r}_n|}}{|\vec{r}_m - \vec{r}_n|} \frac{e^{-ik|\vec{r}_{m'} - \vec{r}_m|}}{|\vec{r}_{m'} - \vec{r}_m|} >$$

$$\alpha_{22}^{(4)} = \iiint p(\vec{r}_m, \vec{r}_n, \vec{r}_{m'}) e^{i\vec{k}_s.(\vec{r}_m - \vec{r}_n)} e^{i\vec{k}_i.(\vec{r}_m - \vec{r}_{m'})} \frac{e^{ik|\vec{r}_m - \vec{r}_n|}}{|\vec{r}_m - \vec{r}_n|} \frac{e^{-ik|\vec{r}_{m'} - \vec{r}_m|}}{|\vec{r}_{m'} - \vec{r}_m|} d\vec{r}_m d\vec{r}_n d\vec{r}_{m'} \tag{3.91}$$

$$\alpha_{22}^{(4)} = \iiint p(\vec{r}_m, \vec{r}_n, \vec{r}_{m'}) e^{i\vec{k}_s.(\vec{r}_m - \vec{r}_n)} e^{i\vec{k}_i.(\vec{r}_m - \vec{r}_{m'})} \frac{e^{ik|\vec{r}_m - \vec{r}_n|}}{|\vec{r}_m - \vec{r}_n|} \frac{e^{-ik|\vec{r}_{m'} - \vec{r}_m|}}{|\vec{r}_{m'} - \vec{r}_m|} d\vec{r}_m d\vec{r}_n d\vec{r}_{m'}$$

This integral is quite difficult to compute. Therefore, we make change of variables in the following manner:

$$\boxed{\begin{aligned}&\vec{r}_1 = \vec{r}_m - \vec{r}_n \\ &\vec{r}_2 = \vec{r}_m - \vec{r}_{m'} \\ &\vec{r}_3 = \frac{\vec{r}_m + \vec{r}_{m'}}{2} \\ &d\vec{r}_1 d\vec{r}_2 d\vec{r}_3 = d\vec{r}_m d\vec{r}_n d\vec{r}_{m'} \quad \left|J(\vec{r}_1, \vec{r}_2, \vec{r}_3)\right| = 1\end{aligned}} \tag{3.92}$$

After the change of variables and using joint probability density function of three point scatterers $p(\vec{r}_m, \vec{r}_n, \vec{r}_{m'}) = p(\vec{r}_m)p(\vec{r}_n)p(\vec{r}_{m'}) = 1/V^3$, we have

$$\alpha_{22}^{(4)} = \frac{1}{V^3}\iiint e^{i\vec{k}_s.(\vec{r}_1)} e^{i\vec{k}_i.(\vec{r}_2)} \frac{e^{ik|\vec{r}_1|}}{|\vec{r}_1|} \frac{e^{-ik|\vec{r}_2|}}{|\vec{r}_2|} d\vec{r}_1 d\vec{r}_2 d\vec{r}_3 \tag{3.93}$$

$$\alpha_{22}^{(4)} = \frac{1}{V^3}\iiint e^{i\vec{k}_s.(\vec{r}_1)} e^{i\vec{k}_i.(\vec{r}_2)} \frac{e^{ikr_1}}{r_1} \frac{e^{-ikr_2}}{r_2} d\vec{r}_1 d\vec{r}_2 d\vec{r}_3 \tag{3.94}$$

$$\alpha_{22}^{(4)} = \frac{1}{V^3}\iiint e^{i\vec{k}_s.(\vec{r}_1)} \frac{e^{ikr_1}}{r_1} e^{i\vec{k}_i.(\vec{r}_2)} \frac{e^{-ikr_2}}{r_2} d\vec{r}_1 d\vec{r}_2 d\vec{r}_3 \tag{3.95}$$

$$\alpha_{22}^{(4)} = \frac{1}{V^3}\int_V d\vec{r}_3 \int_V e^{i\vec{k}_s.(\vec{r}_1)} \frac{e^{ikr_1}}{r_1} d\vec{r}_1 \int_V e^{i\vec{k}_i.(\vec{r}_2)} \frac{e^{-ikr_2}}{r_2} d\vec{r}_2 \tag{3.96}$$

$$\alpha_{22}^{(4)} = \frac{1}{V^3}\int_V d\vec{r}_3 \int_V \frac{e^{i\left[\vec{k}_s.\vec{r}_1 + kr_1\right]}}{r_1} d\vec{r}_1 \int_V \frac{e^{i\left[\vec{k}_i.\vec{r}_2 - kr_2\right]}}{r_2} d\vec{r}_2 \tag{3.97}$$

Now, the above integral is quite complicated. Thus, we separate it into component parts as follows:

$$\alpha_{22}^{(4)} = \frac{1}{V^3} \underbrace{\int_V d\vec{r}_3}_{V} \underbrace{\int_V \frac{e^{i\left[\vec{k}_s.\vec{r}_1 + kr_1\right]}}{r_1} d\vec{r}_1}_{I} \underbrace{\int_V \frac{e^{i\left[\vec{k}_i.\vec{r}_2 - kr_2\right]}}{r_2} d\vec{r}_2}_{I^*} \tag{3.98}$$

where the first integral is equal to volume V. Also, the last two integrals are conjugate of each other (Note that $\vec{k}_s$ and $\vec{k}_i$ are in general different so they are conjugate of each other, too). Hence, with respect to the equivalence $I.I^* = |I|^2$, $\alpha_{22}^{(4)}$ is stated as

$$\alpha_{22}^{(4)} = \frac{1}{V^2}\left|\int_V \frac{e^{i(\vec{k}_s.\vec{r}+kr)}}{r}d\vec{r}\right|^2 \tag{3.99}$$

This result is the same as the result of $\alpha_{22}^{(3)}$. In other words, $\alpha_{22}^{(3)}$ is equal to $\alpha_{22}^{(4)}$:

$$\boxed{\alpha_{22}^{(4)} = \frac{1}{V^2}\left|\int_V \frac{e^{i(\vec{k}_s.\vec{r}+kr)}}{r}d\vec{r}\right|^2 = \alpha_{22}^{(3)}} \tag{3.100}$$

3.2.1.5 Case 5: $m' = m, n' \neq m \,\&\, n' \neq n$

Case 5 is defined by the condition $m' = m, n' \neq m \,\&\, n' \neq n$. In order to get a result, we insert *m* instead of m' into Eq. (3.47) as follows:

$$\alpha_{22}^{(5)} =< e^{i\vec{k}_s.(\vec{r}_{n'}-\vec{r}_n)} e^{i\vec{k}_i.(\vec{r}_m-\vec{r}_m)} \frac{e^{ik|\vec{r}_n-\vec{r}_m|}}{|\vec{r}_n-\vec{r}_m|}\frac{e^{-ik|\vec{r}_{n'}-\vec{r}_m|}}{|\vec{r}_{n'}-\vec{r}_m|} > \tag{3.101}$$

which can be rearranged into the form:

$$\alpha_{22}^{(5)} =< e^{i\vec{k}_s.(\vec{r}_{n'}-\vec{r}_n)} e^{i\vec{k}_i.(\vec{r}_m-\vec{r}_m)} \frac{e^{ik|\vec{r}_m-\vec{r}_n|}}{|\vec{r}_m-\vec{r}_n|}\frac{e^{-ik|\vec{r}_m-\vec{r}_{n'}|}}{|\vec{r}_m-\vec{r}_{n'}|} > \tag{3.102}$$

$$\alpha_{22}^{(5)} =< e^{i\vec{k}_s.(\vec{r}_{n'}-\vec{r}_n)} e^{i\vec{k}_i.(0)} \frac{e^{ik|\vec{r}_m-\vec{r}_n|}}{|\vec{r}_m-\vec{r}_n|}\frac{e^{-ik|\vec{r}_m-\vec{r}_{n'}|}}{|\vec{r}_m-\vec{r}_{n'}|} > \tag{3.103}$$

We obtain an ensemble average of $e^{i\vec{k}_s.(\vec{r}_{n'}-\vec{r}_n)} \frac{e^{ik|\vec{r}_m-\vec{r}_n|}}{|\vec{r}_m-\vec{r}_n|}\frac{e^{-ik|\vec{r}_m-\vec{r}_{n'}|}}{|\vec{r}_m-\vec{r}_{n'}|}$ devoted by $\alpha_{22}^{(5)}$:

$$\alpha_{22}^{(5)} =< e^{i\vec{k}_s.(\vec{r}_{n'}-\vec{r}_n)} \frac{e^{ik|\vec{r}_m-\vec{r}_n|}}{|\vec{r}_m-\vec{r}_n|}\frac{e^{-ik|\vec{r}_m-\vec{r}_{n'}|}}{|\vec{r}_m-\vec{r}_{n'}|} > \tag{3.104}$$

Expression $e^{i\vec{k}_s.(\vec{r}_{n'}-\vec{r}_n)}\left[e^{ik|\vec{r}_m-\vec{r}_n|}/|\vec{r}_m-\vec{r}_n|\right]\left[e^{-ik|\vec{r}_m-\vec{r}_{n'}|}/|\vec{r}_m-\vec{r}_{n'}|\right]$ is multiplied with the probability density function $p(\vec{r}_m,\vec{r}_n,\vec{r}_{n'})$ and then integrated to obtain its ensemble average:

$$\alpha_{22}^{(5)} =< e^{i\vec{k}_s.(\vec{r}_{n'}-\vec{r}_n)} \frac{e^{ik|\vec{r}_m-\vec{r}_n|}}{|\vec{r}_m-\vec{r}_n||\vec{r}_m-\vec{r}_{n'}|} \frac{e^{-ik|\vec{r}_m-\vec{r}_{n'}|}}{|\vec{r}_m-\vec{r}_{n'}|} >$$

$$\alpha_{22}^{(5)} = \iiint p(\vec{r}_m,\vec{r}_n,\vec{r}_{n'}) e^{i\vec{k}_s.(\vec{r}_{n'}-\vec{r}_n)} \frac{e^{ik|\vec{r}_m-\vec{r}_n|}}{|\vec{r}_m-\vec{r}_n||\vec{r}_m-\vec{r}_{n'}|} \frac{e^{-ik|\vec{r}_m-\vec{r}_{n'}|}}{|\vec{r}_m-\vec{r}_{n'}|} d\vec{r}_m d\vec{r}_n d\vec{r}_{n'} \tag{3.105}$$

$$\alpha_{22}^{(5)} = \iiint p(\vec{r}_m,\vec{r}_n,\vec{r}_{n'}) e^{i\vec{k}_s.(\vec{r}_{n'}-\vec{r}_n)} \frac{e^{ik|\vec{r}_m-\vec{r}_n|}}{|\vec{r}_m-\vec{r}_n||\vec{r}_m-\vec{r}_{n'}|} \frac{e^{-ik|\vec{r}_m-\vec{r}_{n'}|}}{|\vec{r}_m-\vec{r}_{n'}|} d\vec{r}_m d\vec{r}_n d\vec{r}_{n'}$$

This integral is quite difficult to compute. Therefore, we make change of variables in the following manner:

$$\boxed{\begin{aligned} &\vec{r}_1 = \vec{r}_m - \vec{r}_n \\ &\vec{r}_2 = \vec{r}_m - \vec{r}_{n'} \quad ==> \vec{r}_1 - \vec{r}_2 = \vec{r}_{n'} - \vec{r}_n \\ &\vec{r}_3 = \frac{\vec{r}_m + \vec{r}_{n'}}{2} \\ &d\vec{r}_1 d\vec{r}_2 d\vec{r}_3 = d\vec{r}_m d\vec{r}_n d\vec{r}_{n'} \quad \left|J(\vec{r}_1,\vec{r}_2,\vec{r}_3)\right| = 1 \end{aligned}} \tag{3.106}$$

After the change of variables and using joint probability density function of three point scatterers $p(\vec{r}_m,\vec{r}_n,\vec{r}_{n'}) = p(\vec{r}_m)p(\vec{r}_n)p(\vec{r}_{n'}) = 1/V^3$, we have

$$\alpha_{22}^{(5)} = \frac{1}{V^3} \iiint e^{i\vec{k}_s.(\vec{r}_1-\vec{r}_2)} \frac{e^{ik|\vec{r}_1|}}{|\vec{r}_1|} \frac{e^{-ik|\vec{r}_2|}}{|\vec{r}_2|} d\vec{r}_1 d\vec{r}_2 d\vec{r}_3 \tag{3.107}$$

$$\alpha_{22}^{(5)} = \frac{1}{V^3} \int_V d\vec{r}_3 \iint_V \frac{e^{i\vec{k}_s.(\vec{r}_1-\vec{r}_2)} e^{ik(r_1-r_2)}}{r_1 r_2} d\vec{r}_1 d\vec{r}_2 \tag{3.108}$$

Now, the above integral is quite complicated. Thus, we separate it into component parts as follows:

$$\alpha_{22}^{(5)} = \frac{1}{V^3} \underbrace{\int_V d\vec{r}_3}_{V} \underbrace{\int_V \frac{e^{i\vec{k}_s.(\vec{r}_1)} e^{ik(r_1)}}{r_1} d\vec{r}_1}_{I} \underbrace{\int_V \frac{e^{-i\vec{k}_s.(\vec{r}_2)} e^{-ik(r_2)}}{r_2} d\vec{r}_2}_{I^*} \tag{3.109}$$

where the first integral is equal to volume V. Also, the last two integrals are conjugate of each other. Hence, with respect to the equivalence $I.I^* = |I|^2$, $\alpha_{22}^{(5)}$ is stated as

$$\alpha_{22}^{(5)} = \frac{1}{V^2} \left| \int_V \frac{e^{i(\vec{k}_s.\vec{r}+kr)}}{r} d\vec{r} \right|^2 \tag{3.110}$$

This result is the same as the result of $\alpha_{22}^{(3)}$. In other words, $\alpha_{22}^{(3)}$ is equal to $\alpha_{22}^{(5)}$:

$$\boxed{\alpha_{22}^{(5)} = \frac{1}{V^2}\left|\int_V \frac{e^{i(\vec{k}_s.\vec{r}+kr)}}{r}d\vec{r}\right|^2 = \alpha_{22}^{(3)}} \tag{3.111}$$

3.2.1.6 Case 6: $m' = n, n' \neq m \,\&\, n' \neq n$

Case 6 is defined by the condition $m' = n, n' \neq m \,\&\, n' \neq n$. In order to get a result, we insert *n* instead of m' into Eq. (3.47) as follows:

$$\alpha_{22}^{(6)} = < e^{i\vec{k}_s.(\vec{r}_{n'}-\vec{r}_n)} e^{i\vec{k}_i.(\vec{r}_m-\vec{r}_n)} \frac{e^{ik|\vec{r}_n-\vec{r}_m|}}{|\vec{r}_n-\vec{r}_m|} \frac{e^{-ik|\vec{r}_{n'}-\vec{r}_n|}}{|\vec{r}_{n'}-\vec{r}_n|} > \tag{3.112}$$

which can be rearranged into the form:

$$\alpha_{22}^{(6)} = < e^{i\vec{k}_s.(\vec{r}_{n'}-\vec{r}_n)} e^{i\vec{k}_i.(\vec{r}_m-\vec{r}_n)} \frac{e^{ik|\vec{r}_m-\vec{r}_n|}}{|\vec{r}_m-\vec{r}_n|} \frac{e^{-ik|\vec{r}_n-\vec{r}_{n'}|}}{|\vec{r}_n-\vec{r}_{n'}|} > \tag{3.113}$$

Expression $e^{i\vec{k}_s.(\vec{r}_{n'}-\vec{r}_n)} e^{i\vec{k}_i.(\vec{r}_m-\vec{r}_n)} \left[e^{ik|\vec{r}_m-\vec{r}_n|} / |\vec{r}_m-\vec{r}_n|\right]\left[e^{-ik|\vec{r}_n-\vec{r}_{n'}|} / |\vec{r}_n-\vec{r}_{n'}|\right]$ is multiplied with the probability density function $p(\vec{r}_m, \vec{r}_n, \vec{r}_{n'})$ and then integrated to obtain its ensemble average:

$$\begin{aligned}
\alpha_{22}^{(6)} &= < e^{i\vec{k}_s.(\vec{r}_{n'}-\vec{r}_n)} e^{i\vec{k}_i.(\vec{r}_m-\vec{r}_n)} \frac{e^{ik|\vec{r}_m-\vec{r}_n|}}{|\vec{r}_m-\vec{r}_n|} \frac{e^{-ik|\vec{r}_n-\vec{r}_{n'}|}}{|\vec{r}_n-\vec{r}_{n'}|} > \\
\alpha_{22}^{(6)} &= \iiint p(\vec{r}_m, \vec{r}_n, \vec{r}_{n'}) e^{i\vec{k}_s.(\vec{r}_{n'}-\vec{r}_n)} e^{i\vec{k}_i.(\vec{r}_m-\vec{r}_n)} \frac{e^{ik|\vec{r}_m-\vec{r}_n|}}{|\vec{r}_m-\vec{r}_n|} \frac{e^{-ik|\vec{r}_n-\vec{r}_{n'}|}}{|\vec{r}_n-\vec{r}_{n'}|} d\vec{r}_m d\vec{r}_n d\vec{r}_{n'} \\
\alpha_{22}^{(6)} &= \iiint p(\vec{r}_m, \vec{r}_n, \vec{r}_{n'}) e^{i\vec{k}_s.(\vec{r}_{n'}-\vec{r}_n)} e^{i\vec{k}_i.(\vec{r}_m-\vec{r}_n)} \frac{e^{ik|\vec{r}_m-\vec{r}_n|}}{|\vec{r}_m-\vec{r}_n|} \frac{e^{-ik|\vec{r}_n-\vec{r}_{n'}|}}{|\vec{r}_n-\vec{r}_{n'}|} d\vec{r}_m d\vec{r}_n d\vec{r}_{n'}
\end{aligned} \tag{3.114}$$

This integral is quite difficult to compute. Therefore, we make change of variables in the following manner:

$$\boxed{\begin{aligned}
&\vec{r}_1 = \vec{r}_m - \vec{r}_n \\
&\vec{r}_2 = \vec{r}_{n'} - \vec{r}_n \\
&\vec{r}_3 = \frac{\vec{r}_m + \vec{r}_{n'}}{2} \\
&d\vec{r}_1 d\vec{r}_2 d\vec{r}_3 = d\vec{r}_m d\vec{r}_n d\vec{r}_{n'} \quad \left|J(\vec{r}_1, \vec{r}_2, \vec{r}_3)\right| = 1
\end{aligned}} \tag{3.115}$$

After the change of variables and using joint probability density function of three point scatterers $p(\vec{r}_m,\vec{r}_n,\vec{r}_{n'}) = p(\vec{r}_m)p(\vec{r}_n)p(\vec{r}_{n'}) = 1/V^3$, we have

$$\alpha_{22}^{(6)} = \frac{1}{V^3}\iiint e^{i\vec{k}_s.(\vec{r}_2)} e^{i\vec{k}_i.(\vec{r}_1)} \frac{e^{ik|\vec{r}_1|}}{|\vec{r}_1|}\frac{e^{-ik|\vec{r}_2|}}{|\vec{r}_2|} d\vec{r}_1 d\vec{r}_2 d\vec{r}_3 \tag{3.116}$$

$$\alpha_{22}^{(6)} = \frac{1}{V^3}\iiint e^{i\vec{k}_s.\vec{r}_2} e^{i\vec{k}_i.\vec{r}_1} \frac{e^{ikr_1}}{r_1}\frac{e^{-ikr_2}}{r_2} d\vec{r}_1 d\vec{r}_2 d\vec{r}_3 \tag{3.117}$$

$$\alpha_{22}^{(6)} = \frac{1}{V^3}\int_V d\vec{r}_3 \int_V e^{i\vec{k}_i.\vec{r}_1}\frac{e^{ikr_1}}{r_1} d\vec{r}_1 \int_V e^{i\vec{k}_s.\vec{r}_2}\frac{e^{-ikr_2}}{r_2} d\vec{r}_2 \tag{3.118}$$

Now, the above integral is quite complicated. Thus, we separate it into component parts as follows:

$$\alpha_{22}^{(6)} = \frac{1}{V^3}\underbrace{\int_V d\vec{r}_3}_{V}\underbrace{\int_V e^{i\vec{k}_i.\vec{r}_1}\frac{e^{ikr_1}}{r_1} d\vec{r}_1}_{I}\underbrace{\int_V e^{i\vec{k}_s.\vec{r}_2}\frac{e^{-ikr_2}}{r_2} d\vec{r}_2}_{I^*} \tag{3.119}$$

where the first integral is equal to volume V. Also, the last two integrals are conjugate of each other (Note that $\vec{k}_s$ and $\vec{k}_i$ are in general different so they are conjugate of each other, too). Hence, with respect to the equivalence $I.I^* = |I|^2$, $\alpha_{22}^{(6)}$ is stated as

$$\alpha_{22}^{(6)} = \frac{1}{V^2}\left|\int_V \frac{e^{i(\vec{k}_i.\vec{r}+kr)}}{r} d\vec{r}\right|^2 \tag{3.120}$$

This result is the same as the result of $\alpha_{22}^{(3)}$. In other words, $\alpha_{22}^{(3)}$ is equal to $\alpha_{22}^{(6)}$:

$$\boxed{\alpha_{22}^{(6)} = \frac{1}{V^2}\left|\int_V \frac{e^{i(\vec{k}_i.\vec{r}+kr)}}{r} d\vec{r}\right|^2 = \alpha_{22}^{(3)}} \tag{3.121}$$

Finally, we note that the last four results of the ensemble averages are equal to each other. This relation can be stated as

$$\boxed{\alpha_{22}^{(3)} = \alpha_{22}^{(4)} = \alpha_{22}^{(5)} = \alpha_{22}^{(6)}} \tag{3.122}$$

3.2.1.7 Case 7: $m' \neq m, m' \neq n, n' \neq m \,\&\, n' \neq n$

Case 7 is defined by the condition $m' \neq m, m' \neq n, n' \neq m \,\&\, n' \neq n$. In order to get a result, we use the general formula of $\alpha_{22}^{(c)}$ as follows:

$$\alpha_{22}^{(7)} = < e^{i\vec{k}_s.(\vec{r}_{n'}-\vec{r}_n)} e^{i\vec{k}_i.(\vec{r}_m-\vec{r}_{m'})} \frac{e^{ik|\vec{r}_n-\vec{r}_m|}}{|\vec{r}_n-\vec{r}_m|} \frac{e^{-ik|\vec{r}_{n'}-\vec{r}_{m'}|}}{|\vec{r}_{n'}-\vec{r}_{m'}|} > \tag{3.123}$$

which can be rearranged into the form:

$$\alpha_{22}^{(7)} = < e^{i\vec{k}_s.(\vec{r}_{n'}-\vec{r}_n)} e^{i\vec{k}_i.(\vec{r}_m-\vec{r}_{m'})} \frac{e^{ik|\vec{r}_m-\vec{r}_n|}}{|\vec{r}_m-\vec{r}_n|} \frac{e^{-ik|\vec{r}_{m'}-\vec{r}_{n'}|}}{|\vec{r}_{m'}-\vec{r}_{n'}|} > \tag{3.124}$$

Expression $e^{i\vec{k}_s.(\vec{r}_{n'}-\vec{r}_n)} e^{i\vec{k}_i.(\vec{r}_m-\vec{r}_{m'})} \left[e^{ik|\vec{r}_m-\vec{r}_n|}/|\vec{r}_m-\vec{r}_n|\right]\left[e^{-ik|\vec{r}_{m'}-\vec{r}_{n'}|}/|\vec{r}_{m'}-\vec{r}_{n'}|\right]$ is multiplied with the probability density function $p(\vec{r}_m, \vec{r}_n, \vec{r}_{m'}, \vec{r}_{n'})$ and then integrated to obtain its ensemble average:

$$\begin{aligned}
\alpha_{22}^{(7)} &= < e^{i\vec{k}_s.(\vec{r}_{n'}-\vec{r}_n)} e^{i\vec{k}_i.(\vec{r}_m-\vec{r}_{m'})} \frac{e^{ik|\vec{r}_m-\vec{r}_n|}}{|\vec{r}_m-\vec{r}_n|} \frac{e^{-ik|\vec{r}_{m'}-\vec{r}_{n'}|}}{|\vec{r}_{m'}-\vec{r}_{n'}|} > \\
\alpha_{22}^{(7)} &= \int\int\int\int p(\vec{r}_m, \vec{r}_n, \vec{r}_{m'}, \vec{r}_{n'}) e^{i\vec{k}_s.(\vec{r}_{n'}-\vec{r}_n)} e^{i\vec{k}_i.(\vec{r}_m-\vec{r}_{m'})} \frac{e^{ik|\vec{r}_m-\vec{r}_n|}}{|\vec{r}_m-\vec{r}_n|} \frac{e^{-ik|\vec{r}_{m'}-\vec{r}_{n'}|}}{|\vec{r}_{m'}-\vec{r}_{n'}|} d\vec{r}_m d\vec{r}_n d\vec{r}_{m'} d\vec{r}_{n'} \\
\alpha_{22}^{(7)} &= \int\int\int\int p(\vec{r}_m, \vec{r}_n, \vec{r}_{m'}, \vec{r}_{n'}) e^{i\vec{k}_s.(\vec{r}_{n'}-\vec{r}_n)} e^{i\vec{k}_i.(\vec{r}_m-\vec{r}_{m'})} \frac{e^{ik|\vec{r}_m-\vec{r}_n|}}{|\vec{r}_m-\vec{r}_n|} \frac{e^{-ik|\vec{r}_{m'}-\vec{r}_{n'}|}}{|\vec{r}_{m'}-\vec{r}_{n'}|} d\vec{r}_m d\vec{r}_n d\vec{r}_{m'} d\vec{r}_{n'}
\end{aligned} \tag{3.125}$$

This integral is quite difficult to compute. Therefore, we make change of variables in the following manner:

$$\begin{aligned}
&\vec{r}_1 = \vec{r}_m - \vec{r}_n, \quad \vec{r}_2 = \vec{r}_{m'} - \vec{r}_{n'} \\
&\vec{r}_3 = \frac{\vec{r}_m + \vec{r}_n}{2}, \quad \vec{r}_4 = -\frac{\vec{r}_{m'} + \vec{r}_{n'}}{2} \\
&\vec{r}_{n'} - \vec{r}_n = \frac{1}{2}\vec{r}_1 - \frac{1}{2}\vec{r}_2 - \vec{r}_3 - \vec{r}_4 \\
&\vec{r}_m - \vec{r}_{m'} = \frac{1}{2}\vec{r}_1 - \frac{1}{2}\vec{r}_2 + \vec{r}_3 + \vec{r}_4 \\
&d\vec{r}_1 d\vec{r}_2 d\vec{r}_3 d\vec{r}_4 = d\vec{r}_m d\vec{r}_n d\vec{r}_{m'} d\vec{r}_{n'} \quad \left|J(\vec{r}_1, \vec{r}_2, \vec{r}_3, \vec{r}_4)\right| = 1
\end{aligned} \tag{3.126}$$

After the change of variables and using joint probability density function of four point scatterers $p(\vec{r}_m, \vec{r}_n, \vec{r}_{m'}, \vec{r}_{n'}) = p(\vec{r}_m)p(\vec{r}_n)p(\vec{r}_{m'})p(\vec{r}_{n'}) = 1/V^4$, we have

$$\alpha_{22}^{(7)} = \frac{1}{V^4}\int\int\int\int e^{i\vec{k}_s.(\frac{1}{2}\vec{r}_1-\frac{1}{2}\vec{r}_2-\vec{r}_3-\vec{r}_4)} e^{i\vec{k}_i.(\frac{1}{2}\vec{r}_1-\frac{1}{2}\vec{r}_2+\vec{r}_3+\vec{r}_4)} \frac{e^{ik|\vec{r}_1|}}{|\vec{r}_1|}\frac{e^{-ik|\vec{r}_2|}}{|\vec{r}_2|} d\vec{r}_1 d\vec{r}_2 d\vec{r}_3 d\vec{r}_4 \quad (3.127)$$

which is separated into component parts, and then we have

$$\begin{aligned}\alpha_{22}^{(7)} = \frac{1}{V^4}\int_V e^{i\vec{k}_s.(\frac{1}{2}\vec{r}_1)} e^{i\vec{k}_i.(\frac{1}{2}\vec{r}_1)} \frac{e^{ikr_1}}{r_1} d\vec{r}_1 \int_V e^{i\vec{k}_s.(-\frac{1}{2}\vec{r}_2)} e^{i\vec{k}_i.(-\frac{1}{2}\vec{r}_2)} \frac{e^{-ikr_2}}{r_2} d\vec{r}_2 \\ \int_V e^{i\vec{k}_s.(-\vec{r}_3)} e^{i\vec{k}_i.(\vec{r}_3)} d\vec{r}_3 \int_V e^{i\vec{k}_s.(-\vec{r}_4)} e^{i\vec{k}_i.(\vec{r}_4)} d\vec{r}_4\end{aligned} \quad (3.128)$$

$$\begin{aligned}\alpha_{22}^{(7)} = \frac{1}{V^4} \underbrace{\int_V \frac{e^{i\left[(\vec{k}_s+\vec{k}_i).(\vec{r}_1/2)+kr_1\right]}}{r_1} d\vec{r}_1}_{I_1} \underbrace{\int_V \frac{e^{-i\left[(\vec{k}_s+\vec{k}_i).(\vec{r}_2/2)+kr_2\right]}}{r_2} d\vec{r}_2}_{I_1^*} \\ \underbrace{\int_V e^{i(\vec{k}_i-\vec{k}_s).\vec{r}_3} d\vec{r}_3}_{I_2} \underbrace{\int_V e^{i(\vec{k}_i-\vec{k}_s).\vec{r}_4} d\vec{r}_4}_{I_2^*}\end{aligned} \quad (3.129)$$

where the first two and the last two integrals are conjugate of each other (Note that $\vec{k}_s$ and $\vec{k}_i$ are in general different so they are conjugate of each other, too). With respect to the equivalences $I_1.I_1^* = |I_1|^2$ and $I_2.I_2^* = |I_2|^2$, $\alpha_{22}^{(7)}$ is stated as

$$\alpha_{22}^{(7)} = \frac{1}{V^4}\left|\int_V \frac{e^{i\left[(\vec{k}_s+\vec{k}_i).(\vec{r}_1/2)+kr_1\right]}}{r_1} d\vec{r}_1\right|^2 \left|\int_V e^{i(\vec{k}_i-\vec{k}_s).\vec{r}_3} d\vec{r}_3\right|^2 \quad (3.130)$$

Now, the above integral is quite complicated. It is expressed by

$$\alpha_{22}^{(7)} = \frac{1}{V^4} \underbrace{\left|\int_V \frac{e^{i\left[(\vec{k}_s+\vec{k}_i).(\vec{r}_1/2)+kr_1\right]}}{r_1} d\vec{r}_1\right|^2}_{I_3^2} \underbrace{\left|\int_V e^{i(\vec{k}_i-\vec{k}_s).\vec{r}_3} d\vec{r}_3\right|^2}_{I_4^2} \quad (3.131)$$

After making use of the sum of the incident and scattered wave vectors $\vec{\sigma} = \vec{k}_s + \vec{k}_i = 2k\sin(\theta_s/2)\hat{\sigma}$, the solution to the integral I_3^2 can be stated as

$$I_3^2 = \frac{8\pi^2}{\sin^2\frac{\theta_s}{2}\cos^4\frac{\theta_s}{2}k^4}\left[\begin{array}{l} 3-\cos(\theta_s)-2\cos(ka)\cos(ka\sin\frac{\theta_s}{2})+ \\ 2\cos(ka)\cos(\theta_s)\cos(ka\sin\frac{\theta_s}{2})- \\ \cos^2(ka\sin\frac{\theta_s}{2})-\cos\theta_s\cos^2(ka\sin\frac{\theta_s}{2})- \\ 4\sin(ka)\sin\frac{\theta_s}{2}\sin(ka\sin\frac{\theta_s}{2}) \end{array}\right] \quad (3.132)$$

Note that, at the backscattering direction ($\theta_s \to 0$), the result of the integral I_3^2 approaches

$$\lim_{\theta_s\to 0} I_3^2 = \frac{32\pi^2}{k^4}\left[1+\frac{a^2k^2}{2}-\cos(ka)-ka\sin(ka)\right] \quad (3.133)$$

After the functional graphic of the term $\left[1+\left(a^2k^2/2\right)-\cos(ka)-ka\sin(ka)\right]$ is analyzed, it is evaluated that this term is always smaller than $\left[a^2k^2\right]$. After this examination, I_3^2 can be given by

$$\lim_{\theta_s\to 0} I_3^2 \le \frac{32\pi^2}{k^4}\left[a^2k^2\right] \quad (3.134)$$

Finally, at the backscattering direction ($\theta_s \to 0$), the result of the integral I_3^2 attains its max value as follows:

$$I_3^2 \le \frac{32\pi^2}{k^2}a^2 \quad (3.135)$$

After making use of the sum of the incident and scattered wave vectors $\vec{\sigma} = \vec{k}_s + \vec{k}_i = 2k\sin(\theta_s/2)\hat{\sigma}$, the solution to the integral I_4^2 can be stated as

$$I_4^2 = 16\pi^2a^6\left[\frac{x\cos x-\sin x}{x^3}\right]^2 \quad ; x = 2ka\cos(\frac{\theta_s}{2}) \quad (3.136)$$

At the backscattering direction ($\theta_s \to 0$), this term $x = 2ka\cos(\theta_s/2)$ is to be $x = 2ka$ and also the result of the integral I_4^2 is

$$\lim_{\theta_s \to 0} I_4^2 = 16\pi^2 a^6 \left[\frac{(2ka)(\cos 2ka) - (\sin 2ka)}{(2ka)^3} \right]^2 \tag{3.137}$$

When we consider infinite volume assumption for the sphere ($a \to \infty$), the term $\left[((2ka)(\cos 2ka) - (\sin 2ka))/((2ka)^3)\right]^2$ can approach this term $\left[1/(2ka)^2\right]^2$. Finally, Note that, at the backscattering direction ($\theta_s \to 0$), the result of the integral I_4^2 approaches

$$I_4^2 \approx \frac{\pi^2 a^2}{k^4} \tag{3.138}$$

If we insert the approximate values of these integrals I_3^2 and I_4^2 into Eq. (3.131) $\left(\alpha_{22}^{(7)} = (1/V^4) I_3^2 I_4^2\right)$, $\alpha_{22}^{(7)}$ can be stated as

$$\alpha_{22}^{(7)} \le \frac{1}{V^4} \frac{32\pi^2}{k^2} a^2 \frac{\pi^2 a^2}{k^4} \tag{3.139}$$

After expressing the volume of the sphere in terms of its radius as $V = (4/3)\pi a^3$ and simplifying the above equation, $\alpha_{22}^{(7)}$ is given by

$$\boxed{\alpha_{22}^{(7)} \le \frac{81}{8k^6 a^8}} \tag{3.140}$$

After finding the values of seven possible cases, we can now calculate $\alpha_{22}^{(c)}$ by using below expression:

$$\alpha_{22}^{(c)} = N(N-1)\begin{bmatrix} \alpha_{22}^{(1)} + \alpha_{22}^{(2)} + (N-2)\,\alpha_{22}^{(3)} + (N-2)\,\alpha_{22}^{(4)} + \\ (N-2)\,\alpha_{22}^{(5)} + (N-2)\,\alpha_{22}^{(6)} + (N-2)(N-3)\,\alpha_{22}^{(7)} \end{bmatrix} \tag{3.141}$$

Eq. (3.141) can be simplified by using the equality $\alpha_{22}^{(3)} = \alpha_{22}^{(4)} = \alpha_{22}^{(5)} = \alpha_{22}^{(6)}$

$$\alpha_{22}^{c} = N(N-1)\left[\alpha_{22}^{(1)} + \alpha_{22}^{(2)} + (N-2)\,4\alpha_{22}^{(3)} + (N-2)(N-3)\,\alpha_{22}^{(7)}\right] \tag{3.142}$$

After expressing the volume of the sphere in terms of its radius as $V = (4/3)\pi a^3$ and inserting the ensemble average terms of double scattering, $\alpha_{22}^{(c)}$ can be stated as

$$\alpha_{22}^{(c)} = \frac{k^2}{k^2} N(N-1) \left(\underbrace{\frac{3}{(a)^2}}_{\alpha_{22}^{(1)}} + \underbrace{\frac{3}{(a)^2} \frac{Si(a\sigma)}{a\sigma}}_{\alpha_{22}^{(2)}} + (N-2) 4 \underbrace{\frac{9}{4k^2 a^4}}_{\alpha_{22}^{(3)}} + (N-2)(N-3) \underbrace{\frac{81}{8k^6 a^8}}_{\alpha_{22}^{(7)}} \right) \tag{3.143}$$

Arranging Eq. (3.143), we have

$$\alpha_{22}^{(c)} = k^2 N(N-1) \left(\underbrace{\frac{3}{(ka)^2}}_{\alpha_{22}^{(1)}/k^2} + \underbrace{\frac{3}{(ka)^2} \frac{Si(a\sigma)}{a\sigma}}_{\alpha_{22}^{(2)}/k^2} + (N-2) \underbrace{\frac{9}{(ka)^4}}_{4\alpha_{22}^{(3)}/k^2} + (N-2)(N-3) \underbrace{\frac{81}{8(ka)^8}}_{\alpha_{22}^{(7)}/k^2} \right) \tag{3.144}$$

After inserting this constant $f = [i4\pi T]/k$ into Eq. (3.46), we get

$$< I_{22} >= \frac{T^4}{k^4 r_a^2} \left[\alpha_{22}^{(c)} \right] \tag{3.145}$$

Substituting Eq. (3.144) into Eq. (3.145), we obtain the mean field intensity due to double scattering from spherical distribution:

$$\boxed{< I_{22} >= \frac{|T|^4}{(kr_a)^2} N(N-1) \left(\underbrace{\frac{3}{(ka)^2}}_{\alpha_{22}^{(1)}/k^2} + \underbrace{\frac{3}{(ka)^2} \frac{Si(a\sigma)}{a\sigma}}_{\alpha_{22}^{(2)}/k^2} + (N-2) \underbrace{\frac{9}{(ka)^4}}_{4\alpha_{22}^{(3)}/k^2} + (N-2)(N-3) \underbrace{\frac{81}{8(ka)^8}}_{\alpha_{22}^{(7)}/k^2} \right)} \tag{3.146}$$

3.2.1.8 Some Results about Double Scattering

I) We expect $\alpha_{22}^{(2)}$ to give the backscattering enhancement. As far as infinite volume assumption ($a \to \infty$) is concerned, $\alpha_{22}^{(2)}$ approaches $\pi^2 / [Vk \sin(\theta_s/2)]$. Due to its form, a narrow peak in the backscattering direction ($\theta_s \to 0$) is observed.

$$\lim_{a\to\infty}\alpha_{22}^{(2)}=\frac{\pi^2}{Vk\sin\left(\frac{\theta_s}{2}\right)} \tag{3.147}$$

$$\lim_{\theta_s\to 0}\frac{\pi^2}{Vk\sin\left(\frac{\theta_s}{2}\right)}=\infty \tag{3.148}$$

II) The mean field intensity due to double scattering is stated as

$$<I_{22}>=\frac{|T|^4}{(kr_a)^2}N(N-1)\left\{\begin{array}{l}\frac{3}{(ka)^2}+\frac{3}{(ka)^2}\frac{Si(a\sigma)}{a\sigma}+(N-2)\frac{9}{(ka)^4}+\\(N-2)(N-3)\frac{81}{8(ka)^8}\end{array}\right\} \tag{3.149}$$

If we want the effect of $\alpha_{22}^{(3-6)}$ to be negligible as compared to $\alpha_{22}^{(7)}$, we must have

$$(N-2)\frac{9}{(ka)^4}>>(N-2)(N-3)\frac{81}{8(ka)^8} \tag{3.150}$$

Considering some assumptions, we can find relationship between the diameter of sphere $D=2a$ and the number of scatterers N in the following manner:

$$\begin{aligned}&N\frac{9}{(ka)^4}>>N^2\frac{81}{8(ka)^8}\\&(ka)^4>>N\frac{9}{8}\\&(ka)^4>N\frac{90}{8}\\&(ka)^4>N(11.25)\end{aligned} \tag{3.151}$$

The effect of the third term $\alpha_{22}^{(3-6)}$ is negligible as compared to that of the last term $\alpha_{22}^{(7)}$ if the diameter of sphere $(ka)^4$ is larger than the number of scatterers $N(11.25)$, such as $(ka)^{(4)}>N(11.25)$. So, an approximate formula of the mean field intensity due to double scattering is stated as

$$<I_{22}>\cong\frac{|T|^4}{(kr_a)^2}N(N-1)\left\{\frac{3}{(ka)^2}+\frac{3}{(ka)^2}\frac{Si(a\sigma)}{a\sigma}+(N-2)\frac{9}{(ka)^4}\right\} \tag{3.152}$$

where $(ka)^{(4)} > N(11.25)$.

III) If we want the effect of $\alpha_{22}^{(3-6)}$ to be negligible as compared to that of $\alpha_{22}^{(1)}$ and $\alpha_{22}^{(2)}$, we must have

$$\frac{3}{(ka)^2} >> (N-2)\frac{9}{(ka)^4}$$
$$(ka)^2 > 30N \tag{3.153}$$

We also note that this inequality ensures that the last term $\alpha_{22}^{(7)}$ is also much smaller than both the first term $\alpha_{22}^{(1)}$ and the second term $\alpha_{22}^{(2)}$. Therefore, $\alpha_{22}^{(7)}$ is negligible as compared to the first two terms. The effects of the third term $\alpha_{22}^{(3-6)}$ and the last term $\alpha_{22}^{(7)}$ are negligible as compared to that of both the first term $\alpha_{22}^{(1)}$ and the second term $\alpha_{22}^{(2)}$ if the diameter of sphere $(ka)^2$ is larger than the number of scatterers $30N$, like $(ka)^2 > 30N$. So, the approximate formula of the mean field intensity due to double scattering is stated as

$$\boxed{< I_{22} > \cong \frac{|T|^4}{(kr_a)^2} N(N-1)\left\{\frac{3}{(ka)^2} + \frac{3}{(ka)^2}\frac{Si(a\sigma)}{a\sigma}\right\}} \tag{3.154}$$

where $(ka)^2 > 30N$. As can be seen from the above equation, $< I_{22} >$ has the Sine integral divided by $a\sigma$ and also σ depends on the scattering angle. Therefore, we expect $< I_{22} >$ to give the backscattering enhancement. In previous section, we present that this Sine integral term $[Si(a\sigma)]/a\sigma$ comes from $\alpha_{22}^{(2)}$. We note that the double scattering phenomenon is the first multiple scattering mechanism in the distribution volume and the approximate formula of the mean field intensity due to double scattering is obtained in an analytical manner and given by Eq. (3.154). In order to depict this case, we arrange Eq. (3.154) and then we get

$$< I_{22} > \cong \frac{N^2 |T|^4}{(kr_a)^2}\frac{3}{(ka)^2}\left\{1 + \frac{Si(a\sigma)}{a\sigma}\right\} \tag{3.155}$$

$$< I_{22} > \frac{(kr_a)^2}{|T|^4} \cong N^2 \frac{3}{(ka)^2}\left\{1+\frac{Si(a\sigma)}{a\sigma}\right\} \qquad (3.156)$$

The above equation is shown in Figure 3.9 as a function of the scattering angle.

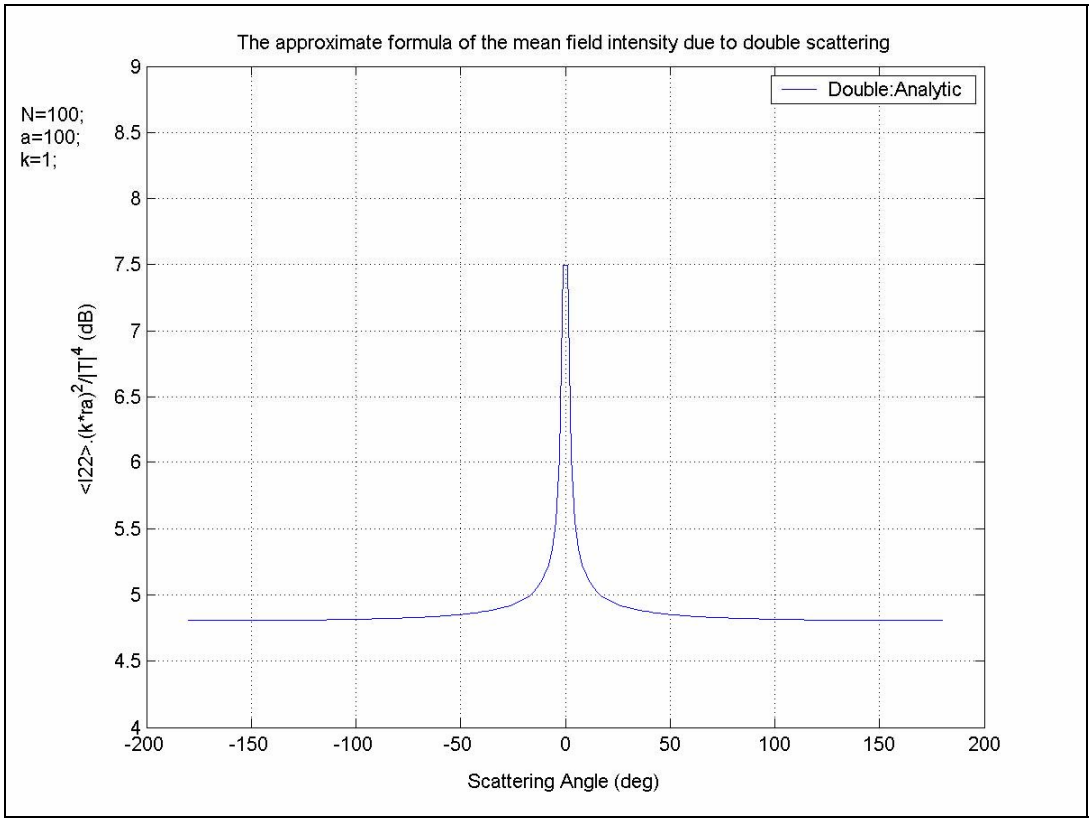

Figure 3.9: The approximate formula of the mean field intensity due to double scattering: N=100 and a=100.

In Figure 3.9, the approximate formula of the mean field intensity due to double scattering $< I_{22} >$ is given for N=100, a=100 and k=1 (note that $(ka)^2$ =10000; 30N=3000). As far as the backscattering enhancement is concerned, the approximate formula gives quiet satisfactory result.

IV) Define r to be the ratio of the mean field intensity in the backscattering direction to the mean field intensity at any other direction:

$$r = \frac{\text{The Field Intensity in the Backscattering Direction}}{\text{The Field Intensity in the Any Other Direction}}$$
$$r = \frac{< I_{22}(\theta_s = 0 >}{< I_{22}(\theta_s \neq 0, \pi >} \tag{3.157}$$

$$r \cong \frac{2 + \dfrac{3}{(ka)^2} N}{1 + \dfrac{3}{(ka)^2} N} \quad \Rightarrow \quad \lim_{N \to \infty} \frac{2 + \dfrac{3}{(ka)^2} N}{1 + \dfrac{3}{(ka)^2} N} = 1 \tag{3.158}$$

which becomes very small for large values of point scatterers number *N*. This means that if the point scatterers number *N* is getting larger, the backscattering enhancement is to disappear because of the shadow effect. We also note that the shadow effect is explained in Section 4.6 and we observed that same result for multiple scattering, too.

3.3 Mean Field Intensity due to Interaction of Single and Double Scattering Phenomenon

3.3.1 The Particles are Distributed within a Sphere

In Eq. (3.4), the mean field intensity due to interaction of single and double scattering is found as

$$< I_{12} >= 2\,\mathrm{Re} < \psi^{(1)}(\vec{r}_a)\psi^{(2)^*}(\vec{r}_a) > \tag{3.159}$$

Substituting the single scattered field $\psi^{(1)}(\vec{r}_a)$ and conjugate of the double scattered field $\psi^{(2)^*}(\vec{r}_a)$ expressions into Eq. (3.159), we have

$$< I_{12} >= 2\,\mathrm{Re} < \sum_{n=1}^{N} \sum_{\substack{m',n' \\ m' \neq n'}}^{N} \frac{-f\,|\,f\,|^2}{(4\pi)^3} \frac{e^{ik|\vec{r}_a - \vec{r}_n|}}{|\,\vec{r}_a - \vec{r}_n\,|} \frac{e^{-ik|\vec{r}_a - \vec{r}_{n'}|}}{|\,\vec{r}_a - \vec{r}_{n'}\,|} \frac{e^{-ik|\vec{r}_{n'} - \vec{r}_{m'}|}}{|\,\vec{r}_{n'} - \vec{r}_{m'}\,|} e^{i\vec{k}_i \cdot (\vec{r}_n - \vec{r}_{m'})} > \tag{3.160}$$

where the variable n is used for $\psi^{(1)}(\vec{r}_a)$ and the variables m' and n' are used for $\psi^{(2)^*}(\vec{r}_a)$. After arranging Eq. (3.160), we have

$$< I_{12} >= 2\,\mathrm{Re}\frac{-f\,|\,f\,|^2}{(4\pi)^3 r_a^2}\underbrace{\sum_{n=1}^{N}\sum_{\substack{m',n'\\ m'\neq n'}}^{N} < \frac{e^{-ik|\vec{r}_{n'}-\vec{r}_{m'}|}}{|\,\vec{r}_{n'}-\vec{r}_{m'}\,|} e^{-i\vec{k}_s.(\vec{r}_n-\vec{r}_{n'})} e^{i\vec{k}_i.(\vec{r}_n-\vec{r}_{m'})} >}_{\alpha_{12}^{(c)}}$$

$$< I_{12} >= 2\,\mathrm{Re}\frac{-f\,|\,f\,|^2}{(4\pi)^3 r_a^2}\underbrace{\sum_{n=1}^{N}\sum_{n'=1}^{N}\sum_{\substack{m'=1\\ m'\neq n'}}^{N} < \frac{e^{-ik|\vec{r}_{n'}-\vec{r}_{m'}|}}{|\,\vec{r}_{n'}-\vec{r}_{m'}\,|} e^{-i\vec{k}_s.(\vec{r}_n-\vec{r}_{n'})} e^{i\vec{k}_i.(\vec{r}_n-\vec{r}_{m'})} >}_{\alpha_{12}^{(c)}} \tag{3.161}$$

We can use shorthand symbol $\alpha_{12}^{(c)}$ in order to denote an ensemble average of $\sum_{n=1}^{N}\sum_{n'=1}^{N}\sum_{\substack{m'=1\\ m'\neq n'}}^{N}\frac{e^{-ik|\vec{r}_{n'}-\vec{r}_{m'}|}}{|\,\vec{r}_{n'}-\vec{r}_{m'}\,|} e^{-i\vec{k}_s.(\vec{r}_n-\vec{r}_{n'})} e^{i\vec{k}_i.(\vec{r}_n-\vec{r}_{m'})}$ which defines the interaction of single and double scattering expression for all cases and the superscript *c* stands for the cases that are defined below. The mean field intensity due to interaction of single and double scattering in Eq. (3.161) can be written in a simple way:

$$< I_{12} >= 2\,\mathrm{Re}\frac{-f\,|\,f\,|^2}{(4\pi)^3 r_a^2}\left[\alpha_{12}^{(c)}\right] \tag{3.162}$$

and $\alpha_{12}^{(c)}$ is stated clearly as

$$\boxed{\alpha_{12}^{(c)} = \sum_{n=1}^{N}\sum_{n'=1}^{N}\sum_{\substack{m'=1\\ m'\neq n'}}^{N} < \frac{e^{-ik|\vec{r}_{n'}-\vec{r}_{m'}|}}{|\,\vec{r}_{n'}-\vec{r}_{m'}\,|} e^{-i\vec{k}_s.(\vec{r}_n-\vec{r}_{n'})} e^{i\vec{k}_i.(\vec{r}_n-\vec{r}_{m'})} >} \tag{3.163}$$

The expression $\sum_{n=1}^{N}\sum_{n'=1}^{N}\sum_{\substack{m'=1\\ m'\neq n'}}^{N}\frac{e^{-ik|\vec{r}_{n'}-\vec{r}_{m'}|}}{|\,\vec{r}_{n'}-\vec{r}_{m'}\,|} e^{-i\vec{k}_s.(\vec{r}_n-\vec{r}_{n'})} e^{i\vec{k}_i.(\vec{r}_n-\vec{r}_{m'})}$ is to be multiplied with the probability density function $p(\vec{r}_n,\vec{r}_{m'},\vec{r}_{n'})$ and then integrated in order to calculate the expected value of $\alpha_{12}^{(c)}$. This resulting integral can be evaluated for three different possible cases which we consider separately in the following sections. Under these three possible cases $\alpha_{12}^{(c)}$ can be written as (see Figure 3.10) as follows:

$$\alpha_{12}^{(c)} = N(N-1)\alpha_{12}^{(1)} + N(N-1)\alpha_{12}^{(2)} + N(N-1)(N-2)\,\alpha_{12}^{(3)} \tag{3.164}$$

The coefficients of the above equation are the total number of possible ways to choose each one of their conditions (see Figure 3.10). The term $N(N-1)$ of these

coefficients is a common multiplier. Thus, this equation can be simplified in the following way:

$$\alpha_{12}^{(c)} = N(N-1)\left[\alpha_{12}^{(1)} + \alpha_{12}^{(2)} + (N-2)\,\alpha_{12}^{(3)}\right] \tag{3.165}$$

We will next explain what these three possible cases are and how the total number of possible ways can be computed. Depending on the choice of *n*, we are evaluating the correlation of the ray with a different ray. There are three possible cases shown in Figure 3.10. In this figure, the dashed line refers to conjugate of the double scattered field $\psi^{(2)^*}(\vec{r}_a)$ and the continuous line refers to the single scattered field $\psi^{(1)}(\vec{r}_a)$. We use basic principle of counting to determine the number of different ways occurring in Figure 3.10. Let us describe how this principle is applied to our cases.

In case 1, we can choose point scatter m' to be the same scatterer as n th one. From *N* randomly distributed point scatterers, this can be done in *N* different ways. After this, there remain (*N*−1) point scatterers. Thus, $n' \neq n$ can be chosen in (*N*−1) different ways from the remaining (*N*−1) point scatterers. After the sequence of these two choosing processes, the total number of possible ways to choose $m' = n \,\&\, n' \neq n$ is *N*(*N*−1).

Case 2 has the same kind of choosing processes as case 1. Therefore, we can say directly the total number of possible ways to choose $m' \neq n \,\&\, n' = n$ is again *N*(*N*−1).

In case 3, we can choose the point scatter m' from *N* randomly distributed point scatterers in *N* different ways. After this, there remain (*N*−1) point scatterers among which $n' \neq n$ can be chosen in (*N*−1) different ways. Then, there remain (*N*−2) point scatterers. Thus, n can be chosen in (*N*−2) different ways from the remaining (*N*−2) point scatterers. After the sequence of these three choosing processes, the total number of possible ways to choose $m' \neq n, n' \neq n \,\&\, n$ is *N*(*N*−1)(*N*−2).

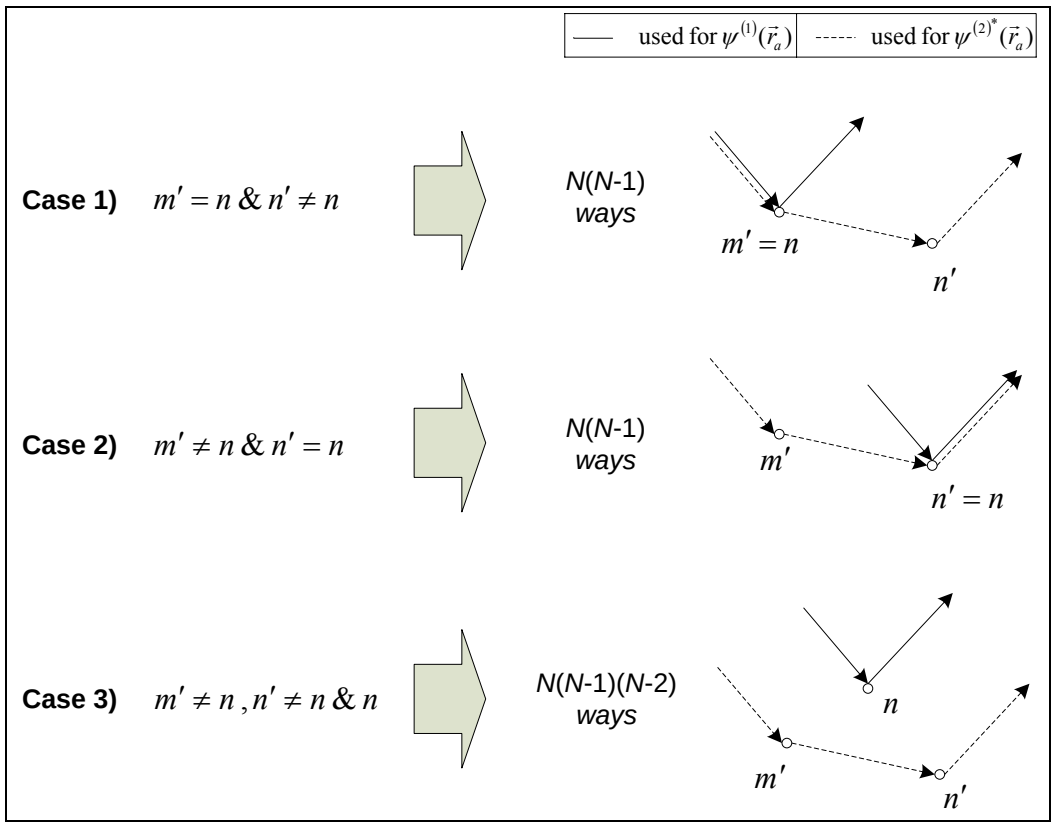

Figure 3.10: Three possible cases of $\alpha_{12}^{(c)}$.

3.3.1.1 Case 1: $m' = n \,\&\, n' \neq n$

Case 1 is defined by the condition $m' = n \,\&\, n' \neq n$. In order to get a result, we insert n instead of m' into Eq. (3.163) as follows:

$$\alpha_{12}^{(1)} =< \frac{e^{-ik|\vec{r}_{n'} - \vec{r}_n|}}{|\vec{r}_{n'} - \vec{r}_n|} e^{-i\vec{k}_s.(\vec{r}_n - \vec{r}_{n'})} e^{i\vec{k}_i.(\vec{r}_n - \vec{r}_n)} > \tag{3.166}$$

which can be rearranged into the form:

$$\alpha_{12}^{(1)} =< \frac{e^{-ik|\vec{r}_n - \vec{r}_{n'}|}}{|\vec{r}_n - \vec{r}_{n'}|} e^{-i\vec{k}_s.(\vec{r}_n - \vec{r}_{n'})} e^{i\vec{k}_i.(\vec{r}_n - \vec{r}_n)} > \tag{3.167}$$

$$\alpha_{12}^{(1)} =< \frac{e^{-ik|\vec{r}_n - \vec{r}_{n'}|}}{|\vec{r}_n - \vec{r}_{n'}|} e^{-i\vec{k}_s.(\vec{r}_n - \vec{r}_{n'})} e^{i\vec{k}_i.(0)} > \tag{3.168}$$

After all, we obtain an ensemble average of $\left[e^{-ik|\vec{r}_n-\vec{r}_{n'}|}/|\vec{r}_n-\vec{r}_{n'}|\right]e^{-i\vec{k}_s.(\vec{r}_n-\vec{r}_{n'})}$ and it is denoted by $\alpha_{12}^{(1)}$:

$$\alpha_{12}^{(1)} = < \frac{e^{-ik|\vec{r}_n-\vec{r}_{n'}|}}{|\vec{r}_n-\vec{r}_{n'}|} e^{-i\vec{k}_s.(\vec{r}_n-\vec{r}_{n'})} > \tag{3.169}$$

Expression $\left[e^{-ik|\vec{r}_n-\vec{r}_{n'}|}/|\vec{r}_n-\vec{r}_{n'}|\right]e^{-i\vec{k}_s.(\vec{r}_n-\vec{r}_{n'})}$ is multiplied with the probability density function $p(\vec{r}_n,\vec{r}_{n'})$ and then integrated to obtain its ensemble average:

$$\begin{aligned}
\alpha_{12}^{(1)} &= < \frac{e^{-ik|\vec{r}_n-\vec{r}_{n'}|}}{|\vec{r}_n-\vec{r}_{n'}|} e^{-ik_s.(\vec{r}_n-\vec{r}_{n'})} > \\
\alpha_{12}^{(1)} &= \iint p(\vec{r}_n,\vec{r}_{n'}) \frac{e^{-ik|\vec{r}_n-\vec{r}_{n'}|}}{|\vec{r}_n-\vec{r}_{n'}|} e^{-i\vec{k}_s.(\vec{r}_n-\vec{r}_{n'})} d\vec{r}_n d\vec{r}_{n'} \\
\alpha_{12}^{(1)} &= \iint p(\vec{r}_n,\vec{r}_{n'}) \frac{e^{-ik|\vec{r}_n-\vec{r}_{n'}|}}{|\vec{r}_n-\vec{r}_{n'}|} e^{-i\vec{k}_s.(\vec{r}_n-\vec{r}_{n'})} d\vec{r}_n d\vec{r}_{n'}
\end{aligned} \tag{3.170}$$

This integral is quite difficult to compute. Therefore, we make change of variables in the following manner:

$$\boxed{\begin{aligned}
&\vec{r}_1 = \vec{r}_n - \vec{r}_{n'} \\
&\vec{r}_2 = \frac{\vec{r}_n + \vec{r}_{n'}}{2} \\
&d\vec{r}_1 d\vec{r}_2 = d\vec{r}_n d\vec{r}_{n'} \quad |J(\vec{r}_1,\vec{r}_2)| = 1
\end{aligned}} \tag{3.171}$$

After the change of variables and using joint probability density function of two point scatterers $p(\vec{r}_n,\vec{r}_{n'}) = p(\vec{r}_n)p(\vec{r}_{n'}) = 1/V^2$, we have

$$\alpha_{12}^{(1)} = \frac{1}{V^2} \iint \frac{e^{-ik|\vec{r}_1|}}{|\vec{r}_1|} e^{-i\vec{k}_s.(\vec{r}_1)} d\vec{r}_1 d\vec{r}_2 \tag{3.172}$$

$$\alpha_{12}^{(1)} = \frac{1}{V^2} \underbrace{\int_V d\vec{r}_2}_{V} \int_V \frac{e^{-ikr_1}}{r_1} e^{-i\vec{k}_s.(\vec{r}_1)} d\vec{r}_1 \tag{3.173}$$

$$\alpha_{12}^{(1)} = \frac{1}{V} \int_V \frac{e^{-ikr_1}}{r_1} e^{-i\vec{k}_s.(\vec{r}_1)} d\vec{r}_1 \tag{3.174}$$

After the change of variables, the volume of above integral is also varied. In a condition of the infinite volume assumption, we can take integral over the sphere and this gives us the approximate result. Solution to the above integral is

$$\alpha_{12}^{(1)} = \frac{\pi}{k^2 V}\left(1 - e^{-2iak} - 2iak\right) \tag{3.175}$$

We first write the below approximated serial expansion:

$$e^{x} \cong 1 + x + \frac{x^2}{2} + \ldots \tag{3.176}$$

So, we can write e^{-2iak} in the same manner,

$$e^{-2iak} \cong 1 + \left(-2iak\right) + \frac{\left(-2iak\right)^2}{2} + \ldots \tag{3.177}$$

When we consider the above approximated serial expansion, the term $\left(1 - e^{-2iak} - 2iak\right)$ can approach this term $\left(2a^2k^2\right)$. After this approximation, $\alpha_{12}^{(1)}$ is stated as

$$\alpha_{12}^{(1)} \cong \frac{2\pi a^2}{V} \tag{3.178}$$

Expressing the volume of the sphere in terms of its radius as $V = (4/3)\pi a^3$, we get

$$\boxed{\alpha_{12}^{(1)} \cong \frac{3}{2a}} \tag{3.179}$$

3.3.1.2 Case 2: $m' \neq n \;\&\; n' = n$

Case 2 is defined by the condition $m' \neq n \;\&\; n' = n$. In order to get a result, we insert n instead of n' into Eq. (3.163) as follows:

$$\alpha_{12}^{(2)} = < \frac{e^{-ik|\vec{r}_n - \vec{r}_{m'}|}}{|\vec{r}_n - \vec{r}_{m'}|} e^{-i\vec{k}_s \cdot (\vec{r}_n - \vec{r}_n)} e^{i\vec{k}_i \cdot (\vec{r}_n - \vec{r}_{m'})} > \tag{3.180}$$

which can be rearranged into the form:

$$\alpha_{12}^{(2)} =< \frac{e^{-ik|\vec{r}_{m'}-\vec{r}_n|}}{|\vec{r}_{m'}-\vec{r}_n|} e^{-i\vec{k}_s.(\vec{r}_n-\vec{r}_n)} e^{i\vec{k}_i.(\vec{r}_n-\vec{r}_{m'})} > \tag{3.181}$$

$$\alpha_{12}^{(2)} =< \frac{e^{-ik|\vec{r}_{m'}-\vec{r}_n|}}{|\vec{r}_{m'}-\vec{r}_n|} e^{-i\vec{k}_s.(0)} e^{i\vec{k}_i.(\vec{r}_n-\vec{r}_{m'})} > \tag{3.182}$$

After all, we obtain an ensemble average of $\left[e^{-ik|\vec{r}_{m'}-\vec{r}_n|}/|\vec{r}_{m'}-\vec{r}_n|\right]e^{i\vec{k}_i.(\vec{r}_n-\vec{r}_{m'})}$ and it is denoted by $\alpha_{12}^{(2)}$:

$$\alpha_{12}^{(2)} =< \frac{e^{-ik|\vec{r}_{m'}-\vec{r}_n|}}{|\vec{r}_{m'}-\vec{r}_n|} e^{i\vec{k}_i.(\vec{r}_n-\vec{r}_{m'})} > \tag{3.183}$$

Expression $\left[e^{-ik|\vec{r}_{m'}-\vec{r}_n|}/|\vec{r}_{m'}-\vec{r}_n|\right]e^{i\vec{k}_i.(\vec{r}_n-\vec{r}_{m'})}$ is multiplied with the probability density function $p(\vec{r}_n,\vec{r}_{m'})$ and then integrated to obtain its ensemble average:

$$\begin{aligned}
\alpha_{12}^{(2)} &=< \frac{e^{-ik|\vec{r}_{m'}-\vec{r}_n|}}{|\vec{r}_{m'}-\vec{r}_n|} e^{i\vec{k}_i.(\vec{r}_n-\vec{r}_{m'})} > \\
\alpha_{12}^{(2)} &= \iint p(\vec{r}_n,\vec{r}_{m'}) \frac{e^{-ik|\vec{r}_{m'}-\vec{r}_n|}}{|\vec{r}_{m'}-\vec{r}_n|} e^{i\vec{k}_i.(\vec{r}_n-\vec{r}_{m'})} d\vec{r}_n d\vec{r}_{m'} \\
\alpha_{12}^{(2)} &= \iint p(\vec{r}_n,\vec{r}_{m'}) \frac{e^{-ik|\vec{r}_{m'}-\vec{r}_n|}}{|\vec{r}_{m'}-\vec{r}_n|} e^{i\vec{k}_i.(\vec{r}_n-\vec{r}_{m'})} d\vec{r}_n d\vec{r}_{m'}
\end{aligned} \tag{3.184}$$

This integral is quite difficult to compute. Therefore, we make change of variables in the following manner:

$$\boxed{\begin{aligned}
&\vec{r}_1 = \vec{r}_n - \vec{r}_{m'} \\
&\vec{r}_2 = \frac{\vec{r}_n + \vec{r}_{m'}}{2} \\
&d\vec{r}_1 d\vec{r}_2 = d\vec{r}_n d\vec{r}_{m'} \quad |J(\vec{r}_1,\vec{r}_2)| = 1
\end{aligned}} \tag{3.185}$$

After the change of variables and using joint probability density function of two point scatterers $p(\vec{r}_n,\vec{r}_{m'}) = p(\vec{r}_n)p(\vec{r}_{m'}) = 1/V^2$, we have

$$\alpha_{12}^{(2)} = \frac{1}{V^2} \iint \frac{e^{-ik|\vec{r}_1|}}{|\vec{r}_1|} e^{i\vec{k}_i.(\vec{r}_1)} d\vec{r}_1 d\vec{r}_2 \tag{3.186}$$

$$\alpha_{12}^{(2)} = \frac{1}{V^2}\int_V d\vec{r}_2 \int_V \frac{e^{-ikr_1}}{r_1} e^{i\vec{k}_i.\vec{r}_1} d\vec{r}_1 \tag{3.187}$$

$$\alpha_{12}^{(2)} = \frac{1}{V^2}\underbrace{\int_V d\vec{r}_2}_{V} \int_V \frac{e^{-ikr_1}}{r_1} e^{i\vec{k}_i.\vec{r}_1} d\vec{r}_1 \tag{3.188}$$

$$\alpha_{12}^{(2)} = \frac{1}{V}\int_V \frac{e^{-ikr_1}}{r_1} e^{i\vec{k}_i.(\vec{r}_1)} d\vec{r}_1 \tag{3.189}$$

Solution to the above integral is

$$\alpha_{12}^{(2)} = \frac{\pi}{k^2 V}\left(1 - e^{-2iak} - 2iak\right) \tag{3.190}$$

This result is the same as the result of $\alpha_{12}^{(1)}$. In other words, $\alpha_{12}^{(1)}$ is equal to $\alpha_{12}^{(2)}$. So, we can directly state $\alpha_{12}^{(2)}$ as

$$\boxed{\alpha_{12}^{(2)} = \alpha_{12}^{(1)} \cong \frac{3}{2a}} \tag{3.191}$$

3.3.1.3 Case 3: $m' \neq n \,\&\, n' \neq n$

Case 3 is defined by the condition $m' \neq n \,\&\, n' \neq n$. In order to get a result, we use the general formula of $\alpha_{12}^{(c)}$ as follows:

$$\alpha_{12}^{(3)} = < \frac{e^{-ik|\vec{r}_{n'} - \vec{r}_{m'}|}}{|\vec{r}_{n'} - \vec{r}_{m'}|} e^{-i\vec{k}_s.(\vec{r}_n - \vec{r}_{n'})} e^{i\vec{k}_i.(\vec{r}_n - \vec{r}_{m'})} > \tag{3.192}$$

which can be rearranged into the form:

$$\alpha_{12}^{(3)} = < \frac{e^{-ik|\vec{r}_{m'} - \vec{r}_{n'}|}}{|\vec{r}_{m'} - \vec{r}_{n'}|} e^{-i\vec{k}_s.(\vec{r}_n - \vec{r}_{n'})} e^{i\vec{k}_i.(\vec{r}_n - \vec{r}_{m'})} > \tag{3.193}$$

Expression $\left[e^{-ik|\vec{r}_{m'} - \vec{r}_{n'}|} \Big/ |\vec{r}_{m'} - \vec{r}_{n'}|\right] e^{-i\vec{k}_s.(\vec{r}_n - \vec{r}_{n'})} e^{i\vec{k}_i.(\vec{r}_n - \vec{r}_{m'})}$ is multiplied with the probability density function $p(\vec{r}_n, \vec{r}_{m'}, \vec{r}_{n'})$ and then integrated to obtain its ensemble average:

$$\alpha_{12}^{(3)} =< \frac{e^{-ik|\vec{r}_{m'}-\vec{r}_{n'}|}}{|\vec{r}_{m'}-\vec{r}_{n'}|} e^{-i\vec{k}_s.(\vec{r}_n-\vec{r}_{n'})} e^{i\vec{k}_i.(\vec{r}_n-\vec{r}_{m'})} >$$

$$\alpha_{12}^{(3)} = \iiint p(\vec{r}_n,\vec{r}_{m'},\vec{r}_{n'}) \frac{e^{-ik|\vec{r}_{m'}-\vec{r}_{n'}|}}{|\vec{r}_{m'}-\vec{r}_{n'}|} e^{-i\vec{k}_s.(\vec{r}_n-\vec{r}_{n'})} e^{i\vec{k}_i.(\vec{r}_n-\vec{r}_{m'})} d\vec{r}_n d\vec{r}_{m'} d\vec{r}_{n'} \tag{3.194}$$

$$\alpha_{12}^{(3)} = \iiint p(\vec{r}_n,\vec{r}_{m'},\vec{r}_{n'}) \frac{e^{-ik|\vec{r}_{m'}-\vec{r}_{n'}|}}{|\vec{r}_{m'}-\vec{r}_{n'}|} e^{-i\vec{k}_s.(\vec{r}_n-\vec{r}_{n'})} e^{i\vec{k}_i.(\vec{r}_n-\vec{r}_{m'})} d\vec{r}_n d\vec{r}_{m'} d\vec{r}_{n'}$$

This integral is quite difficult to compute. Therefore, we make change of variables in the following manner:

$$\boxed{\begin{aligned} &\vec{r}_1 = \vec{r}_{n'} - \vec{r}_{m'} \\ &\vec{r}_2 = \vec{r}_n - \vec{r}_{m'} \quad \vec{r}_2 - \vec{r}_1 = \vec{r}_n - \vec{r}_{n'} \\ &\vec{r}_3 = \frac{\vec{r}_n + \vec{r}_{n'}}{2} \\ &d\vec{r}_1 d\vec{r}_2 d\vec{r}_3 = d\vec{r}_n d\vec{r}_{m'} d\vec{r}_{n'} \quad \left|J(\vec{r}_1,\vec{r}_2,\vec{r}_3)\right| = 1 \end{aligned}} \tag{3.195}$$

After the change of variables and using joint probability density function of three point scatterers $p(\vec{r}_n,\vec{r}_{m'},\vec{r}_{n'}) = p(\vec{r}_n)p(\vec{r}_{m'})p(\vec{r}_{n'}) = 1/V^3$, we have

$$\alpha_{12}^{(3)} = \frac{1}{V^3} \iiint \frac{e^{-ik|\vec{r}_1|}}{|\vec{r}_1|} e^{-i\vec{k}_s.(\vec{r}_2-\vec{r}_1)} e^{i\vec{k}_i.(\vec{r}_2)} d\vec{r}_1 d\vec{r}_2 d\vec{r}_3 \tag{3.196}$$

$$\alpha_{12}^{(3)} = \frac{1}{V^3} \iiint \frac{e^{-ikr_1}}{r_1} e^{i\vec{k}_s.\vec{r}_1} e^{i(\vec{k}_i-\vec{k}_s).\vec{r}_2} d\vec{r}_1 d\vec{r}_2 d\vec{r}_3 \tag{3.197}$$

which is separated into component parts, and then we have

$$\alpha_{12}^{(3)} = \frac{1}{V^3} \underbrace{\int_V d\vec{r}_3}_{V} \int_V \frac{e^{-ikr_1}}{r_1} e^{i\vec{k}_s.\vec{r}_1} d\vec{r}_1 \int_V e^{i(\vec{k}_i-\vec{k}_s).\vec{r}_2} d\vec{r}_2 \tag{3.198}$$

where $\vec{\delta} = \vec{k}_i - \vec{k}_s = 2k\cos(\theta_s/2)\hat{\delta}$ is the subtraction of the incident and scattered wave vectors. The solution to Eq. (3.198) is given by

$$\alpha_{12}^{(3)} = \frac{\pi}{k^2 V}(1 - e^{-2iak} - 2iak)\frac{3(\sin x - x\cos x)}{x^3} \quad ; x = 2ka\cos\frac{\theta_s}{2} \tag{3.199}$$

In the backscattering direction ($\theta_s \to 0$), the term $x = 2ka\cos(\theta_s/2)$ approaches to $x = 2ka$. Therefore, $\alpha_{12}^{(3)}$ can be stated as

$$\alpha_{12}^{(3)} = \frac{\pi}{k^2 V}(1 - e^{-2iak} - 2iak)\frac{-3(2ka\cos 2ka - \sin 2ka)}{(2ka)^3} \tag{3.200}$$

When we consider the infinite volume assumption for the sphere ($a \to \infty$) and the volume of the sphere in terms of its radius as $V = (4/3)\pi a^3$, $\alpha_{22}^{(2)}$ can approach

$$\boxed{\alpha_{12}^{(3)} \cong \frac{-9}{8k^2 a^3}} \tag{3.201}$$

After finding the values of three possible cases, we can calculate $\alpha_{12}^{(c)}$ by using below expression:

$$\alpha_{12}^{(c)} = N(N-1)\left[\alpha_{12}^{(1)} + \alpha_{12}^{(2)} + (N-2)\,\alpha_{12}^{(3)}\right] \tag{3.202}$$

$$\alpha_{12}^{(c)} = N(N-1)\left[\frac{3}{2a} + \frac{3}{2a} + (N-2)\frac{-9}{8k^2 a^3}\right] \tag{3.203}$$

$$\alpha_{12}^{(c)} = \frac{3}{2a}N(N-1)\left[2 - (N-2)\frac{3}{4(ka)^2}\right] \tag{3.204}$$

After expressing the volume of the sphere in terms of its radius as $V = (4/3)\pi a^3$ and this constant $f = [i4\pi T]/k$, we obtain the mean field intensity due to interaction of single and double scattering as

$$\boxed{< I_{12} >= 2i\frac{|T|^2\ \mathrm{Re}(T)}{k^3 r_a^2}\left[\alpha_{12}^{(c)}\right]} \tag{3.205}$$

When inserting the value of $\alpha_{12}^{(c)}$ into the above equation, we get the mean field intensity due to interaction of single and double scattering as

$$\boxed{< I_{12} >= i\frac{|T|^2\ \mathrm{Re}(T)}{(kr_a)^2}\frac{3}{ka}N(N-1)\left[2 - (N-2)\frac{3}{4(ka)^2}\right]} \tag{3.206}$$

We note that the mean field intensity due to interaction of single and double scattering $< I_{12} >$ is in the same order as the mean field intensity due to double scattering $< I_{22} >$ apart from the factor Re(T) and it is to be zero if T-matrix (T) has an only imaginary component. Therefore, the effect of the mean field intensity due to interaction of single and double scattering $< I_{12} >$ can be neglected in most cases.

3.4 Comparison of the Mean Field Intensities due to Single and Double Scattering

From the previous calculation, we see that α_{11} approaches zero ($\alpha_{11} \to 0$) when infinite volume assumption is considered ($D \to \infty$) in the backscattering direction. Hence, the mean field intensity due to single scattering is stated as

$$< I_{11} >= \frac{|f|^2}{(4\pi r_a)^2}\left[N + \sum_{n=1}^{N}\sum_{\substack{n'=1 \\ n' \neq n}}^{N} \underbrace{< e^{i\left[(\vec{k}_i - \vec{k}_s).(\vec{r}_n - \vec{r}_{n'})\right]} >}_{\alpha_{11} \to 0}\right] \tag{3.207}$$

After arranging and substituting $f = [i4\pi T]/k$ into Eq. (3.207), we have an approximate formula of the mean field intensity due to single scattering:

$$< I_{11} > \cong \frac{N|T|^2}{(kr_a)^2} \tag{3.208}$$

which is valid for infinite volume assumption ($D \to \infty$)

In the previous section, we state the approximate formula of the mean field intensity due to double scattering as

$$< I_{22} > \cong \frac{N^2|T|^4}{(kr_a)^2}\frac{3}{(ka)^2}\left\{1 + \frac{Si(a\sigma)}{a\sigma}\right\} \tag{3.209}$$

In order to find effectiveness of the double scattering, we express the ratio of the approximate formula of the mean field intensity due to double scattering to the approximate formula of the mean field intensity due to single scattering as

$$\frac{< I_{22} >}{< I_{11} >} \cong N|T|^2 \frac{3}{(ka)^2}\left\{1 + \frac{Si(a\sigma)}{a\sigma}\right\} \tag{3.210}$$

This result demonstrates that for the double scattering to be effective, we must have

$$N|T|^2 \frac{3}{(ka)^2} > 0.1 \tag{3.211}$$

In other words, as far as effectiveness of the backscattering enhancement is concerned, we must have the above value because double scattering has dominant effect on the backscattering enhancement.

If we only consider single scattering and double scattering, the approximate formula of the total scattered mean field intensity is written as

$$< I_{sca} > \cong < I_{11} > + < I_{22} > \tag{3.212}$$

where the higher-order scattering terms are not taken into account. Inserting the values of both the approximate formula of the mean field intensity due to single scattering $< I_{11} >$ and the approximate formula of the mean field intensity due to double scattering $< I_{22} >$ into the above equation, the approximate formula of the total scattered mean field intensity is obtained as

$$< I_{sca} > \cong \frac{N \mid T \mid^2}{(kr_a)^2} + \frac{N^2 \mid T \mid^4}{(kr_a)^2} \frac{3}{(ka)^2} \left\{ 1 + \frac{Si(a\sigma)}{a\sigma} \right\} \tag{3.213}$$

where $Si(a\sigma) = \int_0^{a\sigma} \frac{\sin t}{t} dt$ is the Sine integral and $\sigma = \left|\vec{\sigma}\right| = \left|\vec{k}_s + \vec{k}_i\right| = 2k \sin(\theta_s / 2)$ is the amplitude of the sum of the incident and scattered wave vectors. Some properties of the Sinc function and the Sine integral are given in Appendix G. As can be seen from the above equation, $< I_{sca} >$ has the form Sine integral divided by $a\sigma$ and also σ depends on the scattering angle. Therefore, we expect $< I_{sca} >$ to give rise to the backscattering enhancement. In previous sections, we present that this Sine integral term $\left[Si(a\sigma)\right]/a\sigma$ comes from $\alpha_{22}^{(2)}$ which is the main cause of the backscattering enhancement. We can arrange Eq. (3.213) by multiplying both sides of this equation with constant $(kr_a)^2$, and then we get

$$< I_{sca} > (kr_a)^2 \cong N \mid T \mid^2 + N^2 \mid T \mid^4 \frac{3}{(ka)^2} \left\{ 1 + \frac{Si(a\sigma)}{a\sigma} \right\} \tag{3.214}$$

This is the approximate formula of the total scattered mean field intensity from spherical distribution and it is given in Figure 3.11 with single and double scattered mean field intensities by using MATLAB programming language

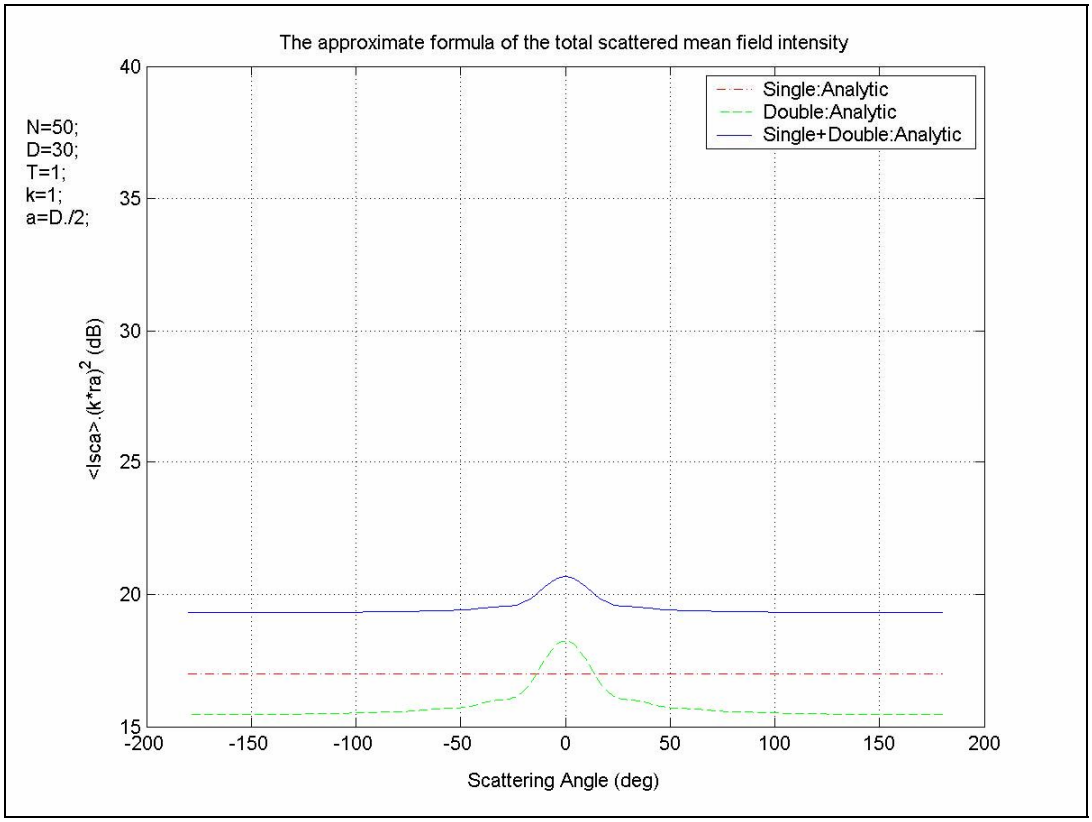

Figure 3.11: The approximate formula of the total scattered mean field intensity: $< I_{sca} >=< I_{11} > + < I_{22} >$.

We note that Figure 3.11 shows the approximate formula of the total scattered mean field intensity: $< I_{sca} >=< I_{11} > + < I_{22} >$ as a function of the scattered angle θ_s (continuous line). The total scattered mean field intensity has a peak in the backscattering direction and it is called as the backscattering enhancement. In addition, the backscattering enhancement due to double scattering is absorbed by other peaks in other directions because single scattering $< I_{11} >$ has large variation. Therefore, the backscattering enhancement due to total scattering is less than expected intensity of the enhancement. As can be seen from this Figure, the intensity of the backscattering enhancement due to total scattering (nearly 1.4 dB) is less than the intensity of the backscattering enhancement due to double scattering (nearly 2.8 dB). The variation of single scattering can not be clearly seen from Figure 3.11 because of the display resolution. Note that the variance of the mean field intensity due to single scattering is calculated in Section 4.1.3.

CHAPTER 4

SIMULATED INVESTIGATION OF THE BACKSCATTERING ENHANCEMENT FROM RANDOMLY DISTRIBUTED POINT SCATTERERS

This Chapter thoroughly includes simulated studies of the backscattering enhancement from randomly distributed point scatterers. We initially begin this investigation with defining simulation as a computer version of real life or an imitation model of some real thing, state of affairs, or process. Its computer version runs on a computer by operating mathematical models. The simulating of something basically requires representing acceptable behaviors or characteristics of a selected physical system, [4].

A computer simulation is a trial to model of a real-life situation on a computer so that it can be carefully examined to recognize how the system works. By changing variables, sensible predictions may be made about the acceptable behavior of the system without potential risks. Traditionally, the formal modeling of systems has been via a mathematical model, which attempts to find analytical solutions to problems which enable the prediction of the behavior of the system from a set of parameters and initial conditions. Computer simulation is often used as a substitution for modeling systems for which simple closed form analytic solutions are not possible. There are many different types of computer simulation; the common feature they try to generate a sample of representative scenarios for a model in which all possible states of the model would be impossible. Some computer-based simulations are the modeling almost effortless and simple, [4], one of them is the Monte Carlo simulation model which is used for simulated investigation of the backscattering enhancement from randomly distributed point scatterers in this thesis.

Monte Carlo simulation is a technique which uses random variables distributed on the interval [0, 1]. Monte Carlo simulation is named after Monte Carlo, the coastal city in Monaco. This city is the center of games of chance. All of these games exhibit random behaviors or repetitive events with known probabilities.

The most important requirement of the Monte Carlo simulation is the probability density function (pdf). The scenario representing a physical system, for example some point scatterers distributed within a cube or a sphere, must be described by a set of pdf's. Random samplings are taken from these probability density functions (pdf) and then these operations are executed repetitively in the Monte Carlo simulation model.

The primary components of the Monte Carlo simulation method are listed below:

- **Probability distribution functions (pdf's):** The physical (or mathematical) system, which needs to be simulated, must be described by a set of pdf's.
- **Random number generator:** A source of random numbers which are uniformly distributed on the unit interval must be available.
- **Sampling rule:** An instruction for sampling from the specified pdf's must be given while assuming random numbers on the unit interval.
- **Error estimation:** An estimate of the statistical error (variance) as a function of the number of trials.
- **Variance reduction techniques:** Methods for reducing the variance in the estimated solution to reduce the computational time, [5].

Let us describe fundamental principle of the Monte Carlo method. The expected value of a function $f(x)$ with a probability density function $p(x)$ is written as:

$$E = \int_V p(x) f(x) dx \tag{4.1}$$

The above integral is too difficult to evaluate. Therefore, E can be estimated by taking N samples $x_1, x_2, x_3, ..., x_N$ and evaluating the average of $f(x)$, [22].

$$\int_V p(x)f(x)dx \approx \frac{1}{N}\sum_{j=1}^{N} f(x_j) \tag{4.2}$$

$$E \approx \frac{1}{N}\sum_{j=1}^{N} f(x_j) \tag{4.3}$$

where E is the expected value of a function $f(x)$ and the x_j are chosen at random from the volume V. This process is done within a uniform distribution.

Let us explain the way how this calculation can be done. We note that this calculation will have a very large loop (or a very great MC) if we want a minimum error estimation for numerical integration. We first write a piece of pseudo-program to explain how this expected variable E can be calculated by directly utilizing the Monte Carlo method and it is stated as

```
1. E=0;
2. for run=1:MC
3. %Choose x at random from V
4. E = E + f(x);
5. end
6. E=E/MC;
```

In the first line, we initialize the variable E which denotes the expected value of a function $f(x)$ to be calculated by the Monte Carlo method. In the second line, we write a loop for x_j and MC is the run number of that loop; in other words, this loop runs MC times. In the third line, we choose x_j at random from a large volume V with a uniform distribution. In the fourth line, for every loop step we repeatedly add the function $f(x_j)$ to E. In the last line, the average (or mean value) of the total expected variable E is calculated by dividing it by the run number MC.

We also note that the MATLAB Programming Language is used in order to evaluate the simulation results through the next sections.

4.1 Mean Field Intensity due to Single Scattering

The single scattering phenomenon is clearly shown in Figure 2.3 (a) and the mean field intensity due to single scattering $< I_{11} >$ is given by

$$< I_{11} >= \sum_{n=1}^{N}\sum_{n'=1}^{N} \frac{|f|^2}{(4\pi r_a)^2} < e^{i\left[(\vec{k}_i - \vec{k}_s).(\vec{r}_n - \vec{r}_{n'})\right]} > \tag{4.4}$$

$$< I_{11} >= \frac{|f|^2}{(4\pi r_a)^2}\left[N + \sum_{n=1}^{N}\sum_{\substack{n'=1 \\ n' \neq n}}^{N} \underbrace{< e^{i\left[(\vec{k}_i - \vec{k}_s).(\vec{r}_n - \vec{r}_{n'})\right]} >}_{\alpha_{11}} \right] \tag{4.5}$$

where $\vec{k}_i = k\hat{r}_i$ is the incident wave vector and $\hat{r}_i$ is a unit vector in the direction from the source to the point scatterer and $\vec{k}_s = k\hat{r}_s$ is the scattered wave vector and $\hat{r}_s$ is a unit vector in the direction from the point scatterer to the observation point (see Figure 2.3 (a)). We can use shorthand symbol α_{11} to denote the ensemble average of $e^{i\left[(\vec{k}_i - \vec{k}_s).(\vec{r}_n - \vec{r}_{n'})\right]}$ (see Eq. (4.5)) and it is given by

$$\alpha_{11} =< e^{i\left[(\vec{k}_i - \vec{k}_s).(\vec{r}_n - \vec{r}_{n'})\right]} > \tag{4.6}$$

The expression $e^{i\left[(\vec{k}_i - \vec{k}_s).(\vec{r}_n - \vec{r}_{n'})\right]}$ is to be multiplied with the probability density function $p(\vec{r}_n, \vec{r}_{n'})$ and then the following integral must be evaluated.

$$\alpha_{11} = \iint p(\vec{r}_n, \vec{r}_{n'}) e^{i\left[(\vec{k}_i - \vec{k}_s).(\vec{r}_n - \vec{r}_{n'})\right]} d\vec{r}_n d\vec{r}_{n'} \tag{4.7}$$

Since the scatterers are the point scatterers, it is assumed that their positions are independent, i.e., under this assumption, we have

$$p(\vec{r}_n, \vec{r}_{n'}) = p(\vec{r}_n)\, p(\vec{r}_{n'}) \tag{4.8}$$

and also that if the density $p(\vec{r}_n)$ is uniform throughout the total volume V, the probability density functions are given by

$$p(\vec{r}_n) = p(\vec{r}_{n'}) = \frac{1}{V} \tag{4.9}$$

$$p(\vec{r}_n, \vec{r}_{n'}) = p(\vec{r}_n)\,p(\vec{r}_{n'}) = \frac{1}{V^2} \tag{4.10}$$

Finally, substituting Eq. (4.10) into Eq. (4.7), we get integral form of α_{11}:

$$\boxed{\alpha_{11} = \iint \frac{1}{V^2} e^{i\left[(\vec{k}_i - \vec{k}_s).(\vec{r}_n - \vec{r}_{n'})\right]} d\vec{r}_n d\vec{r}_{n'}} \tag{4.11}$$

In Chapter 3, we compute the above integral in an analytical manner and then substituting this obtained result into the mean field intensity due to single scattering $< I_{11} >$ formula (see Eq. (4.5)). Finally, solution to the last evaluated integral is the analytic result of the mean field intensity due to single scattering $< I_{11} >$.

In this chapter, we basically estimate the above integral by utilizing the Monte Carlo method. To be able to find Monte Carlo simulation result of the mean field intensity due to single scattering $< I_{11} >$, we first obtain the MC simulation result of α_{11} and then we substitute this MC simulation result into the mean field intensity due to single scattering $< I_{11} >$ formula. After all that, this last evaluated result is the Monte Carlo simulation result of the mean field intensity due to single scattering $< I_{11} >$. This Monte Carlo method is carefully applied to both cubical and spherical distribution scenarios in the next sections.

4.1.1 The Particles are Distributed within a Cube

In this section, we use same scenario depicted in Figure 3.1. In this scenario, the particles are distributed within a cube whose dimension is *D=2d*. In Section 3.1.1, an analytic result of the mean field intensity due to single scattering from cubical distribution is found and depicted in Figure 3.3. In this section, we find out the MC simulation result of the mean field intensity due to single scattering $< I_{11} >$ from cubical distribution by using MATLAB Programming Language. In Figure 4.1, we depict our scenario which is presented as the particles are distributed within a cube thanks to the MATLAB programming language.

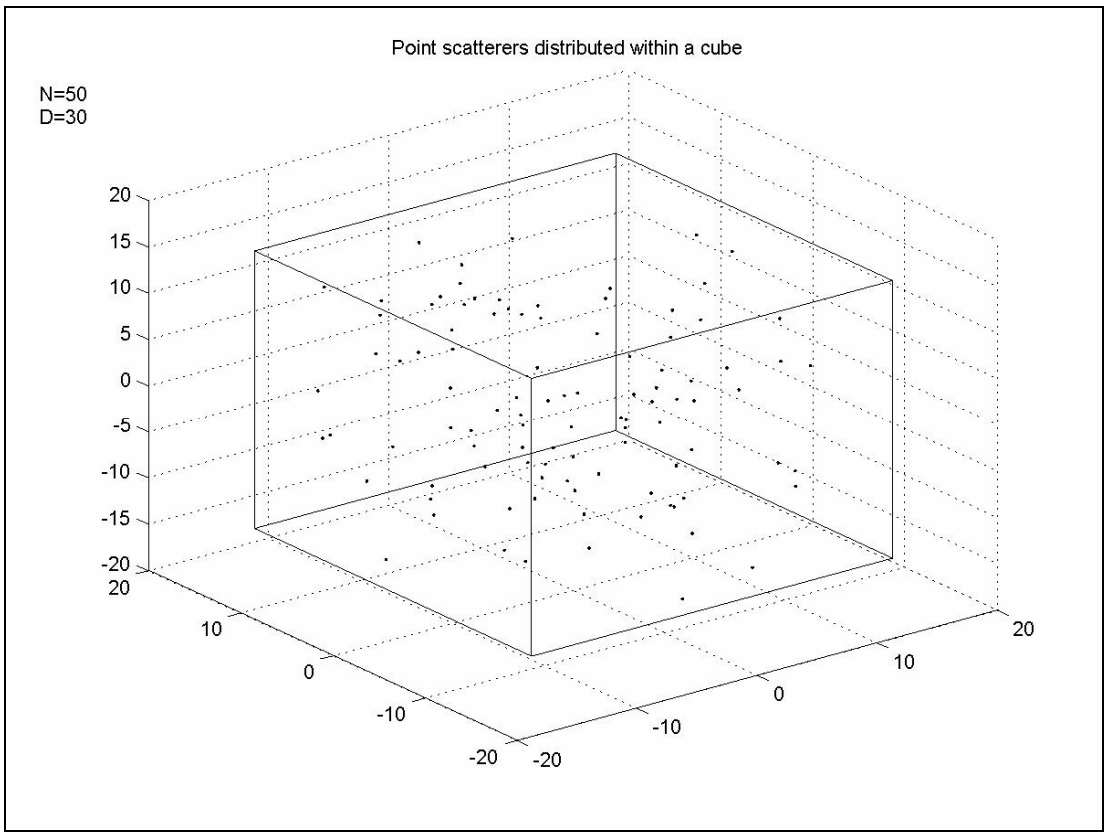

Figure 4.1: Point scatterers distributed within a cube: N=50 and D=30.

The MC simulation and the analytic result of the mean field intensity due to single scattering $< I_{11} >$ from cubical distribution are obtained and shown in Figure 4.2. We see that approximate result is quite accurate for this case. The MC simulation was run for MC=100000 trials as shown in Figure 4.2.

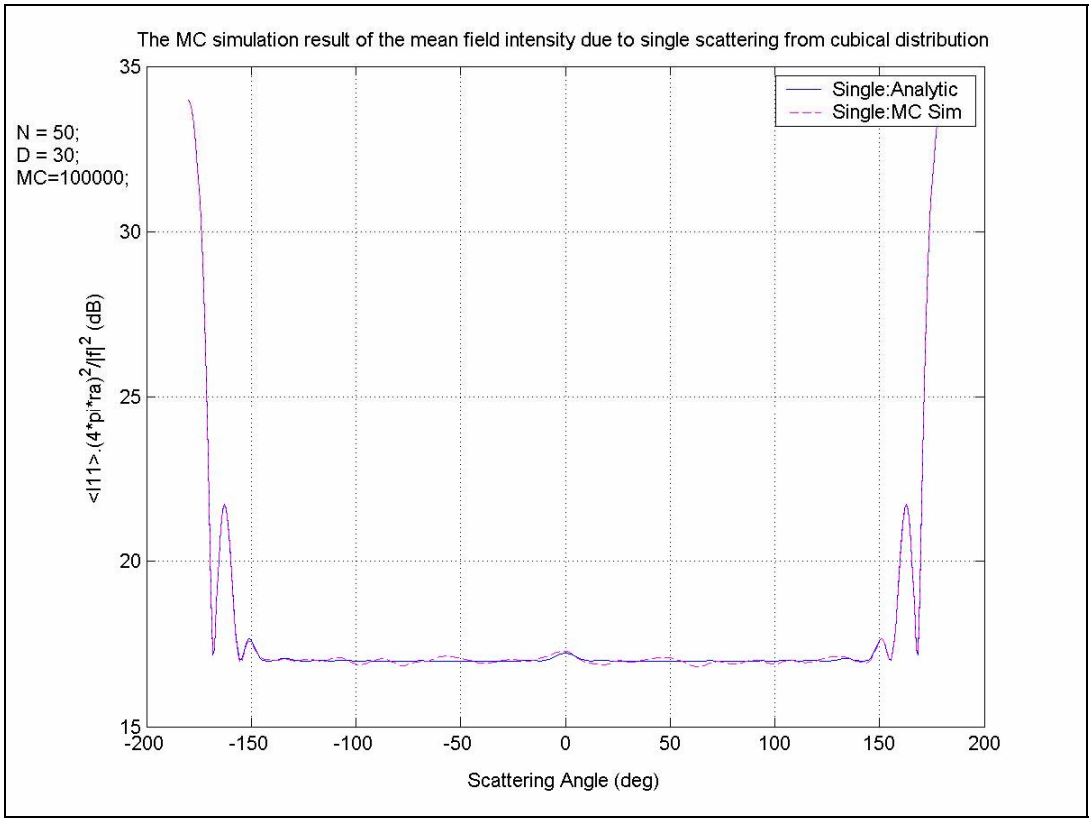

Figure 4.2: The MC simulation result of the mean field intensity due to single scattering from cubical distribution: N=50, D=30 and MC=100000.

We also note that these above results are obtained by using MATLAB programming language and its codes are given in Appendix A.

In Figure 4.2, the MC simulation result of the mean field intensity due to single scattering $< I_{11} >$ from cubical distribution (dashed line) and the analytic result of the mean field intensity due to single scattering $< I_{11} >$ from cubical distribution (continuous line) are very similar to each others. This basically verifies the analytic expression obtained in Chapter 3. In other words, the run number MC = 100000 of the MC simulation is sufficient to explain the single scattering phenomenon from cubical distribution. As can be seen from Figure 4.2, there is a peak in the 0 degrees direction or there is an enhancement in the backscattering direction. However, it is not called as a backscattering enhancement; it is actually specular reflection. Why it is a specular enhancement is explained in more detail in Section 4.3. In this study,

we also prove that the backscattering enhancement can only occur due to multiple scattering.

4.1.2 The Particles are Distributed within a Sphere

In this section, we use the same scenario as depicted in Figure 3.4. In this scenario, the particles are distributed within a sphere whose diameter is $D=2a$. In Section 3.1.2, an analytic result of the mean field intensity due to single scattering from spherical distribution is found and plotted in Figure 3.5. In this section, we find out the MC simulation result of the mean field intensity due to single scattering $< I_{11} >$ from spherical distribution by using MATLAB Programming Language. In Figure 4.3, we depict our scenario which is presented as the particles are distributed within a sphere thanks to the MATLAB programming language.

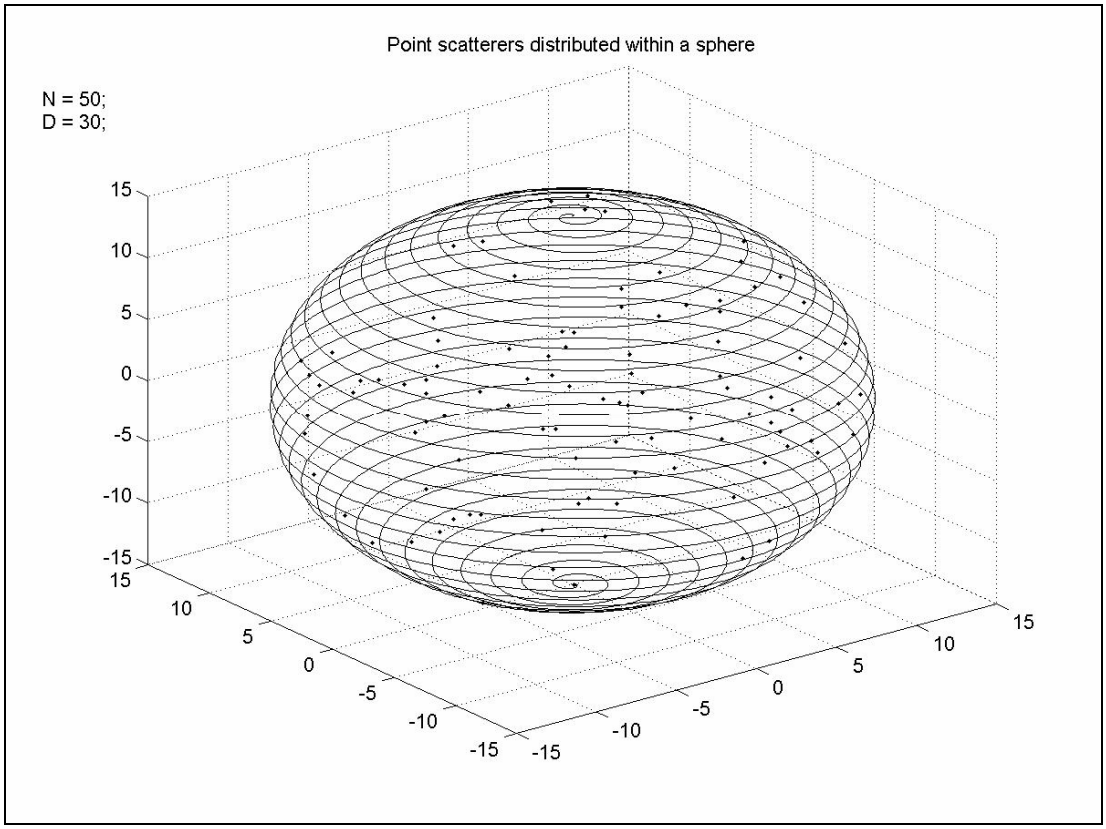

Figure 4.3: Point scatterers distributed within a sphere: N=50 and D=30.

The MC simulation and the analytic result of the mean field intensity due to single scattering $< I_{11} >$ from spherical distribution are obtained and shown in Figure 4.4. This MC simulation result verifies the analytic expression obtained in Chapter 3. The MC simulation was run for *MC*=100000 trials as shown in Figure 4.4.

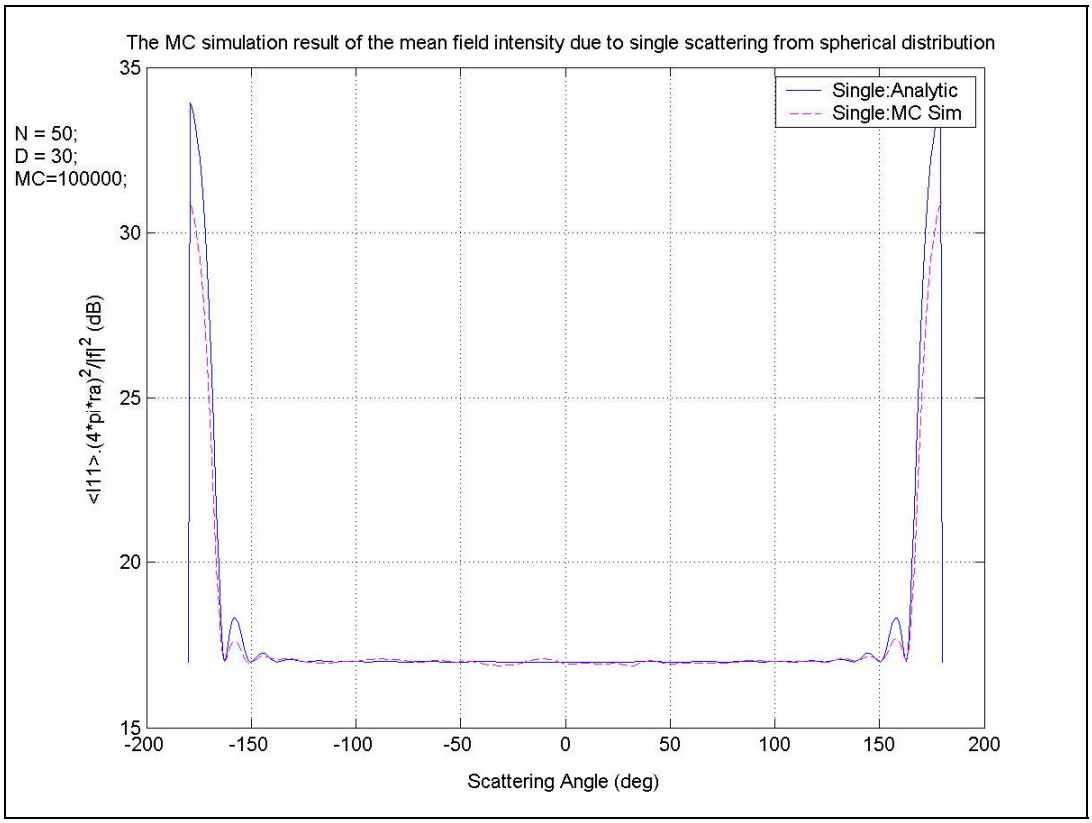

Figure 4.4: The MC simulation result of the mean field intensity due to single scattering from spherical distribution: *N*=50, *D*=30 and *MC*=100000.

We also note that these above results are obtained by using MATLAB programming language and its codes are given in Appendix B.

In Figure 4.4, the MC simulation result of the mean field intensity due to single scattering $< I_{11} >$ from spherical distribution (dashed line) and the analytic result of the mean field intensity due to single scattering $< I_{11} >$ from spherical distribution (continuous line) are very similar to each others. This basically indicates that the

approximate expression is quite accurate for this scenario and also that the number of MC trials, MC = 100000, is sufficient.

As can be seen from Figure 4.4, there is no peak in the 0 degrees direction or there is no enhancement in any direction due to single scattering from spherical distribution.

4.1.3 The 95% Confidence Interval for the MC Simulation Result of the Mean Field Intensity due to Single Scattering

As far as a simulation is concerned, an error estimation is an important subject; because, the simulations yield some approximate answers. Their accuracy depends on some parameters about programming structure but mostly they depend on the run number of simulation. This run number is denoted by MC throughout this thesis. In order to verify the MC simulation results of the mean field intensities due to single scattering, we must calculate the confidence intervals for the MC simulation results for which standard deviations are known. We must show that these confidence intervals are narrow and the simulated mean results are between these two confidence interval results. Thanks to this, we can present that our simulation results are comparatively satisfactory. In order to evaluate the confidence interval results, we first write the variance of this function f $Var(f)$ in the following manner:

$$\boxed{\begin{aligned} Var(f) &= < f^2 > - < f >^2 \\ < f > &= \frac{1}{MC}\sum_{i=1}^{MC} f(x_i) \\ < f^2 > &= \frac{1}{MC}\sum_{i=1}^{MC} f(x_i)^2 \end{aligned}} \qquad (4.12)$$

We note that the standard deviation $Std(f)$ is the square root of the variance $Var(f)$, such as $Std(f) = \sqrt{Var(f)}$.

Because of the fact that the variance is really big value, the standard deviation is a much more useful number. After this general definition of the variance and the

standard deviation, we can write the variance of the MC simulation result of the mean field intensity due to single scattering denoted by $Var(I_{11})$:

$$Var(I_{11}) =< I_{11}^2 > - < I_{11} >^2 \tag{4.13}$$

The mean field intensity due to single scattering can be written as

$$< I_{11} >= \frac{|f|^2}{(4\pi r_a)^2}\left[N + \sum_{n=1}^{N}\sum_{\substack{n'=1 \\ n'=n}}^{N} \underbrace{< e^{i\left[(\vec{k}_i - \vec{k}_s).(\vec{r}_n - \vec{r}_{n'})\right]} >}_{\alpha_{11}} \right] \tag{4.14}$$

Using the subtraction of the incident and scattered wave vectors $\vec{\delta} = \vec{k}_i - \vec{k}_s$, we get

$$I_{11} = \frac{|f|^2}{(4\pi r_a)^2}\left[N + \sum_{n=1}^{N}\sum_{\substack{n'=1 \\ n'=n}}^{N} e^{i\left[\vec{\delta}.(\vec{r}_n - \vec{r}_{n'})\right]} \right] \tag{4.15}$$

Let us consider these constants $y_{nn'} = e^{i\left[\vec{\delta}.(\vec{r}_n - \vec{r}_{n'})\right]}$, $A = |f|/(4\pi r_a)$ and $< y_{nn'} >= \alpha_{11}$, we get a simpler form of the field intensity due to single scattering as follows:

$$I_{11} = A^2\left[N + \sum_{n=1}^{N}\sum_{\substack{n'=1 \\ n'=n}}^{N} y_{nn'} \right] \tag{4.16}$$

In the above equation, the terms in the double summation are independent if $n \neq n'$. Thus, a factor of (N−1) appears for such terms. On the other hand, if $n = n'$, we have $y_{nn'} = 1$ and a factor of N comes from such terms. Thus, the mean field intensity due to single scattering can be expressed as

$$I_{11} = A^2\left[N + N(N-1)y_{nn'} \right] \tag{4.17}$$

and the mean field intensity due to single scattering can be expressed by

$$\begin{aligned} &< I_{11} >= A^2\left[N + N(N-1) < y_{nn'} > \right] \\ &< I_{11} >= A^2\left[N + N(N-1)\alpha_{11} \right] \end{aligned} \tag{4.18}$$

The variance of the mean field intensity due to single scattering is given by

$$\begin{aligned} &Var(I_{11}) = A^2 N(N-1) Var(y_{nn'}) \\ &Var(y_{nn'}) =< y_{nn'}.y^*_{nn'} > - < y_{nn'} >< y_{nn'} >^* = 1 - \alpha_{11}^2 \end{aligned} \tag{4.19}$$

In the limit as the volume goes to infinity, i.e., ($D \to \infty$), α_{11} approaches zero ($\alpha_{11} \to 0$) and then the variance of the mean field intensity due to single scattering can be simplified as follows:

$$Var(I_{11}) = A^2 N(N-1)(1-\alpha_{11}^2) \cong (AN)^2 \tag{4.20}$$

The standard deviation of the mean field intensity due to single scattering is evaluated by using the variance expression as follows:

$$Std(I_{11}) \cong AN \tag{4.21}$$

Both the variance and the standard deviation (especially the variance) have too large values and also they depend on the number of the point scatterers *N*. This means that if we increase the number of the point scatterers, the run number of the MC simulation has to increase so that simulation error can be negligible. This explains the difficulty in observing any kind of the enhancement from the Monte Carlo simulation results of the mean field intensity due to single scattering.

After calculating the standard deviation, let's express the confidence interval formula for which the standard deviation is known and this is given by

$$CI = M \pm \left(z * \frac{Std}{\sqrt{MC}} \right) \tag{4.22}$$

where *M* denotes the mean value, *Std* is the standard deviation, *MC* is the run number of Monte Carlo simulation, and *z* is the *z-score* for the particular confidence interval of interest, [34]. If you need the 95% confidence interval, *z* must be used as 1.96 in the following manner:

$$CI = M \pm \left(1.96 * \frac{Std}{\sqrt{MC}} \right) \tag{4.23}$$

There is nothing special about 95%. It is just a convention that confidence interval is expressed with 95% confidence. Confidence interval can be computed for any desired degree of confidence. Some values of the *z*-scores are given for the other particular confidence intervals of interest in the Table 4.1.

Table 4.1: The *z*-scores for the particular confidence intervals of interest, [32].

Confidence Level	*z*-score
50%	0.674
80%	1.282
90%	1.645
95%	1.960
98%	2.326
99%	2.576

Let us show the 95% confidence interval for the MC simulation result of the mean field intensity due to single scattering from cubical distribution in Figure 4.5 and the 95% confidence interval for the MC simulation result of the mean field intensity due to single scattering from spherical distribution in Figure 4.6. As can be seen from these two graphics, the run numbers MC = 100000 of the MC simulation results are very sufficient because interval estimates are too narrow; actually, they are overlapped with each other. Besides, the mean field intensities due to single scattering overlap with their 95% confidence interval estimates (Confidence Interval Plus and Confidence Interval Minus) and none of the mean field intensities points falls outside of the 95% confidence intervals. Therefore, the results of mean field intensities and confidence intervals are seemed as if one result in these two Figures.

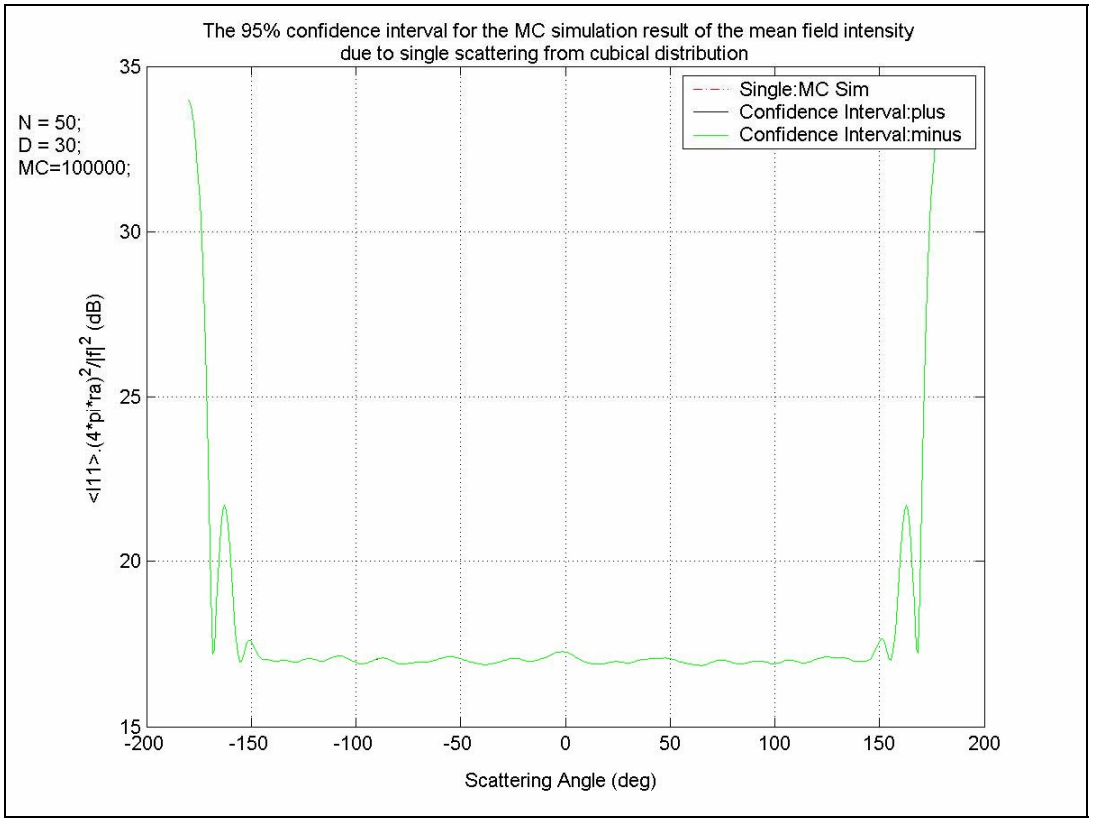

Figure 4.5: The 95% confidence interval for the MC simulation result of the mean field intensity due to single scattering from cubical distribution: N=50, D=30 and MC=100000.

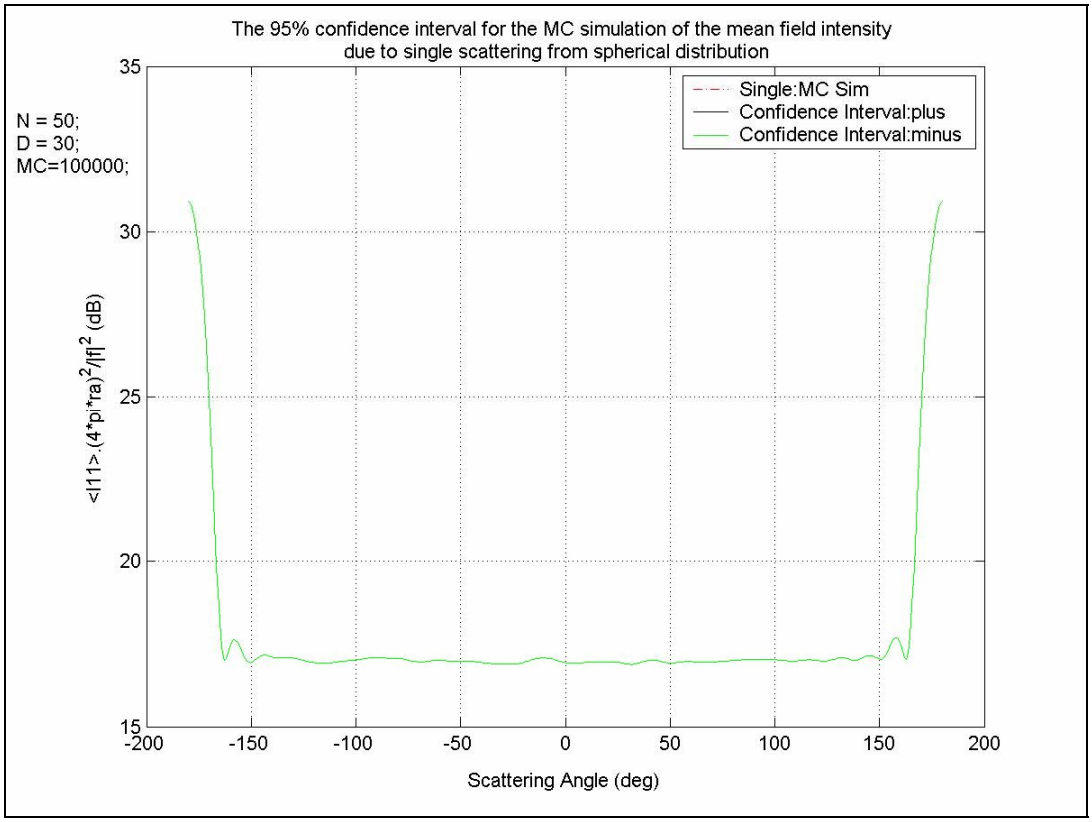

Figure 4.6: The 95% confidence interval for the MC simulation of the mean field intensity due to single scattering from spherical distribution: N=50, D=30 and MC=100000.

We also note that these results are obtained by using MATLAB programming language. Programming codes of Figure 4.5 are given in Appendix C and programming codes of Figure 4.6 have also the same methodology. At these MC simulation programs, the 95% confidence intervals are found out by using below equations as follows:

Variance of the expression x is denoted by $Var(x)$ and it is given by

$$Var(x) = \frac{1}{MC-1}\sum_{i=1}^{MC}(x_i - \hat{x})^2 \tag{4.24}$$

where $\hat{x}$ is the mean of the term x and MC is the run number of the Monte Carlo simulation. Arranging Eq. (4.24), we get

$$Var(x) = \frac{1}{MC-1}\sum_{i=1}^{MC} x_i^2 - \frac{MC}{MC-1}\hat{x}^2 \tag{4.25}$$

Note that standard deviation is the square root of variance, i.e., $Std(x) = \sqrt{Var(x)}$.

4.2 Mean Field Intensity due to Multiple Scattering

As it is explained in Section 2.2, the effective field $\phi(\vec{r}_n)$ consists of the incident wave $\psi_{inc}(\vec{r}_n)$ and the wave scattered from all the particles except the one at $\vec{r}_n$ and it is stated as

$$\phi(\vec{r}_n) = \psi_{inc}(\vec{r}_n) + \sum_{\substack{t=1 \\ t\neq n}}^{N} fG^0(\vec{r}_n, \vec{r}_t)\phi(\vec{r}_t) \tag{4.26}$$

If the effective field $\phi(\vec{r}_n)$ is known at all locations of the point scatterers, the total scattered field $\psi_{sca}(\vec{r}_a)$ for N scatterers at observation point $\vec{r}_a$ can be written as

$$\psi_{sca}(\vec{r}_a) = \sum_{n=1}^{N} fG^0(\vec{r}_a, \vec{r}_n)\phi(\vec{r}_n) \tag{4.27}$$

We note that the effective field $\phi(\vec{r}_n)$ can be eliminated from Eq. (4.27), and a solution to the total scattered field at observation point $\psi_{sca}(\vec{r}_a)$ can be found by using Eq. (4.27). After determining the total scattered field, we can now find the total scattered field intensity (or the field intensity due to multiple scattering) $I_{sca}(\vec{r}_a)$ at the observation point by multiplying the total scattered field $\psi_{sca}(\vec{r}_a)$ and its conjugate $\psi^*_{sca}(\vec{r}_a)$ in the following manner:

$$I_{sca}(\vec{r}_a) = \psi_{sca}(\vec{r}_a)\psi^*_{sca}(\vec{r}_a) \tag{4.28}$$

The ensemble average (or mean) of the total scattered field intensity (or the field intensity due to multiple scattering) over all possible distribution of N particles can be evaluated as follows:

$$\boxed{< I_{sca}(\vec{r}_a) >=< \psi_{sca}(\vec{r}_a)\psi^*_{sca}(\vec{r}_a) >} \tag{4.29}$$

which is the total scattered mean field intensity (or the mean field intensity due to multiple scattering).

However, this calculation of the total scattered mean field intensity is still too complex to be done analytically because of too many unknowns. In Eq. (4.26), we have *N* unknowns which are the effective fields at the positions of the scatterers, i.e. $\phi(\vec{r}_n) \quad ; n = 1,2,...,N$. The effective field $\phi(\vec{r}_n)$ can be written for any *n*=1,2,…,*N* ; thus, Eq. (4.26) defines *N* equations in the *N* unknowns, which are the effective fields at the exact location of the *N* scatterers. This equation can be written in matrix form. To sum up, the mean field intensity due to multiple scattering is not possible to be calculated analytically. However, we can compute the mean field intensity due to multiple scattering in a simulation manner. For this purpose, we develop a certain number of Monte Carlo simulations in this study. We will next explain how these Monte Carlo simulations are gradually developed.

We can rearrange the effective field $\phi(\vec{r}_n)$ for any *n*=1,2,…,*N* by defining Eq. (4.26) as *N* equations in the *N* unknowns for simplifying. After this rearrangement, we can write it in matrix form as follows:

$$\begin{aligned} \bar{\phi} &= \bar{\psi}_{inc} + \bar{\bar{G}}\bar{\phi} \\ \bar{\phi} - \bar{\bar{G}}\bar{\phi} &= \bar{\psi}_{inc} \\ (1 - \bar{\bar{G}})\bar{\phi} &= \bar{\psi}_{inc} \\ (\bar{I} - \bar{\bar{G}})\bar{\phi} &= \bar{\psi}_{inc} \end{aligned} \tag{4.30}$$

Note that the symbol $\bar{\bar{G}}$ is the Green's function matrix which consists of elements depending on both $\vec{r}_n$ and $\vec{r}_t$, $\bar{\phi}$ is the effective field vector which consists of elements depending on $\vec{r}_n$, and $\bar{\psi}_{inc}$ is the incident field vector which consists of elements depending on $\vec{r}_n$. If we write Eq. (4.30) in the following manner:

$$\bar{\phi} = \left[\bar{I} - \bar{\bar{G}}\right]^{-1} \bar{\psi}_{inc} \tag{4.31}$$

The effective field vector $\bar{\phi}$ can be calculated from matrix multiplication of the inverse matrix $\left[\bar{I} - \bar{\bar{G}}\right]^{-1}$ with the incident field vector $\bar{\psi}_{inc}$.

Let us explain how these calculations can be evaluated in the MC simulation programming codes. We can determine the free-space Green's functions by executing computer programming loops over and over again until computing each one of the Green's functions matrix elements. We also note that the MC simulation programming codes developed in this study are given in Appendixes. There are two different kinds of the free-space Green's functions in these equations and they are denoted by $G^0(\vec{r}_n,\vec{r}_t)$ and $G^0(\vec{r}_a,\vec{r}_n)$. Therefore, we use two different kinds of loops computing each one of the Green's function matrix elements by considering each one of the point scatterers' positions. In these loops, we apply a basic principle of filling matrixes whose elements are dependent on the position of the point scatterers in the distribution volume. Similarly, we compose another loop structure which fills the incident field vector $\overline{\psi}_{inc}$ whose elements are also dependent on the position of the point scatterers in the distributed volume. After determining the Green's function matrix and the incident field vector, the effective field vector $\overline{\phi}$ can be calculated from matrix multiplication given by Eq. (4.31). After evaluating the effective field vector $\overline{\phi}$, the total scattered field at any observation point $\psi_{sca}(\vec{r}_a)$ can be calculated from similar matrix multiplication (see Eq. (4.27)). Now, we achieve the MC simulation result of the total scattered field at observation point $\psi_{sca}(\vec{r}_a)$; hence, the MC simulation result of the total scattered field intensity (or the field intensity due to multiple scattering) can be found out by multiplying the MC simulation result of total scattered field $\psi_{sca}(\vec{r}_a)$ and its conjugate $\psi^*_{sca}(\vec{r}_a)$.

In summary, because of the fact that calculation of the effective field vector $\overline{\phi}$ is too complex, the effective field vector $\overline{\phi}$ is not possible to be estimated in an analytic manner. Therefore, we compute it in a simulation manner and we directly apply the Monte Carlo simulation method while evaluating the simulation results. We also verify the accuracy of these MC simulations by presenting their confidence intervals throughout this study.

4.2.1 The Particles are Distributed within a Cube

In this section, we use same scenario depicted in Figure 4.1 where the particles are distributed within a cube whose dimension is $D=2d$. However, this time we interest the multiple scattering phenomenon. It is not possible to calculate the mean field intensity due to multiple scattering $< I_{sca}(\vec{r}_a) >$ from cubical distribution in an analytic manner. Because of the fact that there are too many unknowns in the scattered field equations, we can only achieve the mean field intensity due to multiple scattering $< I_{sca}(\vec{r}_a) >$ from cubical distribution by running the MC simulation computer codes. We also note that, in Section 4.1.1, both the analytic and MC simulation results of the mean field intensity due to single scattering from cubical distribution are properly calculated and also they are depicted in the same graphical result in order to compare their characteristic behaviors.

In this section, the mean field intensity due to multiple scattering from cubical distribution is obtained by running the programming codes in which the MC simulation method is directly utilized. We also note that how the MC method is applied these computer programming codes is mentioned in previous sections. After we run the developed computer programming codes which are composed in order to examine the multiple scattering phenomenon from cubical distribution, we evaluate the MC simulation results of the mean field intensity due to multiple scattering from cubical distribution. In order to be in a standard form, we only achieve the MC simulation result in which these variables N=50, D=30 and MC=10000 are considered and this MC simulation result is given in Figure 4.7. As far as a simulation is concerned, an error estimation is an important subject; because, the simulations yield some approximate answers. Their accuracy depends on some parameters about programming structure but mostly they depend on the run number. Therefore, this result is ultimately achieved by running computer codes 10000 times. This run number is sufficient in order to present the backscattering enhancement due to multiple scattering from cubical distribution and this run number is denoted by MC=10000 in Figure 4.7.

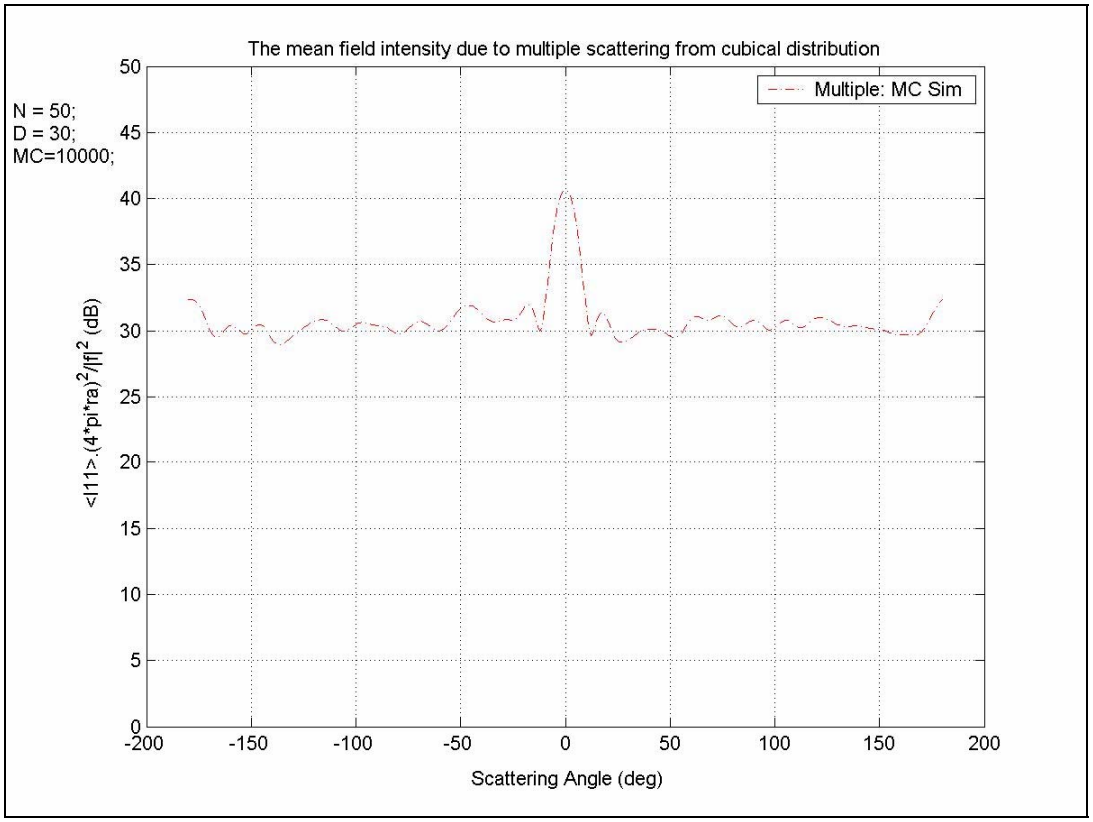

Figure 4.7: The mean field intensity due to multiple scattering from cubical distribution: N=50, D=30 and MC=10000.

We also note that this above result is ultimately achieved by using a MATLAB programming language. Its programming codes are given in Appendix D.

As can be seen from Figure 4.7, there is a peak in the backscattering direction whose intensity is nearly 10 dB. This peak actually comes into being due to the backscattering enhancement phenomenon not the specular enhancement phenomenon. Why this result is determined as the backscattering enhancement is explained in more detail in Section 4.3. In this study, we also prove that the backscattering enhancement is only constituted due to multiple scattering.

4.2.2 The Particles are Distributed within a Sphere

In this section, we use same scenario depicted in Figure 4.3 where the particles are distributed within a sphere whose diameter is $D=2a$. However, this time we only interest the multiple scattering phenomenon. It is not possible to calculate the mean field intensity due to multiple scattering $< I_{sca}(\vec{r}_a) >$ from spherical distribution in an analytic manner. Because of the fact that there are too many unknowns in the scattered field equations, we can only achieve the mean field intensity due to multiple scattering $< I_{sca}(\vec{r}_a) >$ from spherical distribution by running the MC simulation computer codes. We also note that, in Section 4.1.2, both the analytic and the MC simulation results of the mean field intensity due to single scattering from spherical distribution are properly calculated and also they are depicted in the same graphical result in order to compare their characteristic behaviors.

In this section, the mean field intensity due to multiple scattering from spherical distribution is obtained by running the programming codes in which the MC simulation method is directly utilized. We also note that how the MC method is applied these computer programming codes is mentioned in previous sections. After we run the developed computer programming codes which are composed in order to examine the multiple scattering phenomenon from spherical distribution, we evaluate the MC simulation results of the mean field intensity due to multiple scattering from spherical distribution. In order to be in a standard form, we only achieve the MC simulation result in which these variables N=50, D=30 and MC=10000 are considered and this MC simulation result is given in Figure 4.8. As far as a simulation is concerned, an error estimation is an important subject; because, the simulations yield some approximate answers. Their each accuracy depends on some parameters about programming structure but mostly they depend on the run number. Therefore, this result is ultimately achieved by running computer codes 10000 times. This run number is sufficient in order to present the backscattering enhancement due to multiple scattering from spherical distribution and this run number is denoted by MC=10000 in Figure 4.8.

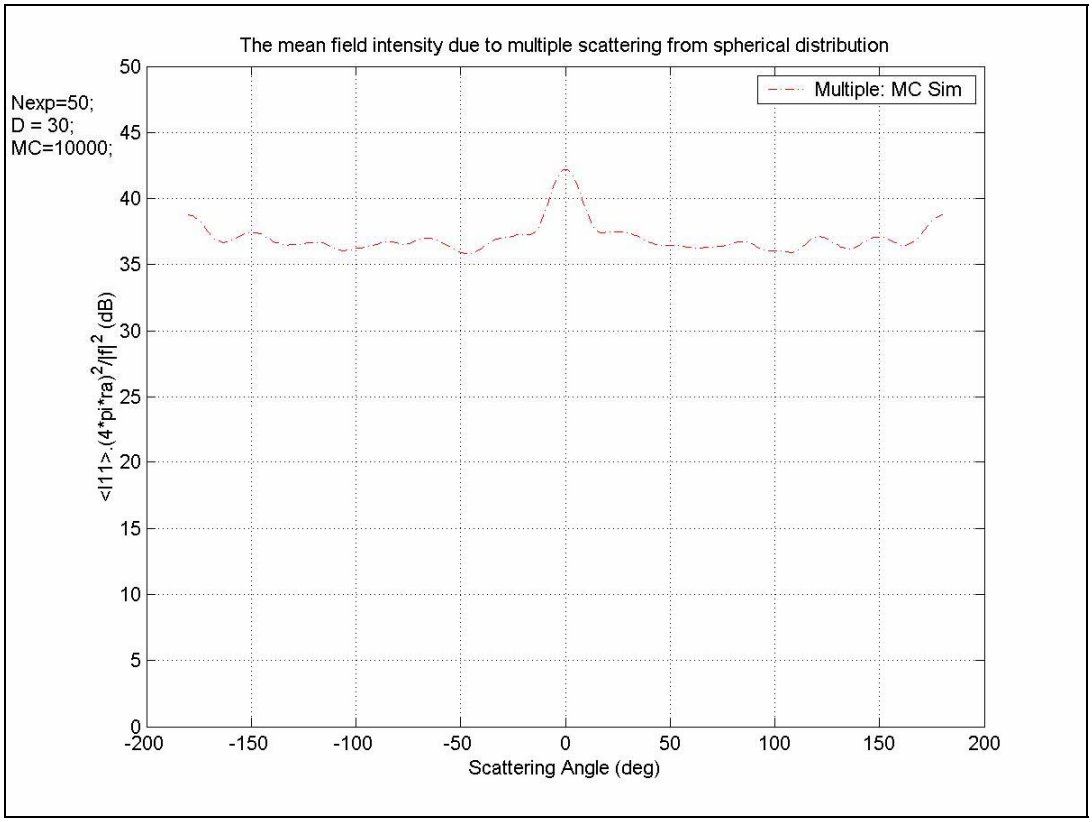

Figure 4.8: The mean field intensity due to multiple scattering from spherical distribution: N=50, D=30 and MC=10000.

We also note that this above result is ultimately achieved by using a MATLAB programming language. Its programming codes are given in Appendix E.

As can be seen from Figure 4.8, there is a peak in the backscattering direction whose intensity is nearly 5 dB. This peak actually comes into being due to the backscattering enhancement phenomenon not the specular enhancement phenomenon. Why this result is determined as the backscattering enhancement is explained in more detail in Section 4.3. In this study, we also prove that the backscattering enhancement is only constituted due to multiple scattering

We also emphasize that cubical distribution has stronger backscattering enhancement intensity than spherical distribution.

4.2.3 The 95% Confidence Interval for the Mean Field Intensity due to Multiple Scattering

The MC simulation results of the mean field intensities need to be verified. Therefore, we must calculate the confidence intervals for the MC simulation results for which standard deviations are known. The 95% confidence intervals for the MC simulation results of the mean field intensities due to single scattering are found for both cubical and spherical distribution in Section 4.1.3. In this section, we present the 95% confidence interval for the mean field intensity due to multiple scattering from cubical distribution in Figure 4.9 and the 95% confidence interval for the mean field intensity due to multiple scattering from spherical distribution in Figure 4.10.

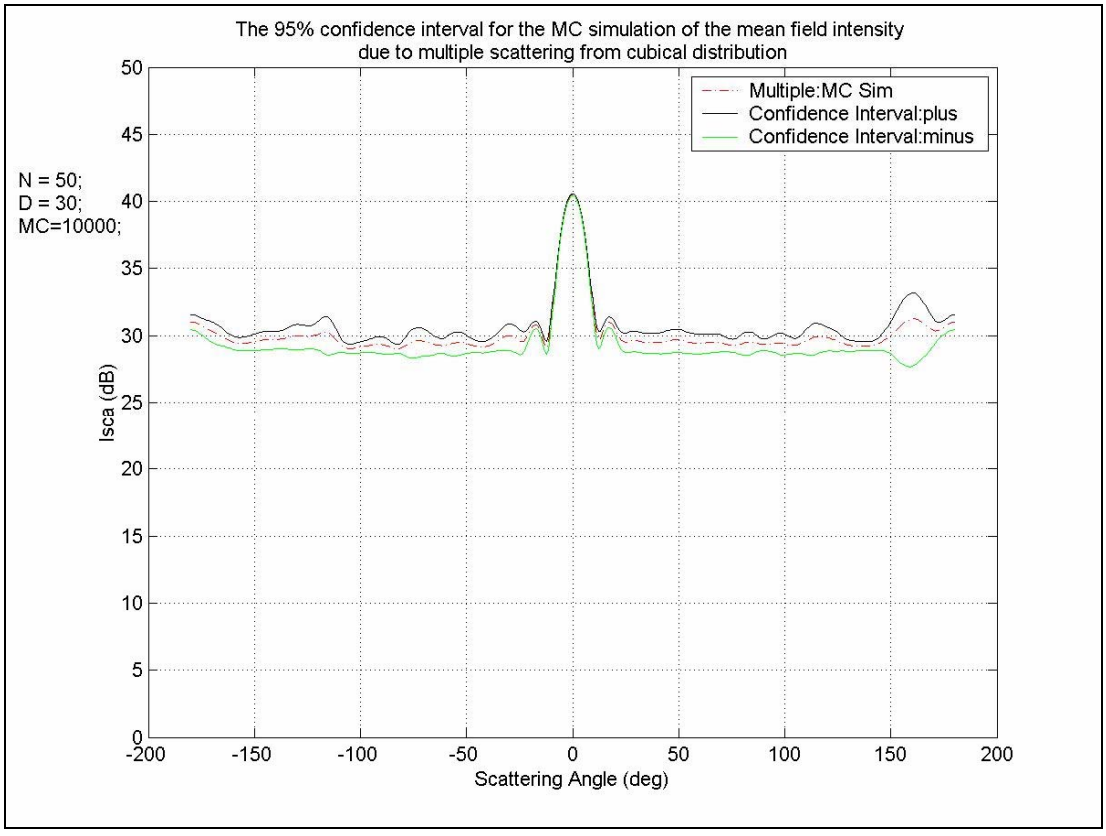

Figure 4.9: The 95% confidence interval for the MC simulation of the mean field intensity due to multiple scattering from cubical distribution: N=50, D=30 and MC=10000.

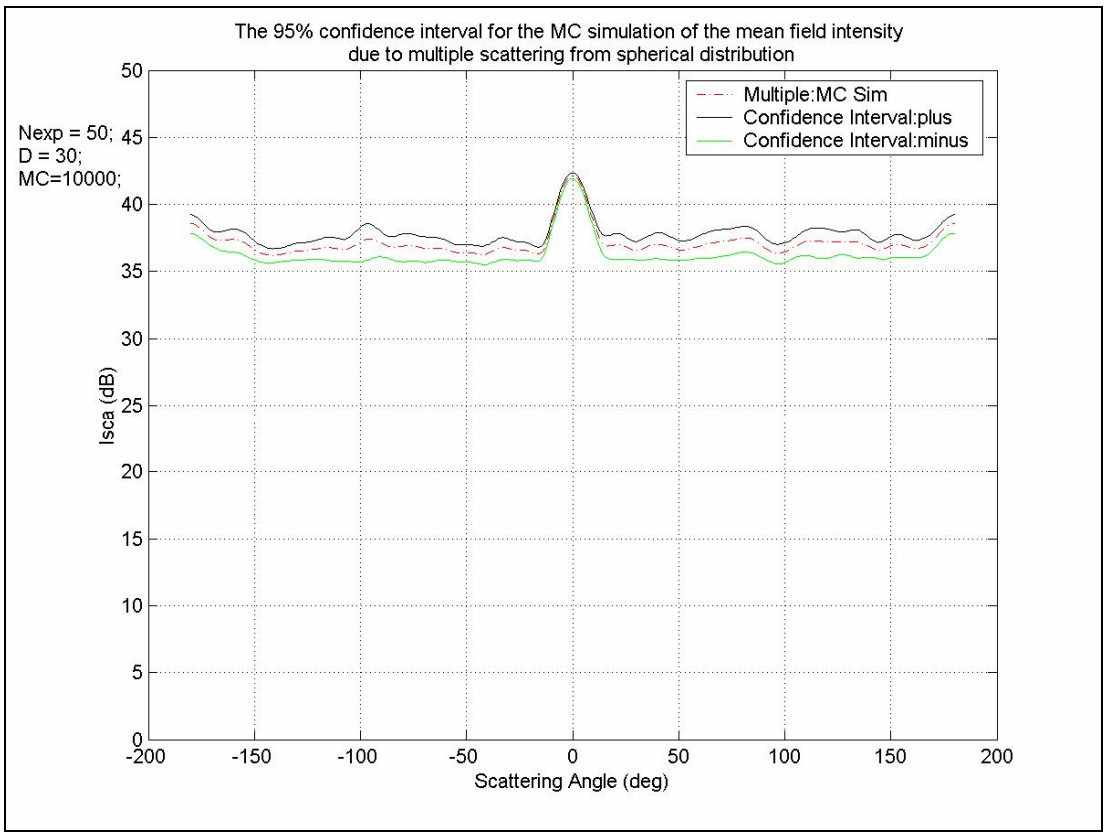

Figure 4.10: The 95% confidence interval for the MC simulation of the mean field intensity due to multiple scattering from spherical distribution: N=50, D=30 and MC=10000.

We also note that these above results are obtained by using MATLAB programming language. Programming codes of Figure 4.9 are given in Appendix F and programming codes of Figure 4.10 have also the same methodology.

As can be seen from these two graphics, the run numbers MC = 10000 of the MC simulation results are sufficient because estimate intervals are narrow and there is a 95% chance that the mean field intensities place within these narrow intervals. Thank for this, accuracies and reliabilities of the MC simulation results have been provided. We note that the mean field intensities due to multiple scattering, in both of these two graphics, are between the 95% confidence interval results and none of the mean field intensities' points fall outside of the 95% confidence intervals.

4.3 Investigation of the Specular Enhancement from Randomly Distributed Point Scatterers

In the previous studies, some enhancement phenomena in the backscattering direction are observed when the incident field comes from the $-z$ direction. That the incident field in the $-z$ direction occasionally causes some unresolved difficulties about deciding what kind of enhancement phenomenon is observed. In other words, the incident field direction perpendicular to the surface of randomly distributed point scatterers may be causing a specular reflection especially when a cubical distribution is taken into consideration. Because, the cubical distribution of the point scatterers has a flat surface and this surface behaves like a mirror for an incident electromagnetic field under proper conditions (see Figure 4.11). In order to distinguish the type of the enhancement phenomenon as a backscattering or a specular, we send the incident field in a direction different than the z axis. Some general characteristic behaviors of the scattered fields are depicted in Figure 4.11. In this figure, the incident field comes from a direction different than the z axis and the scattered field in the backscattering direction has a different scattering angle than the scattered field in the specular direction.

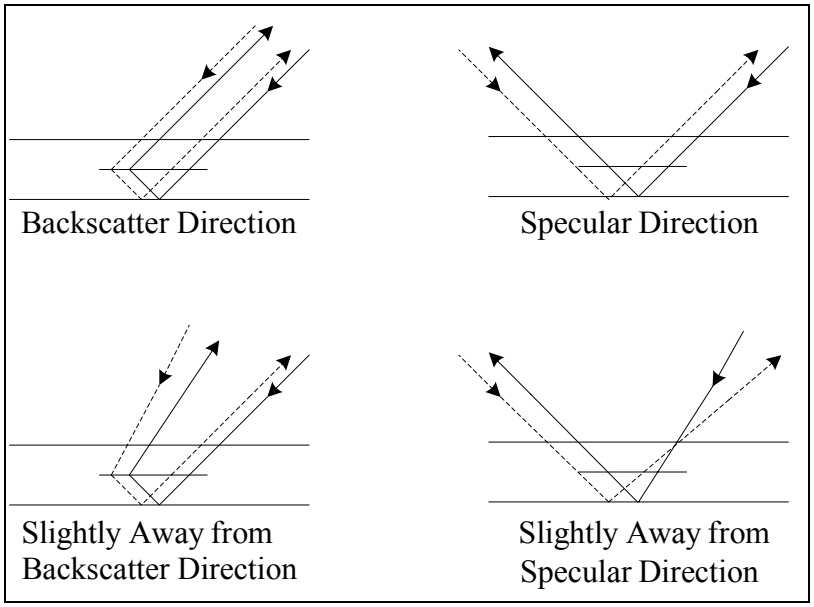

Figure 4.11: The incident field in a direction different than the z axis, [7].

4.3.1 The Particles are Distributed within a Cube

In this part of the study, we examine what kind of the enhancement occurs due to both single and multiple scattering phenomena from cubical distribution.

When we focus on the single scattering from the cubical distribution in Section 3.1.1, an enhancement is observed. However, this enhancement can not be clearly determined as a backscattering or a specular; because, the incident field only comes from the $-z$ direction. In order to resolve this, we send the incident field in a direction different than the z axis and then we get the enhancement results in the different directions. The MC simulation result of the mean field intensity due to single scattering $< I_{11} >$ from cubical distribution while the incident field is in the direction of +45 degrees and the analytic result of the mean field intensity due to single scattering $< I_{11} >$ from cubical distribution while the incident field is in the direction of 0 degrees are obtained and shown in Figure 4.12.

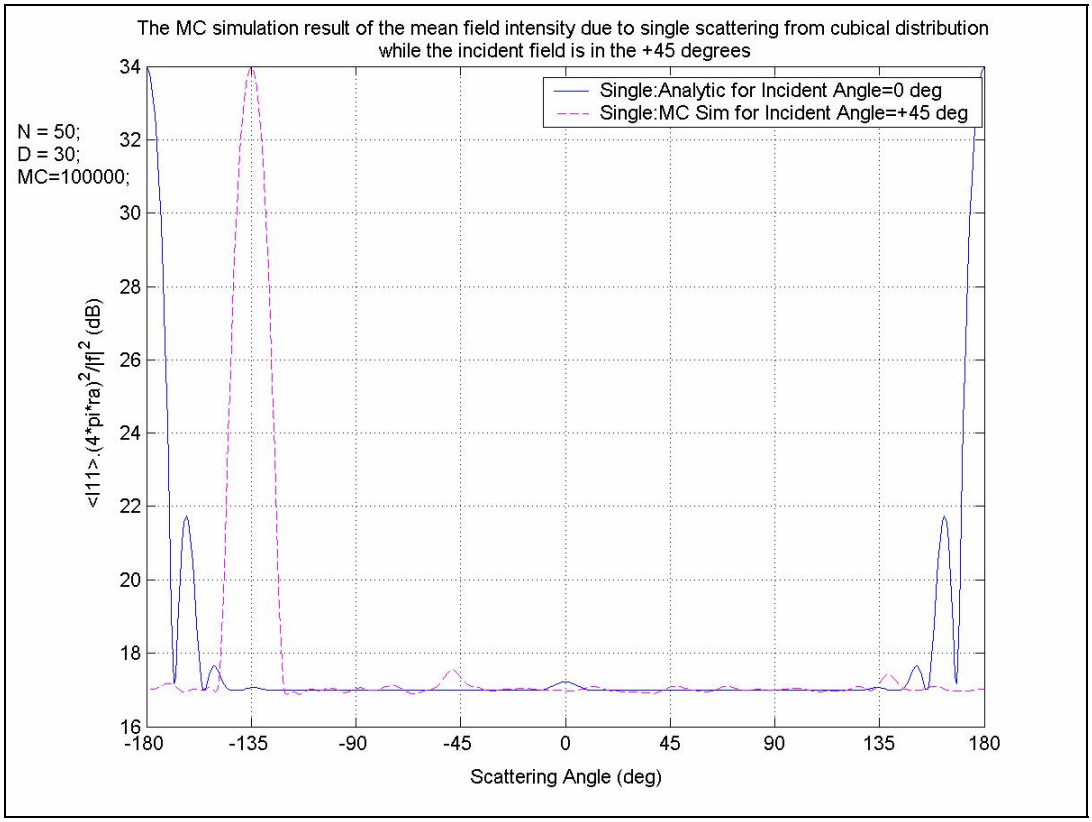

Figure 4.12: The MC simulation result of the mean field intensity due to single scattering from cubical distribution while the incident field is in the +45 degrees: N=50, D=30 and MC=100000.

As can be seen from Figure 4.12, we get an enhancement in the direction of 0 degrees for the analytic result while the incident field is in the direction of 0 degrees and we get an enhancement in the direction of −45 degrees for the MC simulation result while the incident field is in the direction of +45 degrees. The expected results prove obviously that the type of these enhancement phenomena are specular not backscattering enhancements. Thanks to these results, we say clearly that there is no backscattering enhancement due to single scattering from cubical distribution. Meanwhile, the forward scattering intensity in the direction of ± 180 degrees can be seen clearly while the incident field is in the direction of 0 degrees for the analytic result and the forward scattering intensity in the direction of −135 degrees can be seen clearly while the incident field is in the direction of +45 degrees for the MC simulation result.

We next examine what kind of the enhancement occurs due to multiple scattering from cubical distribution. When we focus on the multiple scattering from the cubical distribution in Section 4.2.1, an enhancement is observed. However, this enhancement can not be clearly determined as a backscattering or a specular; because, the incident field only comes from the $-z$ direction. In order to resolve this, we send the incident field in a direction different than the z axis and then we get an enhancement in the backscattering direction. It is stated as follows:

The mean field intensity due to multiple scattering $< I_{sca}(\vec{r}_a) >$ from cubical distribution while the incident field is in the direction of +45 degrees is obtained and shown in Figure 4.13.

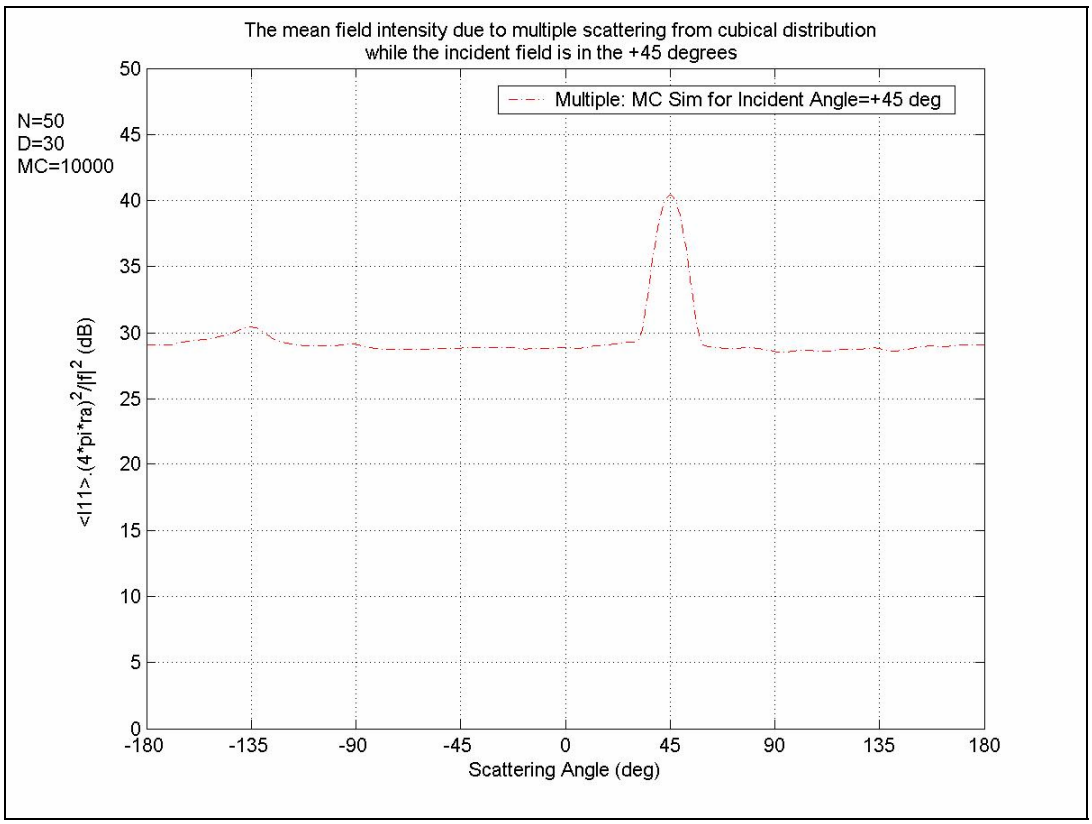

Figure 4.13: The mean field intensity due to multiple scattering from cubical distribution while the incident field is in the +45 degrees: N=50, D=30 and MC=10000.

As can be seen from Figure 4.13, we get an enhancement in the direction of +45 degrees for the mean field intensity due to multiple scattering from cubical distribution while the incident field is in the direction of +45 degrees. The result demonstrates obviously that the type of this enhancement phenomenon is a backscattering not a specular. Its intensity is nearly 10 dB the same as amplitude of intensity in Figure 4.7 where the incident field is in the direction of 0 degrees.

Thanks to the results of cubical distributions, we say clearly that the backscattering enhancement is observed only as regard as multiple scattering conditions. At the same time, this basically means the single scattering phenomenon is not enough alone in order to explain the backscattering enhancement and also the higher-order scattering terms have to be calculated in order to get accurate results in the case of the backscattering enhancement.

4.3.2 The Particles are Distributed within a Sphere

In this part of the study, we examine both the single and multiple scattering phenomena from spherical distribution.

When we focus on the single scattering from the spherical distribution in Section 3.1.2, any kind of an enhancement is not observed. So, we check the result of the spherical distribution when the incident field comes from a direction different than the z axis. The MC simulation result of the mean field intensity due to single scattering $< I_{11} >$ from spherical distribution while the incident field is in the direction of +45 degrees and the analytic result of the mean field intensity due to single scattering $< I_{11} >$ from spherical distribution while the incident field is in the direction of 0 degrees are obtained and shown in Figure 4.14.

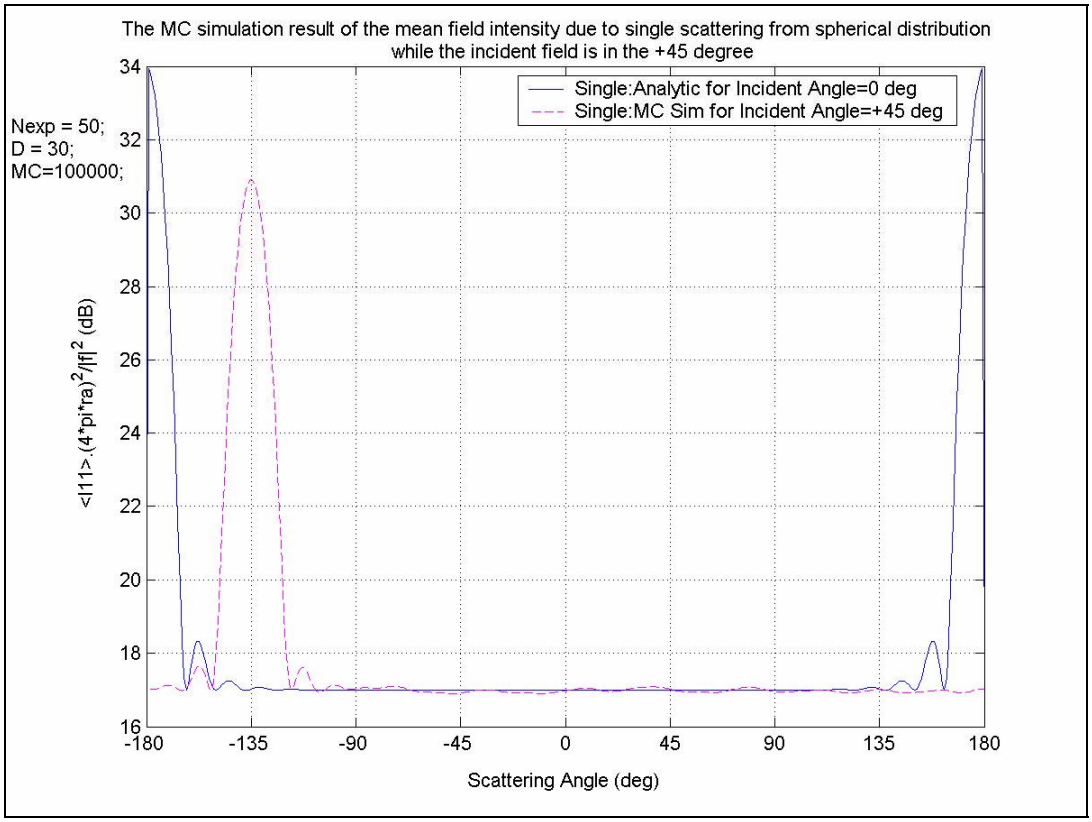

Figure 4.14: The MC simulation result of the mean field intensity due to single scattering from spherical distribution while the incident field is in the +45 degrees: N=50, D=30 and MC=100000.

As can be seen from Figure 4.14, none of the enhancement phenomenon occurs in the direction of 0 degrees for the analytic result while the incident field is in the direction of 0 degrees and none of the enhancement phenomenon occurs in the direction of −45 degrees or +45 degrees for the MC simulation result while the incident field is in the direction of +45 degrees. Those results demonstrate us obviously that there is neither the backscattering enhancement phenomenon nor the specular enhancement phenomenon appearing due to single scattering from spherical distribution. Meanwhile, the forward scattering intensity in the direction of ± 180 degrees can be seen clearly while the incident field is in the direction of 0 degrees for the analytic result and the forward scattering intensity in the direction of −135 degrees can be seen clearly while the incident field is in the direction of +45 degrees for the MC simulation result.

We next examine what kind of the enhancement occurs due to multiple scattering from spherical distribution. When we focus on the multiple scattering from the spherical distribution in Section 4.2.2, an enhancement is observed. However, this enhancement can not be clearly determined as a backscattering or a specular; because, the incident field only comes from the $-z$ direction. In order to resolve this, we send the incident field in a direction different than the z axis and then we get an enhancement in the backscattering direction which is stated as follows:

The mean field intensity due to multiple scattering $< I_{sca}(\vec{r}_a) >$ from spherical distribution while the incident field is in the direction of +45 degrees is obtained and shown in Figure 4.15.

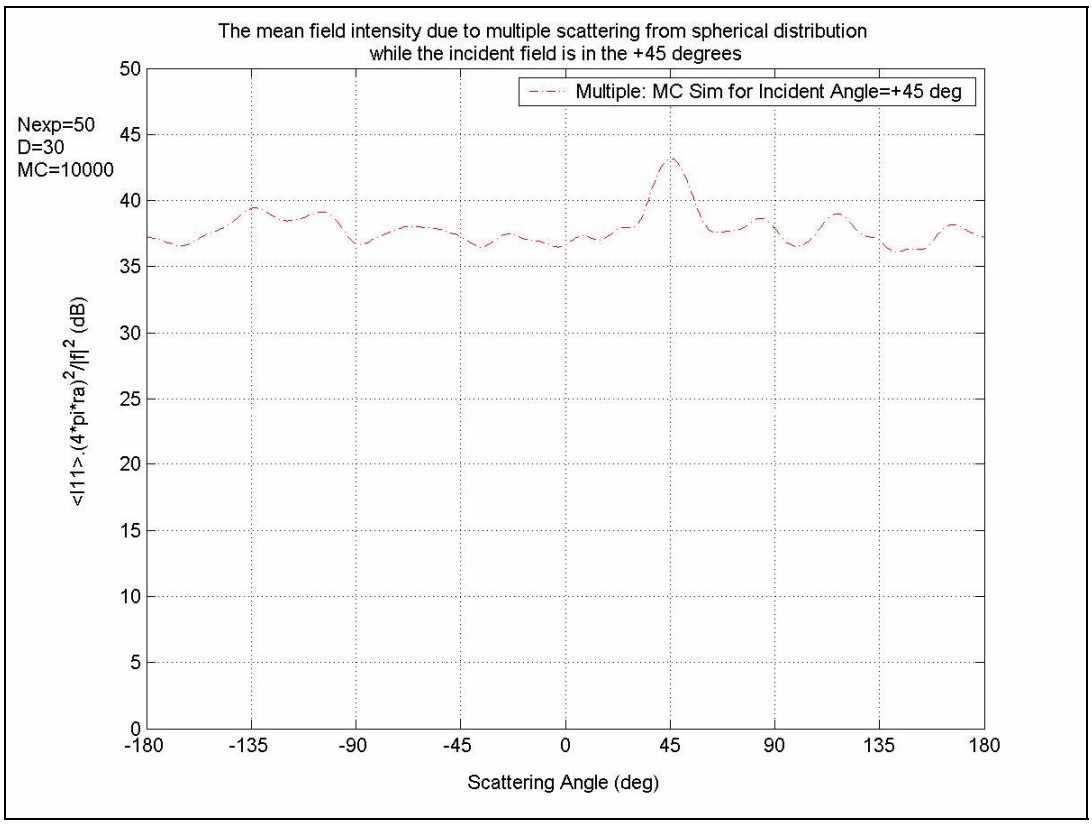

Figure 4.15: The mean field intensity due to multiple scattering from spherical distribution while the incident field is in the +45 degrees: N=50, D=30 and MC=10000.

As can be seen from Figure 4.15, we get an enhancement in the direction of +45 degrees for the mean field intensity due to multiple scattering from spherical distribution while the incident field is in the direction of +45 degrees. The result proves us obviously that the type of this enhancement phenomenon is a backscattering not a specular. Its intensity is nearly 5 dB the same as amplitude of intensity in Figure 4.8 where the incident field is in the direction of 0 degrees.

Thanks to the investigation of the specular enhancement, we say clearly that the backscattering enhancement is observed only as regard as multiple scattering conditions. At the same time, this basically means the single scattering phenomenon is not enough alone in order to explain the backscattering enhancement and also the higher-order scattering terms have to be calculated in order to get accurate results in the case of the backscattering enhancement.

4.4 Multiple Scattering Compared to Single Scattering and Double Scattering Phenomena

In previous investigations, we get a certain number of results regarding multiple, single and double scattering phenomena. In this section, we obviously present them in the same graphical results in order to compare their characteristic behaviors. Multiple scattering compared to single scattering from cubical distribution is carefully examined in Section 4.4.1 and multiple scattering compared to single scattering and double scattering from spherical distribution is looked over in Section 4.4.2.

4.4.1 The Particles are Distributed within a Cube

In Section 4.1.1, the analytic and MC simulation results of the mean field intensity due to single scattering from cubical distribution and in Section 4.2.1, the MC simulation result of the mean field intensity due to multiple scattering from cubical distribution are evaluated. In this section, we compare these results in order to examine differences between the single and multiple scattering phenomena from cubical distribution in Figure 4.16.

As can be seen from Figure 4.16, the backscattering enhancement occurs due to multiple scattering. As for single scattering, the specular enhancement is observed, which is presented in previous sections. As well as this key difference, there is a large amplitude distinction between multiple and single scattering results. Therefore, if we definitely want to obtain general characteristic behaviors of the cubical distribution, we must calculate higher-order scattering terms and consider the multiple scattering phenomenon.

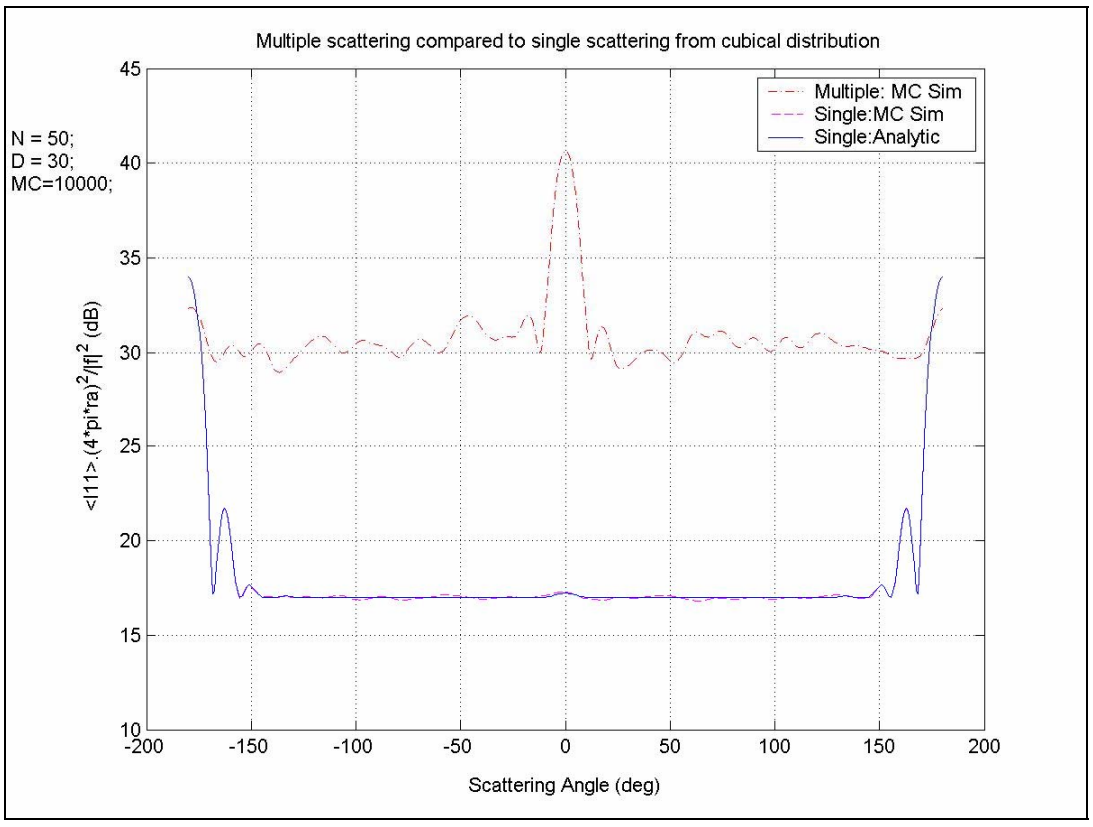

Figure 4.16: Multiple scattering compared to single scattering from cubical distribution: N=50, D=30 and MC=10000.

4.4.2 The Particles are Distributed within a Sphere

In Section 3.2.1 the analytic result of the mean field intensity due to double scattering from spherical distribution, in Section 4.1.2 the analytic and MC

simulation results of the mean field intensity due to single scattering from spherical distribution and in Section 4.2.2 the MC simulation result of the mean field intensity due to multiple scattering from spherical distribution are evaluated. In this section, we compare these four results in order to examine differences among the single, double and multiple scattering phenomena from spherical distribution in Figure 4.17.

As can be seen from Figure 4.17, the backscattering enhancement is observed due to higher-order multiple scattering terms and double scattering term but none of the enhancement is observed due to single scattering. As well as these key differences, there is large amplitude distinction between the higher-order multiple scattering and the low-order scattering phenomena. Therefore, if we specially want to obtain general characteristic behaviors of the spherical distribution, we have to calculate higher-order scattering terms and consider the multiple scattering phenomenon. We have to note that the double scattering phenomenon is the first multiple scattering mechanism and it is also one of the low-order multiple scattering terms. As can be seen from Figure 4.17, double scattering has the dominant effect on the backscattering enhancement. However, it is not enough in order to explain the backscattering enhancement phenomenon alone. Because, the higher-order scattering terms contribute significantly to the backscattering enhancement as much as double scattering.

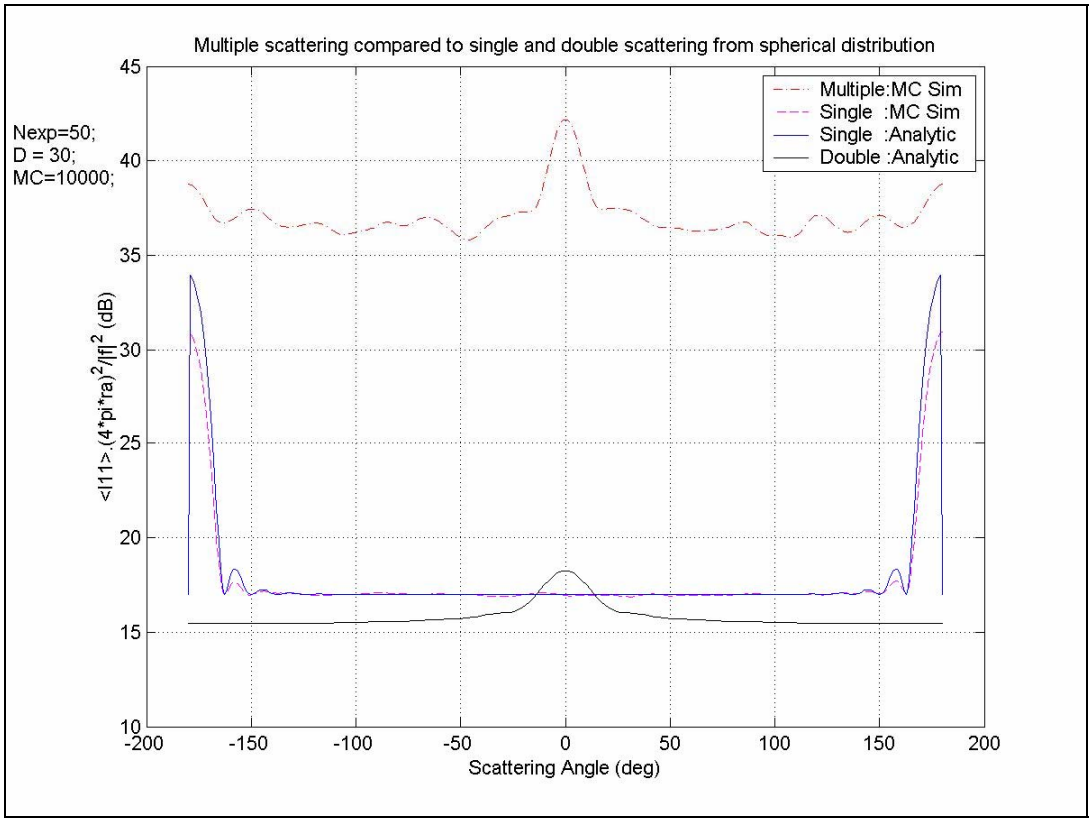

Figure 4.17: Multiple scattering compared to single and double scattering from spherical distribution: N=50, D=30 and MC=10000.

The above comparing results of both the cubical and spherical distribution prove that the backscattering enhancement phenomenon occurs only due to multiple scattering. This conclusion about the cause of the backscattering enhancement is verified for both cubical and spherical distributions.

4.5 The Effect of Incident Field Frequency on the Backscattering Enhancement due to Multiple Scattering

In this section, we show the effect of incident field frequency on the backscattering enhancement due to multiple scattering. In previous sections, we use the incident wave which is assumed as a plane wave and is given by

$$\psi_{inc}(\vec{r}) = e^{i\vec{k}_i.\vec{r}} \tag{4.32}$$

The incident wave vector is denoted by $\vec{k}_i = k\hat{r}_i$ where $\hat{r}_i$ is a unit vector in the direction from the source to the point scatterer and k is the wave number given by

$$k = \frac{2\pi}{\lambda} \tag{4.33}$$

where λ is the wave length which can be written in terms of the speed of propagation v_w and the frequency f, as $\lambda = v_w / f$. Substituting this expression into Eq. (4.33), we get

$$k = \frac{2\pi}{\frac{v_w}{f}} = f\frac{2\pi}{v_w} \tag{4.34}$$

which is the relation between the wave number k and the frequency f in 1/s = Hz. As can be seen from Eq. (4.34), the wave number k and the frequency of a wave f are proportional to each other and it is symbolized by $k \propto f$. As can be seen from this expression, we can increase the wave number k instead of the frequency f in order to see the effect of frequency variation on the backscattering enhancement.

In the previous sections, we use the value k=1 while calculating the mean field intensity due to multiple scattering from spherical distribution. In this section, the wave number is increased from k=1 to k=2 and then the mean field intensity is calculated for the wave number k=2. Lastly, the mean field intensities due to multiple scattering from spherical distribution are rationally compared and depicted for the wave numbers k=1 and k=2 in Figure 4.18.

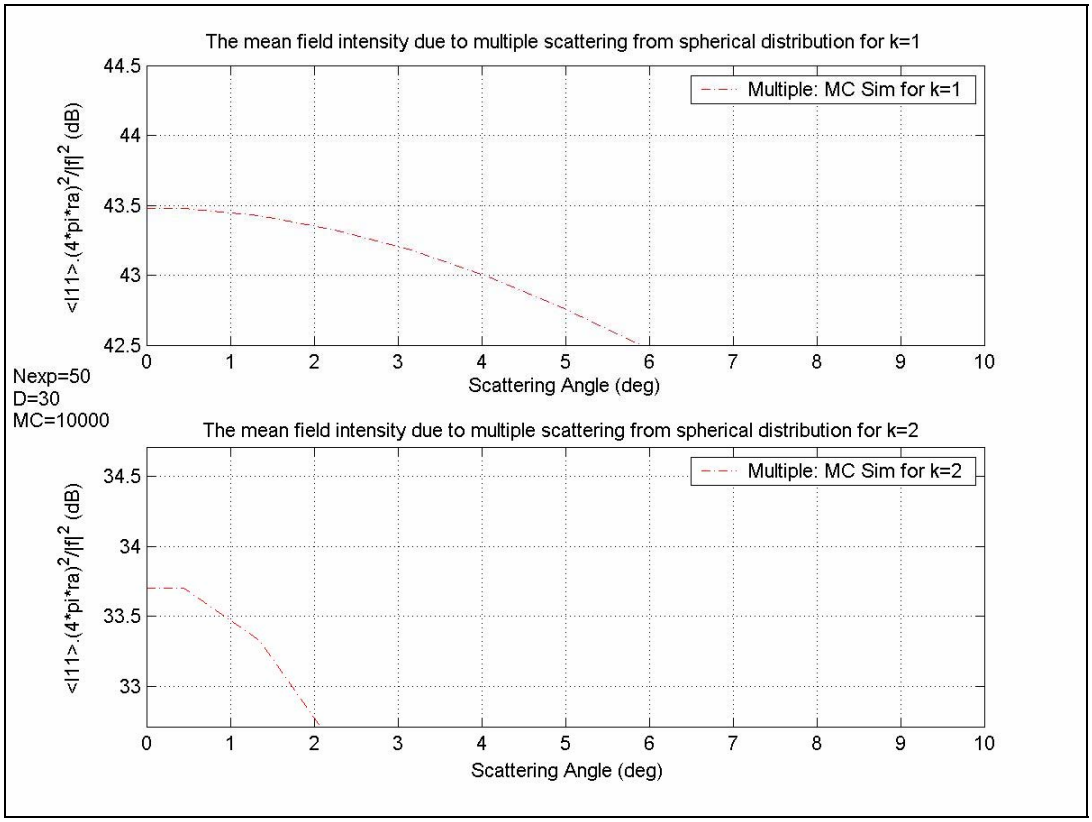

Figure 4.18: The effect of incident field frequency on the backscattering enhancement due to multiple scattering from spherical distribution.

In Figure 4.18, we also note that the mean field intensities due to multiple scattering from spherical distribution are calculated in the decibel (dB) units. The decibel (dB) is a logarithmic unit and clearly defined in a common way when referring to measurements of power or intensity and this is written as $f(x)_{dB} = 10\log_{10}\left(f(x)\right)$.

In Figure 4.18, the angular widths for both wave numbers k=1 and k=2 are shown at the amplitude −1 dB. The angular width for k=1 at −1 dB is approximately 5.9 degrees and the angular width for k=2 at −1 dB is approximately 2.1 degrees. To sum up, increasing incident wave frequency causes the narrower backscattering enhancement angular widths. The backscattering enhancement angular width is necessary in order to define the receiving pattern angular width of the receiver antenna. If the backscattering enhancement angular width is smaller than the receiving pattern angular width of the receiver antenna, the backscattering

enhancement is not likely to be observed. Hence, the incident field frequency is so much important in the remote sensing, [7].

4.6 The Effects of Point Scatterer Density on the Backscattering Enhancement and the Specular Enhancement

Density of the point scatterers distributed within a cube or a sphere can be denoted by N/V where N is the number of distributed point scatterers and V is the volume of distribution. After running a certain number of Monte Carlo simulations, we observe that the point scatterer density has important effects on the backscattering enhancement. In our studies, we also demonstrate that the backscattering enhancement is only constituted due to multiple scattering. The multiple scattering phenomenon is commonly encountered when the density of point scatterers is large enough, so that an incident wave interacts with more than one point scatterer before leaving them, [8]. Therefore, the backscattering enhancement is only observed when the density of point scatterers is in a certain interval. If the distance between point scatterers increase (that is to say, in the lower-density condition), the multiple scattering to be occurring becomes a weak probability. Because of this weak probability, the backscattering enhancement can not occur. If the distance between point scatterers decrease (that is to say, in the higher-density condition), the incident field is to be absorbed in the point scatterers distributed media so there will not be enough returned fields after scattering processes and so once again the backscattering enhancement can not be observed. This phenomenon (the absorption of incident field) is mentioned as the "shadow effect" in [9], [25], [28] and [29]. On the other hand, if the particle density is too high, the structure behaves like a solid.

After all, we need to determine a density interval where the backscattering enhancement occurs. For this purpose, the simulation results about backscattering enhancement are given in the Table 4.2 after running a certain number of Monte Carlo simulations. In these simulations, dimension of cubical distribution and diameter of spherical distribution are considered as D=30. From these results, the density interval for the backscattering enhancement due to multiple scattering from

cubical distribution can be determined as [3/27000 – 99/27000]. This means that the backscattering enhancement is observed in this density interval [3/27000 – 99/27000] or [$1.1\text{x}10^{-4}$ – $36.6\text{x}10^{-4}$]. In the same way, the density interval for the backscattering enhancement due to multiple scattering from spherical distribution can be stated as [3/14137 – 74/14137] or [$2.1\text{x}10^{-4}$ – $52.3\text{x}10^{-4}$]. As can be seen these intervals, the backscattering enhancement from cubical distribution has a larger density interval than spherical distribution has.

Table 4.2: Density intervals for the backscattering enhancement due to multiple scattering from cubical and spherical distributions

Distribution:	Number of Scatterers (*N*):	Volume of Distribution (*V*) for *D*=30:
Cubical	3−99	$D^3 = 27000$
Spherical	3−74	$(4/3)\pi(D/2)^3 = 14137$

We get some specular enhancement results due to single scattering from cubical distribution; because of the cubical structure. From the results of Table 4.3, the density interval can be determined as [7/27000 – *INF*/27000] or [$2.59\text{x}10^{-4} - \infty$]. If the scatterers are in a condition of the lower-density, the specular enhancement does not occur. As for the scattering processes in a condition of higher-density, the specular enhancement always occurs since a flat surface being. Meanwhile, owing to the spherical structure, the specular enhancement results are not observed in any intervals. After all, we prove that both the backscattering and specular enhancements are related to the density of randomly distributed point scatterers.

Table 4.3: Density intervals for the specular enhancement due to single scattering from cubical and spherical distributions

Distribution:	Number of Scatterers (*N*):	Volume of Distribution (*V*) for *D*=30:
Cubical	$7 - INF$	$D^3 = 27000$
Spherical	---	$(4/3)\pi(D/2)^3 = 14137$

where *INF* denotes an infinite number of point scatterers.

CHAPTER 5

CONCLUSIONS

In this thesis, analysis and simulation of the backscattering enhancement phenomenon from randomly distributed point scatterers are investigated. These point scatterers are distributed randomly into two different geometries such as spherical and cubical distributions throughout this study. Analytical explanations of single and multiple scattering phenomena from point scatterers are presented by expanding their general formulas.

T-matrix method is applied while analysis of the backscattering enhancement phenomenon from randomly distributed point scatterers is being investigated in Chapter 3 and also some computer programs using Monte Carlo method to compute the backscattering enhancement phenomenon from randomly distributed point scatterers are developed in Chapter 4.

Mean field intensities due to single scattering from cubical and spherical distributions are properly calculated analytically. Moreover, these mean field intensities are plotted by using MATLAB programming language and an enhancement due to single scattering is observed for only cubical distribution. In the last Chapter, we prove that this enhancement is a kind of the specular enhancement not the backscattering enhancement.

Mean field intensity due to double scattering from spherical distribution is estimated analytically by clearly determining seven possible cases which are evaluated from correlation of two different rays. In addition, this mean field intensity is plotted by using MATLAB programming language and we also present that the second case is the dominant among the other cases as far as the backscattering enhancement is concerned. We note that the double scattering

phenomenon is the first multiple scattering mechanism in the distribution volume and the approximate formula of the mean field intensity due to double scattering is obtained in an analytical manner.

Mean field intensity due to interaction of single and double scattering from spherical distribution is calculated analytically by clearly determining three possible cases which are evaluated from correlation of two different rays. Subsequently, we demonstrate that this intensity is to be zero if T-matrix (T) has an only imaginary component. Therefore, the minimal effect of the mean field intensity due to interaction of single and double scattering can be neglected in the most cases.

Mean field intensities due to single scattering from cubical and spherical distributions are simulated by using Monte Carlo simulation technique. The reliabilities of these simulation results have been checked by comparing their analytical results and computing their 95% confidence intervals.

Mean field intensities due to multiple scattering from cubical and spherical distributions are simulated by using Monte Carlo simulation technique. The reliabilities of these simulation results have been checked by computing their 95% confidence intervals. These results prove that the existence of the backscattering enhancements due to multiple scattering from cubical and spherical distributions. Moreover, we display that the cubical distribution give rise to stronger backscattering enhancement intensity than the spherical distribution. Universal survey studies about the individual existences of the backscattering enhancements from different obstacles are presented in [21]. In addition, the experimental studies about backscattering enhancement can be found in [24], [30] and [31].

The specular enhancement from randomly distributed point scatterers is investigated. This type of the enhancement is observed over cubical distribution when examining the single scattering phenomenon. This proves obviously that specular enhancement occurs due to single scattering from cubical distribution and also this result help us to conclude that the backscattering enhancement is only constituted due to multiple scattering. As for the spherical distribution, the result

presents us that specular enhancement due to single scattering from the spherical distribution is not constituted. The specular enhancement is also observed in [14] which presents that if a surface is flat, this condition corresponds to Snell's law, and the wave is always to be scattered in the specular direction. In [7], both backscattering enhancement and specular enhancement are observed at the same time.

Multiple scattering is compared to single scattering from the cubical distribution and also multiple scattering is compared to single scattering and double scattering from the spherical distribution. We prove that the backscattering enhancement is mainly constituted due to only multiple scattering. Moreover, we demonstrate that the double scattering is the first multiple scattering mechanism and it has dominant effect on the backscattering enhancement. However, it is not enough in order to explain the backscattering enhancement phenomenon alone. In the same manner, the effect of double scattering has been presented in [9] and [27]. In addition, the higher-order multiple scattering terms contributes to magnitude of the mean field intensity. Similar conclusion drawn in [10] is that the significant contribution of multiple scattering can vary by almost an order of magnitude. The similar results about contributions of multiple scattering terms are presented in [11], [26], [27] and [29]. On account of these results, we must include multiple scattering terms in our scattering models to be realistic.

The effect of incident field frequency on the backscattering enhancement due to multiple scattering is illustrated. The result proves that to increase incident wave frequency causes narrower backscattering enhancement angular width and calculating this width is necessary in order to define the receiving pattern angular width of the receiver antenna. The same effect of incident field frequency can be found in [7] and [15], which conclude that the higher the frequency, the narrower the enhancement angle width.

The effects of point scatterer density on the backscattering enhancement and the specular enhancement are illustrated. We present that the backscattering enhancement is commonly encountered when the density of point scatterers is large

enough. If the randomly distributed point scatterers are in a condition of the lower-density, the multiple scattering to be occurring becomes a weak probability. As for the scattering processes in condition of higher-density, the incident field is to be absorbed in the randomly distributed point scatterers' media so there are not enough returned fields interfering constructively to produce the backscattering enhancement. This event (the absorption of incident field) is mentioned as the "shadow effect" in some academic articles, for example [9], [25], [28] and [29]. In the same manner, the effects of density have been presented in [8] and [28]. We also present that the specular enhancement is commonly encountered when the density of point scatterers is large enough for only single scattering from cubical distribution. In a condition of the lower-density, the specular enhancement is not to occur since a flat surface occurring becomes a weak probability. As for the higher-density condition, the specular enhancement is always observed because of a flat surface occurring. Meanwhile, owing to the geometrical structure of the spherical distribution, the specular enhancement results are not observed at any density ratio.

As a future work, the same problems can be solved in the presence of some different distributions, such as cylindrical distribution. Moreover, instead of using point scatterers, three dimensional scatterers can be distributed into the different structures. However, these randomly distributed three dimensional scatterers cause that the analytic solutions are to be more difficult and also the runtime of simulated solutions are to be much longer.

REFERENCES

[1] Akira Ishimaru, Wave Propagation and Scattering in Random Media, Oxford University Press, 1997.

[2] T. A. Nieminen, H. Rubinsztein-Dunlop, N. R. Heckenberg, Calculation of the T-matrix: General Considerations and Application of the Point-Matching Method, Preprint Submitted to Elsevier Preprint, 6 August 2002.

[3] Roger F. Harrington, Time-Harmonic Electromagnetic Fields, McGraw-Hill Book Company, 1961.

[4] Wikimedia Foundation, Simulation, http://en.wikipedia.org/wiki/Simulation, 17 January 2007, Last Accessed at July 2007.

[5] Computational Science Education Project, Introduction to Monte Carlo Methods, http://www.phy.ornl.gov/csep/CSEP/MC/MC.html, 1995, Last Accessed at July 2007.

[6] Lee A. Becker, Confidence Intervals, http://web.uccs.edu/lbecker/SPSS /confintervals.htm, 1999, Last Accessed at February 2007.

[7] R.H. Lang and N. Khadr, Effects of Backscattering Enhancement on Soil Moisture Sensitivity, IEEE 91-72810/92$03.00, 1992.

[8] C. Roze, T. Girasole, L. Mees, G. Grehan, L. Hespel, A. Delfour, Interaction Between Ultra Short Pulses and a Dense Scattering Medium by Monte Carlo Simulation: Consideration of Particle Size Effect, Optics Communications 220 237–245, 2003.

[9] V.P. Tishkovetsa, E.V. Petrovab, K. Jockersc, Optical Properties of Aggregate Particles Comparable in Size to the Wavelength, Journal of Quantitative Spectroscopy & Radiative Transfer 86 241–265, 2004.

[10] V. P. Romanov, D. Yu. Churmakov, E. Berrocal, and I. V. Meglinski, Low-Order Light Scattering in Multiple Scattering Disperse Media, Optics and Spectroscopy, Vol. 97, No. 5, 2004.

[11] Jack F. Paris, A Simple Algorithm to Correct Single-Scattering Model Outputs for Multiple Scattering Effects, IEEE 91-72810/92$03.00, 1992.

[12] Jean-Claude Auger, Brian Stout, A Recursive Centered T-Matrix Algorithm to Solve the Multiple Scattering Equation: Numerical Validation, Journal of Quantitative Spectroscopy & Radiative Transfer 79–80 533–547, 2003.

[13] Z. Q. Meng, M. Tateiba, Bistatic Scattering Enhancement Phenomenon in a Random Medium, Progress in Electromagnetics Research Symposium, 2005.

[14] Yasuo Kuga, Guifu Zhang, Ji-Hae Yea and Akira Ishimaru, Analytical and Numerical Studies of Angular Correlation Function of Waves Scattered from Randomly Distributed Cylinders, Waves in Random Media 8 269–281, 1998.

[15] ZHANG Min, SONG Yue-Xia, WU Zhen-Sen, MA An-Ying, Simulation of Low Grazing Scattering Properties of Vegetation, Chinese Physical Society and IOP Publishing Ltd Vol. 20, No. 4 502, 2003.

[16] Özgür Salih Ergül, Fast Multipole Method for the Solution of Electromagnetic Scattering Problems, Thesis Submitted to Bilkent University, 2003.

[17] David K. Cheng, Second Edition Field and Wave Electromagnetics, Addison-Wesley Publishing Company, 1989.

[18] Constantine A. Balanis, Antenna Theory Analysis and Design Second Edition, John Wiley & Sons, Inc., 1982.

[19] Merrill I. Skolnik, Introduction to Radar Systems Second Edition, McGraw-Hill Book Company, 1981.

[20] Joe King, MATLAB 6 for Engineers, R. T. Edwards. Inc., 2001.

[21] YU. N. Barabanenkov, YU. A. Kravtsov, V. D. Ozrin, and A. I. Saichev, Enhanced Backscattering: The Universal Wave Phenomenon, Proceedings of the IEEE Vol.79, No.10, 1991.

[22] David Adamson, Monte Carlo Methods, http://cs.oberlin.edu/~dadamson/Monte%20Carlo.pdf, 2007, Last Accessed at July 2007.

[23] Shu-Qing Li, Chi Hou Chan, Wen-Bing Wang, and Leung Tsang, Backscattering Enhancement of Electromagnetic Waves from Vegetation Canopies, Microwave and Optical Technology Letters Vol. 24, No. 5, 2000.

[24] Akira Ishimaru, Jei S Chen, Phillip Phu and Kuniaki Yoshitomi, Numerical, Analytical, and Experimental Studies of Scattering from very Rough Surfaces and Backscattering Enhancement, Waves in Random Media 1 S91-SlO7, 1991.

[25] Stankevicha, Shkuratov, Grynko, Muinonen, Computer Simulations for Multiple Scattering of Light Rays in Systems of Opaque Particles, Journal of Quantitative Spectroscopy & Radiative Transfer 76 1–16, 2003.

[26] David M Winker, Effects of Multiple Scattering on Lidar Signals and Influences of Particle Characteristics, Progress in Electromagnetics Research Symposium August 23-26, 2005.

[27] Arturo Quirantes, Francisco Arroyo and Jesus Quirantes-Ros, Multiple Light Scattering by Spherical Particle Systems and Its Dependence on Concentration: A T-Matrix Study, Journal of Colloid and Interface Science 240, 78–82, 2001.

[28] D. Liljequist, Trajectory calculation as an approximation to the exact quantum treatment of multiple elastic scattering, Nuclear Instruments and Methods in Physics Research B 251 27–40, 2006

[29] Eva Cerezo, Frederic Perez, Xavier Pueyo, Francisco J. Seron, Francois X. Sillion, A survey on participating media rendering techniques, Visual Comput 21: 303–328 DOI 10.1007/s00371-005-0287-1, 2005.

[30] Tsz-King Chan, Yasuo Kuga, Akira Ishimaru, Charlie T. C. Le, Experimental Studies of Bistatic Scattering from Two-Dimensional Conducting Random Rough Surfaces, IEEE Transactions on Geoscience and Remote Sensing Vol 34 No 3, 1996.

[31] Julien de Rosny, Arnaud Tourin, and Mathias Fink, Coherent Backscattering for Elastic Waves in a Chaotic Cavity, IEEE 0-7803-5722-1/99/$10.00, 1999.

[32] James Jones, Stats: Introduction to Estimation, http://www.richland.edu/james /lecture/m170/ch08-int.html, 8 January 2007, Last Accessed at July 2007.

[33] Ian Craw, Change of Variable – the Jacobian, http://www.maths.abdn.ac.uk /~igc/ tch/ma2001/notes/node77.html, 07 January 2002, Last Accessed at July 2007.

[34] Ronald E. Wyllys, Confidence Intervals for the Mean of a Population, The University of Texas at Austin School of Information Mathematical Notes for Lis 397.1, 15 January 2003.

APPENDIX A

MATLAB PROGRAM OF FIGURE 4.2

```
clear;

N = 50;
D = 30;
MC=10000;

d=D./2;
k = 1.0;
jey = sqrt(-1);
ths = linspace(-180,180,400).';
thsr = ths*pi/180;
ki = k*[0 0 -1];
ks = k*[zeros(size(thsr)) sin(thsr) cos(thsr)];
alfa11s  = zeros(size(ths));

for run=1:MC;
  Rn = D*(rand(3,N)-0.5);
  Rnp = D*(rand(3,N)-0.5);
  R1 = Rn-Rnp;
  e1 = exp(jey*ki*R1);
  e2 = exp(-jey*ks*R1);
  alfa11s = alfa11s+e2*e1.'/N;

  run
end

alfa11s=alfa11s/MC;
alfa11a=(((sin(k.*D.*(cos(thsr./2)).^2).^2.*((sin(k.*d.*sin(thsr)))
.^2))./(((k.*D).^4).*((cos(thsr./2)).^6).*((sin(thsr./2)).^2))));

I11a=N+N*(N-1)*alfa11a;
I11s=N+N*(N-1)*alfa11s;

plot(ths,10.*log10(I11a),ths,10.*log10(real(I11s)),'m--');
axis([-200 200 15 35]);

title('The MC simulation result of the mean field intensity due to
single scattering from cubical distribution');
xlabel('Scattering Angle (deg)');
ylabel('<I11>.(4*pi*ra)^2/|f|^2 (dB)');
legend('Single:Analytic','Single:MC Sim');
grid on;
```

APPENDIX B

MATLAB PROGRAM OF FIGURE 4.4

```
clear;
Nexp = 50;
D = 30;
MC=10000;
Nc =(6./pi).*Nexp;
d=D./2;
k = 1.0;
jey = sqrt(-1);
ths = linspace(-180,180,400).';
thsr = ths*pi/180;
ki = k*[0 0 -1];
ks = k*[zeros(size(thsr)) sin(thsr) cos(thsr)];
alfa11s  = zeros(size(ths));

for run=1:MC;
  Rn = 2*d*(rand(3,Nc)-0.5);
  r = sqrt(sum(Rn.^2));
  ixn = find(r<=d);

  Rnp = 2*d*(rand(3,Nc)-0.5);
  r = sqrt(sum(Rnp.^2));
  ixnp = find(r<=d);

  L = min([length(ixn) length(ixnp)]);
  Rn = Rn(:,ixn(1:L));
  Rnp = Rnp(:,ixnp(1:L));
  R1 = Rn-Rnp;
  e1 = exp(jey*ki*R1);
  e2 = exp(-jey*ks*R1);
  alfa11s = alfa11s+e2*e1.'/L;
  run
end

alfa11s=alfa11s/MC;
alfa11a=[[9.*[k.*D.*cos(k.*D.*cos(thsr./2)).*cos(thsr./2)-
sin(k.*D.*cos(thsr./2))].^2]./[(k.*D.^6).*[[cos(thsr./2)].^6]]];

I11a=Nexp+Nexp*(Nexp-1)*alfa11a;
I11s=L+L*(L-1)*alfa11s;
plot(ths,10.*log10(I11a),ths,10.*log10(real(I11s)),'m--');
axis([-200 200 15 35]);
title('The MC simulation result of the mean field intensity due to
single scattering from spherical distribution');
xlabel('Scattering Angle (deg)');
ylabel('<I11>.(4*pi*ra)^2/|f|^2 (dB)');
legend('Single:Analytic','Single:MC Sim');
grid on;
```

APPENDIX C

MATLAB PROGRAM OF FIGURE 4.5

```
clear;
N = 50;
D = 30;
MC=10000;
d=D./2;
k = 1.0;
jey = sqrt(-1);
ths = linspace(-180,180,400).';
thsr = ths*pi/180;
ki = k*[0 0 -1];
ks = k*[zeros(size(thsr)) sin(thsr) cos(thsr)];
alfa11s  = zeros(size(ths));
alfa11s2 = zeros(size(ths));

for run=1:MC;
  Rn = D*(rand(3,N)-0.5);
  Rnp = D*(rand(3,N)-0.5);
  R1 = Rn-Rnp;
  e1 = exp(jey*ki*R1);
  e2 = exp(-jey*ks*R1);
  alfa11s = alfa11s+e2*e1.'/N;
  alfa11s2=alfa11s2+(e2*e1.'/N).^2;
  run
end

alfa11s_m=alfa11s/MC;

I11s_m=N+N*(N-1)*alfa11s_m;
I11s2=N+N*(N-1)*alfa11s2;

I11s_v= (1./(MC-1)).*I11s2-(MC./(MC-1))*(I11s_m.^2);
I11s_sd=sqrt(I11s_v);

CIp=I11s_m+(1.96*I11s_sd)./sqrt(MC);
CIm=I11s_m-(1.96*I11s_sd)./sqrt(MC);

plot(ths,10.*log10(I11s_m),'r-
.',ths,10.*log10(CIp),'k',ths,10.*log10(CIm),'g');
axis([-200 200 15 35]);
title('The 95% confidence interval for the MC simulation result of
the mean field intensity due to single scattering from cubical
distribution');
xlabel('Scattering Angle(deg)');
ylabel('<I11>.(4*pi*ra)^2/|f|^2');
legend('Single:MC Sim','Confidence Interval:plus','Confidence
Interval:minus');
grid on;
```

APPENDIX D

MATLAB PROGRAM OF FIGURE 4.7

```
clear;

N = 50;
D = 30;
MC=10000;

d = D./2;
k = 1.0;
T = 1.0;
jey = sqrt(-1);
ths = linspace(-180,180,400).';
thsr = ths*pi/180;
ki = k*[0 0 -1];
ks = k*[zeros(size(thsr)) sin(thsr) cos(thsr)];
f=(jey*4*pi*T)./k;
eRa= [zeros(size(thsr)) sin(thsr) cos(thsr)];
eRa=eRa.';
I_sca = zeros(size(ths));

for run=1:MC;

    Rn = 2*d*(rand(3,N)-0.5);
    I=eye(N);
    Gnt=zeros(N);
    field_inc_n=zeros(1,N);
    Gan=zeros(400,N);
    field_inc_a=zeros(1,400);

    for n=1:N;
        for t=1:N;
            if t~=n
                R1=Rn(:,n)-Rn(:,t);
                r1 = sqrt(sum(R1.^2));
                Gnt(n,t)=-exp(jey*k*r1)./(4*pi*r1);
            else
            end
        end
        field_inc_n(n)=exp(jey*(ki*Rn(:,n)));
    end

    Gnt=Gnt*f;
    A=I-Gnt;
    b=field_inc_n.';
    phi = inv(A)*b;

    for a=1:400;
        for n=1:N;
```

```
            R2=sum(eRa(:,a).*Rn(:,n));
            Gan(a,n)=(exp(jey*k*R2));
        end
    end

    Gan=Gan*f;
    field= Gan*phi;
    field=field.';
    field_conj=conj(field);
    I_sca1=(field.*field_conj);
    I_sca=I_sca+I_sca1.'/N;
    run
end

I_sca_m=I_sca./MC;

plot(ths,10.*log10(I_sca_m),'r-.');
axis([-200 200 0 50]);

title('The mean field intensity due to multiple scattering from
cubical distribution');
xlabel('Scattering Angle (deg)');
ylabel('<I11>.(4*pi*ra)^2/|f|^2 (dB)');
legend('Multiple: MC Sim');
grid on;
```

APPENDIX E

MATLAB PROGRAM OF FIGURE 4.8

```
clear;

Nexp = 50;
D = 30;
MC=10000;

Nc =(6./pi).*Nexp;
d = D./2;
k = 1.0;
T = 1.0;
jey = sqrt(-1);
ths = linspace(-180,180,400).';
thsr = ths*pi/180;
ki = k*[0 0 -1];
ks = k*[zeros(size(thsr)) sin(thsr) cos(thsr)];
f=(jey*4*pi*T)./k;
eRa= [zeros(size(thsr)) sin(thsr) cos(thsr)];
eRa=eRa.';
I_sca = zeros(size(ths));

for run=1:MC;

    Rn = 2*d*(rand(3,Nc)-0.5);
    r = sqrt(sum(Rn.^2));
    ixn = find(r<=d);
    L = length(ixn);
    Rn = Rn(:,ixn(1:L));
    I=eye(L);
    Gnt=zeros(L);
    field_inc_n=zeros(1,L);
    Gan=zeros(400,L);
    field_inc_a=zeros(1,400);

    for n=1:L;
        for t=1:L;
            if t~=n
                R1=Rn(:,n)-Rn(:,t);
                r1 = sqrt(sum(R1.^2));
                Gnt(n,t)=-exp(jey*k*r1)./(4*pi*r1);
            else
            end
        end
        field_inc_n(n)=exp(jey*(ki*Rn(:,n)));
    end

    Gnt=Gnt*f;
    A=I-Gnt;
```

```
    b=field_inc_n.';
    phi = inv(A)*b;

    for a=1:400;
        for n=1:L;
            R2=sum(eRa(:,a).*Rn(:,n));
            Gan(a,n)=(exp(jey*k*R2));
        end
    end

    Gan=Gan*f;
    field= Gan*phi;
    field=field.';
    field_conj=conj(field);
    I_sca1=(field.*field_conj);
    I_sca=I_sca+I_sca1.'/L;
    run
end

I_sca_m=I_sca./MC;

plot(ths,10.*log10(I_sca_m),'r-.');
axis([-200 200 0 50]);

title('The mean field intensity due to multiple scattering from
spherical distribution');
xlabel('Scattering Angle (deg)');
ylabel('<I11>.(4*pi*ra)^2/|f|^2 (dB)');
legend('Multiple: MC Sim');
grid on;
```

APPENDIX F

MATLAB PROGRAM OF FIGURE 4.9

```
clear;

N = 50;
D = 30;
MC=10000;

d = D./2;
k = 1.0;
T = 1.0;
jey = sqrt(-1);
ths = linspace(-180,180,400).';
thsr = ths*pi/180;
ki = k*[0 0 -1];
ks = k*[zeros(size(thsr)) sin(thsr) cos(thsr)];
f=(jey*4*pi*T)./k;
eRa= [zeros(size(thsr)) sin(thsr) cos(thsr)];
eRa=eRa.';
I_sca = zeros(size(ths));
I_sca2 = zeros(size(ths));

for run=1:MC;

    Rn = 2*d*(rand(3,N)-0.5);
    I=eye(N);
    Gnt=zeros(N);
    field_inc_n=zeros(1,N);
    Gan=zeros(400,N);
    field_inc_a=zeros(1,400);

    for n=1:N;
        for t=1:N;
            if t~=n
                R1=Rn(:,n)-Rn(:,t);
                r1 = sqrt(sum(R1.^2));
                Gnt(n,t)=-exp(jey*k*r1)./(4*pi*r1);
            else
            end
        end
        field_inc_n(n)=exp(jey*(ki*Rn(:,n)));
    end

    Gnt=Gnt*f;
    A=I-Gnt;
    b=field_inc_n.';
    phi = inv(A)*b;

    for a=1:400;
```

```
        for n=1:N;
            R2=sum(eRa(:,a).*Rn(:,n));
            Gan(a,n)=(exp(jey*k*R2));
        end
    end

    Gan=Gan*f;
    field= Gan*phi;
    field=field.';
    field_conj=conj(field);
    I_sca1=(field.*field_conj);
    I_sca=I_sca+I_sca1.'/N;
    I_sca2 = I_sca2+(I_sca1.'/N).^2;
    run
end

I_sca_m=I_sca./MC;
I_sca_v=(1./(MC-1)).*I_sca2-(MC./(MC-1))*(I_sca_m.^2);
I_sca_sd=sqrt(I_sca_v);

CIp=I_sca_m+(1.96*I_sca_sd)./sqrt(MC);
CIm=I_sca_m-(1.96*I_sca_sd)./sqrt(MC);

plot(ths,10.*log10(I_sca_m),'r-
.',ths,10.*log10(CIp),'k',ths,10.*log10(CIm),'g');
axis([-200 200 0 50]);

title('The 95% confidence interval for the MC simulation of the
mean field intensity due to multiple scattering from cubical
distribution');
xlabel('Scattering Angle (deg)');
ylabel('Isca (dB)');
legend('Multiple:MC Sim','Confidence Interval:plus','Confidence
Interval:minus');
grid on;
```

APPENDIX G

SINC FUNCTION AND SINE INTEGRAL

Sinc Function:

The Sinc function is denoted by $Sinc(x)$ and it is the function of the Sine function $\sin(x)$ divided by x, such as $Sinc(x) = [\sin(x)]/x$. The Sinc function is also known as the "Sampling Function" and it is shown in Figure G.1 as dashed line.

Some Properties of the Sinc Function:

- The Sinc function is the frequency spectrum of the rectangular pulse. That is, the sinc function and the rectangular pulse are Fourier transform pairs
- The Sinc function is the spherical Bessel fuction of the first kind of order zero
- The Sinc function is also determined as

$$Sinc(x) = \begin{cases} 1 & ; x = 0 \\ \dfrac{\sin(x)}{x} & ; otherwise \end{cases}$$

Sine Integral:

The Sine integral is denoted by $Si(x)$ and it is the integral of the Sinc function, such as $Si(x) = \int_0^x \frac{\sin t}{t} dt$ or $Si(x) = \int_0^x Sinc(t) dt$. The Sine integral divided by x $\left[\frac{Si(x)}{x}\right]$ is shown in Figure G.1 as continuous line.

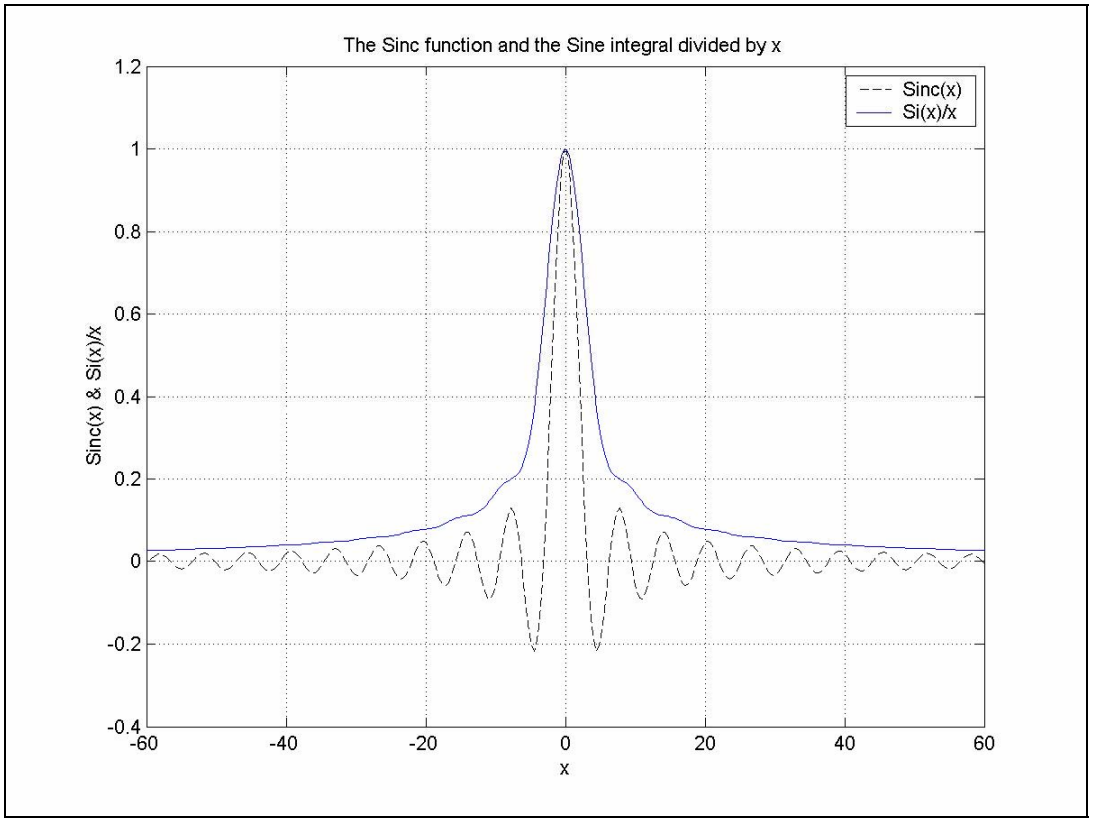

Figure G.1: The Sinc function and the Sine integral divided by *x*

Matlab Program of Figure G.1:

```
clear;
x = linspace(-180,180,1000);

sinc_func =sin(x)./(x);
sine_int_x=sinint(x)./(x);

plot(x,sinc_func,'k--',x,sine_int_x);

axis([-60 60 -0.4 1.2]);
title('Sinc Function & Sine Integral divided by x');
xlabel('x');
ylabel('Sinc(x) & Si(x)/x');
legend('Sinc(x)','Si(x)/x');
grid on;
```